SOME INVESTIGATIONS ON PARAMAGNETIC RELAXATION AT RADIO FREQUENCIES

J. G. A. HILLAERT

SOME INVESTIGATIONS ON PARAMAGNETIC RELAXATION AT RADIO FREQUENCIES

PROEFSCHRIFT

TER VERKRIJGING VAN DE GRAAD VAN DOCTOR IN DE WISKUNDE EN NATUURWETENSCHAPPEN AAN DE RIJKSUNIVERSITEIT TE LEIDEN, OP GEZAG VAN DE RECTOR MAGNIFICUS DR. A.E. COHEN, HOOGLERAAR IN DE FACULTEIT DER LETTEREN, VOLGENS BESLUIT VAN HET COLLEGE VAN DEKANEN TE VERDEDIGEN OP WOENSDAG 28 NOVEMBER 1973 TE KLOKKE 14.15 UUR

door

Johannes Gustaaf Anna Hillaert
Geboren te Hulst in 1941

Krips Repro - Meppel

PROMOTOR: *PROF. DR. C.J. GORTER*

DIT PROEFSCHRIFT IS TOT STAND GEKOMEN
ONDER LEIDING VAN *DR. J.C. VERSTELLE*

STELLINGEN

1. Voor een paramagnetische stof die aan de wet van Curie voldoet volgt uit de gemeten waarde van χ_{ad}/χ_0 rechtstreeks b/C. Om van een stof welke beschreven wordt met de wet van Curie-Weiss b/C te bepalen, dient een temperatuur afhankelijke correctie te worden aangebracht. Deze kan eenvoudig thermodynamisch worden afgeleid.

   Dit proefschrift, hoofdstuk 1, §4.

2. Indien voor een paramagnetische stof bestaande uit een spin-systeem, een systeem van laagfrequent fononen en een vast aan het bad gekoppeld roostersysteem de energieuitwisseling tussen de systemen evenredig is met het temperatuurverschil, treden in een lineaire benadering twee niet eenvoudig te herkennen relaxatietijden op.

   Dit proefschrift, hoofdstuk 4.

   Herzfeld, K.F. and Litovitz, T.A., Absorption and Dispersion of Ultrasonic Waves.

3. Tussen de theoretische voorspellingen van de spin-spin relaxatietijd in een paramagnetische stof van Mazur en Terwiel enerzijds en Sauermann anderzijds bestaat in velden groot ten opzichte van het inwendige veld een discrepantie van een faktor die ongeveer gelijk is aan $(1 - \chi'_{bet}/\chi_{ad})^2$.

   Dit proefschrift, hoofdstuk 3, §4.

4. Bij de berekening van de spin-spin relaxatietijd verwaarloost Caspers ten onrechte termen welke belangrijk kunnen zijn.

   Caspers, W.J., Physica 26 (1966) 798.

   Caspers, W.J., Theory of Spin Relaxation, Interscience Publ., New York (1964).

5. In resolutie 3 en 4 van de 13de Conférence Générale des Poids et Mesures (1967-1968) komt onvoldoende tot uiting dat 1 °C = 1 K.

   13de Conférence Générale des Poids et Mesures (1967-1968) Metrologia 5 (1969) 35.

6. De conclusies welke Emori et al. trekken uit het feit dat de gemeten en berekende susceptibiliteit in Diisothiocyanatobis (thiourea) nickel (II) en analoge complexe verbindingen overeenstemmen zijn aanvechtbaar.

   Emori, S., Inoue, M. and Kubo, M., Bull. Chem. Soc. Japan 44 (1971) 3299.

7. Bij het meten van de verandering van de viscositeit van gassen onder invloed van een uitwendig magneetveld dienen de zogenaamde Knudsen correcties in rekening te worden gebracht. Een duidelijk onderscheid moet gemaakt worden tussen de efficientie waarmee moleculen reoriënteren bij gas-gas botsingen en die waarmee zij reoriënteren bij botsingen met de wand.

8. Om een Internationale Praktische Temperatuur Schaal tussen 4 en 14 K vast te leggen met een nauwkeurigheid van 0.5 mK, zijn minstens drie vaste punten nodig. Het verdient aanbeveling te onderzoeken of magnetische overgangspunten hiervoor in aanmerking komen.

   Temperature, Its Measurement and Control in Science and Industry, Instrument Society of America, Pittsburg (1972) Vol. 4, Part 2, page 815.

9. Het valt niet te verwachten dat bij vergroting van het aantal beschikbare cardiogrammen, een zuiver statistische analyse van deze cardiogrammen alléén een bruikbare methode zal opleveren voor een bevolkingsonderzoek naar hartafwijkingen.

10. Het door Alonso en Finn bij de behandeling van een inductieverschijnsel van de 2de soort ingevoerde begrip equivalente veldsterkte doet afbreuk aan de overigens fraaie behandeling van de electromagnetische verschijnselen.

    Alonso, M. and Finn, E.J., Fundamental University Physics, Vol. II, Chapter 17.4, Addison-Wesley Comp., Massachusetts, USA.

11. De aanduidingen "voor" en "achter" op perrons van de Nederlandse Spoorwegen zijn onduidelijk als men niet weet in welke richting de trein zal gaan rijden.

Stellingen behorende bij het proefschrift van J.G.A. Hillaert.

Leiden, november 1973.

Aan mijn ouders
Aan Corry en poppedruif

CONTENTS

CHAPTER I

SURVEY OF THE THEORY

1.1 *Introduction*

By paramagnetic relaxation is meant those phenomena which occur when the magnetization of a paramagnetic substance tends towards equilibrium after a disturbance in the external magnetic field. The phenomena comprise a number of different processes, such as parallel field resonance, spin-spin relaxation, spin-lattice relaxation, and lattice-bath relaxation, from which in the following only spin-spin and spin-lattice relaxation will be discussed.

1.2 *Static susceptibility*

Normal paramagnetics are those substances for which the magnetization $\vec{M}$ induced by the magnetic field $\vec{H}$ varies approximately inversely with the temperature T, according to Curie's law

$$\vec{M} = \frac{\overline{\overline{C}}}{T} \cdot \vec{H} = \overline{\overline{\chi}}_0 \cdot \vec{H} \quad ; \tag{1.01}$$

$\overline{\overline{C}}$ is called the Curie constant and $\overline{\overline{\chi}}_0$ the static susceptibility. In general, the vectors $\vec{M}$ and $\vec{H}$ are not in the same direction, and $\overline{\overline{\chi}}_0$ is thus a second order tensor. $\overline{\overline{\chi}}_0$ is a diagonal tensor if the principal axes of $\overline{\overline{\chi}}_0$ are chosen as the reference system, and $\overline{\overline{\chi}}_0$ reduces to a scalar if the magnetic field is applied along one of these principal axes, which will be called z axis. In that case, $\vec{M}$ and $\vec{H}$ have the same direction, and we may write

$$\vec{M} = \frac{C}{T} \vec{H} = \chi_0 \vec{H} \quad . \tag{1.02}$$

Normal paramagnetism occurs in salts involving elements of the so-called transition groups in the periodic system, which possess a not completely filled inner shell.

If we consider a large number N of free paramagnetic ions each with a permanent magnetic moment $\vec{\mu}$, placed in a magnetic field $\vec{H}$, in thermal equilibrium at a temperature T, then the magnetization is given by

$$M = Ng\mu_B JB_J(x) \quad , \tag{1.03}$$

where

$$B_J(x) = \frac{2J + 1}{2J} \operatorname{ctgh}\left(\frac{2J + 1}{2J}x\right) - \frac{1}{2J} \operatorname{ctgh}\left(\frac{x}{2J}\right)$$

and

$$x = \frac{g\mu_B JH}{kT} \quad .$$

In this expression g is the Landé factor, μ_B is the Bohr magneton (μ_B = 0.9271 erg Oe^{-1}), and J the total angular momentum quantum number.
If $x << 1$, we can simplify expression (1.03) and write

$$M = N \frac{g^2\mu_B^2 J(J + 1)}{3kT} H \quad , \tag{1.04}$$

which we can identify with Curie's law

$$M = \chi_0 H = \frac{C}{T} H \quad ,$$

so that

$$C = N \frac{g^2\mu_B^2 J(J + 1)}{3k} \quad . \tag{1.05}$$

Van Vleck [1] has given a quantum mechanical derivation of (1.04), assuming that the energy spectrum of the ions consists of a group of low lying energy levels with spacings between consecutive levels small compared to kT, and a group of high energy levels at a distance large compared to kT. Besides the temperature dependent susceptibility, he obtained an expression for the temperature independent contribution.

The paramagnetism of the rare earth ions is caused by the not completely filled inner shell of the 4f electrons. The influence of the crystal field on the paramagnetic ions in the crystal is rather small, and we deal with almost free ions.
Apart from a few exceptions, Curie's constant is given by (1.05). In the ions of the iron group, the paramagnetism originates from the 3d electrons which are not shielded by outer electrons. The crystal field has a great influence on the electrons, and causes splittings of about $10^4 cm^{-1}$. The orbital angular momentum is quenched, and only the spin remains free. This means that Curie's constant is given by

$$C = N \frac{g^2 \mu_B^2 S(S+1)}{3k} \qquad (1.06)$$

in which S is the spin quantum number, and g has a value of about the free spin value 2.

Only a few salts follow Curie's law down to very low temperatures. A better description of the susceptibility is given by the Curie-Weiss law,

$$\chi_0 = \frac{C}{T - \Theta} \qquad (1.07)$$

in which Θ can contain, besides a contribution due to the crystal fields, terms caused by interactions between the ions.

1.3 *Linear response theory*

From a paramagnetic system in equilibrium (for which the magnetization is given by Curie's law or the Curie-Weiss law) the field is varied a little during a certain time, which will result in a variation of the magnetization. For the magnetic field H along the z axis, we write

$$H(t) = H_z + \Delta H_z(t) \quad , \qquad (1.08)$$

and for the magnetization M along the z-axis

$$M(t) = M_z + \Delta M_z(t) \quad . \qquad (1.09)$$

H_z and M_z are the equilibrium values, $\Delta H_z(t)$ is the variation of the magnetic field and $\Delta M_z(t)$ the resulting variation of the magnetization.

Linearity

It is assumed that the field variation $\Delta H_z(t)$ is small enough to give a description in a linear approximation.

Response function

A δ-peak like variation in the magnetic field at the time $t = \tau$

$$\Delta H_z(t) = \delta(t - \tau)h \quad , \qquad (1.10)$$

will cause a variation of the magnetization at the time $t > \tau$ which we can write as

$$\Delta M_z(t) = R_{zz}(t - \tau)h = R_{zz}(t - \tau)\Delta H_z(\tau) \quad . \tag{1.11}$$

$R_{zz}(t)$ will be called the response function. It is the zz element of the response tensor $\bar{\bar{R}}(t)$.

Principle of causality

As a variation in the magnetic field at the time τ cannot cause a variation of the magnetization at times $t < \tau$, one has

$$R_{zz}(t - \tau) = 0 \text{ for } t < \tau \quad . \tag{1.12}$$

This is called the principle of causality. Furthermore, we demand that a finite disturbance produces finite after-effects in time as well as in amplitude. This implies that $\lim_{t\to\infty} R_{zz}(t) = 0$. An arbitrary field variation at the time t may be written as a sum of δ-functions:

$$\Delta H_z(t) = \int_{-\infty}^{+\infty} \delta(t - \tau)\Delta H_z(\tau)d\tau \quad . \tag{1.13}$$

The contribution to the variation of the magnetization of one δ-function is given by (1.11), and because all contributions may be added due to linearity, the variation of the magnetization as response to an arbitrary field may be written as

$$\begin{aligned} \Delta M_z(t) &= \int_{-\infty}^{t} R_{zz}(t - \tau)\Delta H_z(\tau)d\tau \\ &= \int_{0}^{\infty} R_{zz}(\tau)\Delta H_z(t - \tau)d\tau \quad . \end{aligned} \tag{1.14}$$

A contribution due to diamagnetic effects has been omitted.

1.3.1 *Relaxation function*

The relaxation function $\phi_{zz}(t)$ is, except for an additive constant, defined as

$$-\frac{d}{dt}\phi_{zz}(t) = R_{zz}(t) \quad . \tag{1.15}$$

The additive constant is determined by the value of $\phi_{zz}(t)$ in the limit for large t.

If we consider for instance the response of the magnetization to a negative

field step

$$H(t) = \begin{cases} H + h & \text{for } t < 0 \\ H & \text{for } t > 0 \end{cases} , \tag{1.16}$$

then the variation of magnetization is given by

$$\Delta M_z(t) = M_z(t) - M_z(t = 0, H+h) = - \int_0^t R_{zz}(t - \tau, H+h) h d\tau . \tag{1.17}$$

In a linear approximation, this can be written as

$$M_z(t) - M_z(0,H) = \{\frac{\partial M_z(0,H)}{\partial H} + \int_t^\infty R_{zz}(\tau,H) d\tau - \int_0^\infty R_{zz}(\tau,H) d\tau\} h . \tag{1.18}$$

If, as is frequently done, $\phi_{zz}(t)$ is defined as

$$M_z(t) - M_z(0,H) = \phi_{zz}(t) h , \tag{1.19}$$

by which the additive constant in (1.15) has been fixed, we have

$$\phi_{zz}(t) = \{\frac{\partial M_z(0,H)}{\partial H} + \int_t^\infty R_{zz}(\tau,H) d\tau - \int_0^\infty R_{zz}(\tau,H) d\tau\} . \tag{1.20}$$

The value of

$$\lim_{t\to\infty} \phi_{zz}(t) = \{\frac{\partial M_z(0,H)}{\partial H} - \int_0^\infty R_{zz}(\tau,H) d\tau\} \tag{1.21}$$

is in general different from zero.

1.3.2 *Complex susceptibility*

Let us consider the response of the magnetization to an oscillating field of amplitude h and frequency ω

$$\Delta H_z(t) = \mathrm{Re}\, h\, e^{i\omega t} ; \tag{1.22}$$

then the variation of the magnetization is given by

$$\begin{aligned} \Delta M_z(t) &= \mathrm{Re} \int_0^\infty d\tau R_{zz}(\tau) e^{-i\omega\tau} h\, e^{i\omega t} \\ &\equiv \mathrm{Re}\chi(\omega) h\, e^{i\omega t} \end{aligned} \tag{1.23}$$

$\chi(\omega)$ is the complex frequency dependent susceptibility

$$\chi(\omega) = \chi'(\omega) - i\chi''(\omega) = \int_0^\infty dt R_{zz}(t) e^{-i\omega t} \quad . \tag{1.24}$$

As R(t) is a real function, we have

$$\chi'(\omega) = \int_0^\infty dt R_{zz}(t) \cos\omega t \quad \text{and} \tag{1.25a}$$

$$\chi''(\omega) = \int_0^\infty dt R_{zz}(t) \sin\omega t \quad . \tag{1.25b}$$

The Laplace transform of the response function $R_{zz}(t)$ is defined as

$$R_{zz}(p) = \int_0^\infty dt e^{-pt} R_{zz}(t) \quad , \tag{1.26}$$

so that

$$\chi(\omega) = R_{zz}(i\omega) \quad . \tag{1.27}$$

If we define $\Phi(t) = \phi_{zz}(t) - \lim_{t\to\infty} \phi_{zz}(t)$, then partial integration of (1.24) gives (as $\lim_{t\to\infty} \Phi(t) = 0$)

$$\chi(\omega) = \chi(0) - i\omega \int_0^\infty dt \Phi(t) e^{-i\omega t} \tag{1.28}$$

or

$$\chi'(\omega) = \chi(0) - \omega \int_0^\infty dt \Phi(t) \sin\omega t \quad , \tag{1.29a}$$

and

$$\chi''(\omega) = \omega \int_0^\infty dt \Phi(t) \cos\omega t \quad . \tag{1.29b}$$

$\chi(0)$ is the limiting value of $\chi(\omega)$ for $\omega \to 0$. In section 1.4, we will see that for spin-lattice relaxation, $\chi(0) = \chi_0$, the static susceptibility, and for spin-spin relaxation $\chi(0) = \chi_{ad}$, the so-called adiabatic susceptibility. The Fourier transform of $\Phi(t)$ is defined as

$$\Phi(\omega) = \frac{1}{2\pi} \int_{-\infty}^{\infty} dt e^{-i\omega t} \Phi(t) \quad . \tag{1.30}$$

If $\Phi(-t) = \Phi(t)$, then

$$\Phi(\omega) = \frac{\chi''(\omega)}{\pi\omega} \quad . \tag{1.31}$$

1.3.3 *Kramers-Kronig relations*

According to formulae (1.25a) and (1.25b), $\chi'(\omega)$ and $\chi''(\omega)$ may be derived from one function $R_{zz}(t)$. Elimination of $R_{zz}(t)$ leads to the Kramers-Kronig relations

$$\chi'(\omega) - \chi'(\infty) = \frac{1}{\pi} P\int_{-\infty}^{+\infty} \frac{\chi''(\omega_1)}{\omega_1 - \omega}\, d\omega_1 \tag{1.32}$$

and

$$\chi''(\omega) = -\frac{1}{\pi} P\int_{-\infty}^{+\infty} \frac{\chi'(\omega_1) - \chi'(\infty)}{\omega_1 - \omega}\, d\omega_1 \quad , \tag{1.33}$$

where the symbol P stands for taking the principal value of the integral. A more practical form of the Kramers-Kronig relation is

$$\chi'(\omega) - \chi'(\infty) = \frac{2}{\pi}\int_0^{\infty} \frac{\omega_1\chi''(\omega_1) - \omega\chi''(\omega)}{\omega_1^2 - \omega^2}\, d\omega_1 \quad , \tag{1.34}$$

$$\chi''(\omega) = -\frac{2\omega}{\pi}\int_0^{\infty} \frac{\chi'(\omega_1) - \chi'(\omega)}{\omega_1^2 - \omega^2}\, d\omega_1 \quad . \tag{1.35}$$

If we take $\omega = 0$ in relation (1.34), we obtain the useful relation

$$\chi'(0) - \chi'(\infty) = \frac{2}{\pi}\int_0^{\infty} \frac{\chi''(\omega)}{\omega}\, d\omega \quad , \tag{1.36}$$

which tells us that the total intensity of $\chi''(\omega)/\omega$ over the frequency range (including the negative frequency range) in which spin-spin relaxation takes place equals $\pi\chi_{ad}$ if $\chi'(\infty) = 0$.

1.3.4 *Moments of $\chi''(\omega)/\omega$*

If $\Phi(-t) = \Phi(t)$, then the reciprocal relation of (1.30),

$$\Phi(t) = \int_{-\infty}^{+\infty} d\omega e^{i\omega t}\Phi(\omega) \quad , \tag{1.37}$$

leads together with relation (1.31) to

$$\Phi(t) = \int_{-\infty}^{+\infty} d\omega e^{i\omega t}\, \frac{\chi''(\omega)}{\pi\omega} \quad . \tag{1.38}$$

The moments of $\chi''(\omega)/\omega$ can be derived from this relation by differentiation

$$<\omega^n> \equiv \frac{\int_{-\infty}^{+\infty} (\chi''(\omega)/\omega)\omega^n d\omega}{\int_{-\infty}^{+\infty} (\chi''(\omega)/\omega) d\omega} = (-i)^n \frac{\left[\frac{d^n \Phi(t)}{dt^n}\right]_{t=0}}{\Phi(0)} \qquad (1.39)$$

1.3.5 *Debye formulae*

If we consider a relaxation which takes place according to a single exponential decay

$$\Phi(t) = \{\chi(0) - \chi'(\infty)\}e^{-\frac{t}{\tau}} \quad \text{for } t > 0 \quad , \qquad (1.40)$$

then the susceptibility is given by (see relations (1.29a) and (1.29b))

$$\chi'(\omega) = \chi'(\infty) + \{\chi(0) - \chi'(\infty)\} \frac{1}{1 + \omega^2\tau^2} \qquad (1.41a)$$

and

$$\chi''(\omega) = \{\chi(0) - \chi'(\infty)\} \frac{\omega\tau}{1 + \omega^2\tau^2} \quad . \qquad (1.41b)$$

These are the formulae of Debye, which will be used frequently in this thesis. $\chi(0)$ is the value of $\chi(\omega)$ at frequencies $\omega << \tau^{-1}$, and $\chi(\infty)$ the value of $\chi(\omega)$ at frequencies $\omega >> \tau^{-1}$. $\chi'(\omega)/\chi(0)$ has been plotted versus ω on a logarithmic scale in fig. 1.1a and $\chi''(\omega)/\chi(0)$ versus ω on a double logarithmic scale in fig. 1.1b. The relaxation time τ is the inverse of the frequency for which $\chi''(\omega)/\chi(0)$ has a maximum and $\chi'(\omega)/\chi(0)$ is halfway between its initial and final value. If we plot $\chi''(\omega)/\chi(0)$ versus $\chi'(\omega)/\chi(0)$, we obtain a semicircle, symmetric around the point $\omega\tau = 1$. This so-called Cole-Cole diagram has also been used to determine the relaxation time. The variations of $\chi'(\omega)$ and $\omega\chi''(\omega)$ are called dispersion resp. absorption which names are also used for $\chi'(\omega)$ and $\chi''(\omega)$ itself.

1.4 *Thermodynamic theory*

In the theory of Casimir and Du Pré [2] for spin-lattice relaxation, the paramagnetic salt is supposed to consist of two thermodynamic systems: the spin system determining all the magnetic properties of the sample, and the lattice system describing the remaining properties. Internal equilibrium in both systems is assumed, each with a characteristic temperature T_S or T_L. Equilibrium in the whole system is established by spin-lattice interactions, by which energy is

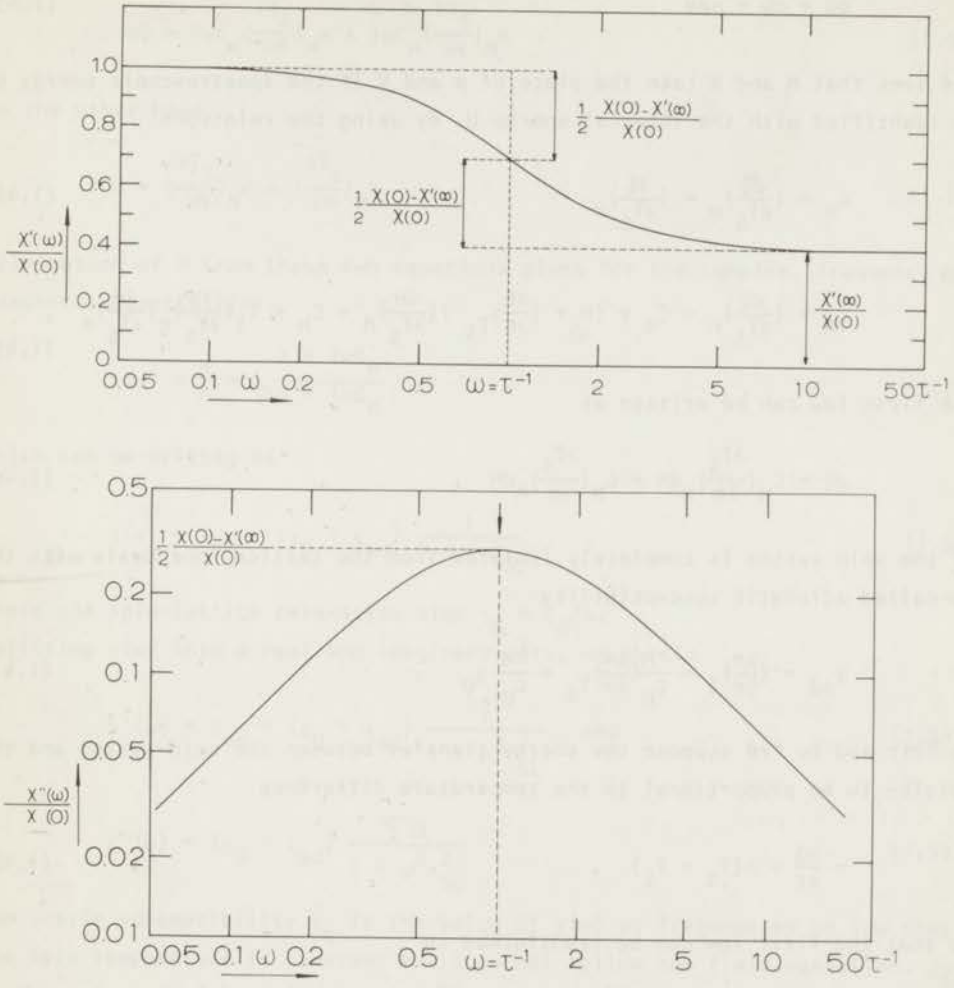

Fig. 1.1 Debye curves for $\chi'(\omega)/\chi(0)$ and $\chi''(\omega)/\chi(0)$.

transferred from the spin system to the lattice. In the simplest model, the contact between lattice and surrounding heat bath is so effective that the lattice temperature is constant. The first law of thermodynamics for the spin system reads

$$dQ = dE + MdH \ , \tag{1.42}$$

in which E is the magnetic enthalpy, called by Gorter the spectroscopic energy.

If one compares this equation with the standard form of the first law

$$dQ = dU + pdV \quad , \tag{1.43}$$

one sees that M and H take the place of p and V if the spectroscopic energy E is identified with the internal energy U. By using the relations

$$C_H = \left(\frac{dQ}{dT_S}\right)_H = \left(\frac{\partial E}{\partial T_S}\right)_H \tag{1.44}$$

and

$$C_M = \left(\frac{dQ}{dT_S}\right)_M = C_H + \left\{M + \left(\frac{\partial E}{\partial H}\right)_{T_S}\right\}\left(\frac{\partial H}{\partial T_S}\right)_M = C_H + T_S\left(\frac{\partial M}{\partial T_S}\right)_H\left(\frac{\partial H}{\partial T_S}\right)_M \quad , \tag{1.45}$$

the first law can be written as

$$dQ = C_H\left(\frac{\partial T_S}{\partial M}\right)_H dM + C_M\left(\frac{\partial T_S}{\partial H}\right)_M dH \quad . \tag{1.46}$$

If the spin system is completely isolated from the lattice, one deals with the so-called adiabatic susceptibility

$$\chi_{ad} = \left(\frac{\partial M}{\partial H}\right)_S = \frac{C_M}{C_H}\left(\frac{\partial M}{\partial H}\right)_{T_S} = \frac{C_M}{C_H}\chi_0 \quad . \tag{1.47}$$

Casimir and Du Pré suppose the energy transfer between the spin system and the lattice to be proportional to the temperature difference

$$-\frac{dQ}{dt} = \alpha(T_S - T_L) \quad , \tag{1.48}$$

so that the first law can be transformed to

$$-\alpha(T_S - T_L) = C_H\left(\frac{\partial T_S}{\partial M}\right)\frac{dM}{dt} + C_M\left(\frac{\partial T_S}{\partial H}\right)_M\frac{dH}{dt} \quad . \tag{1.49}$$

In the measuring procedure the total field consists of a constant part and a small oscillating part of some fixed frequency ω. In a linear approximation, M and T will fluctuate with the same frequency around their equilibrium values M_0 resp. T_L.

Substitution of

$$H = H_0 + \mathrm{Re}(h\, e^{i\omega t}) \quad ,$$
$$M = M_0 + \mathrm{Re}(m\, e^{i\omega t}) \quad , \text{ and}$$
$$T_S = T_L + \mathrm{Re}(\theta\, e^{i\omega t})$$

in equation (1.49) gives

$$-\alpha\Theta = i\omega C_H \left(\frac{\partial T_S}{\partial M}\right)_H m + i\omega C_M \left(\frac{\partial T_S}{\partial H}\right)_M h \quad . \tag{1.50}$$

On the other hand,

$$\Theta = \left(\frac{\partial T_S}{\partial M}\right)_H m + \left(\frac{\partial T_S}{\partial H}\right)_M h \quad . \tag{1.51}$$

Elimination of Θ from these two equations gives for the complex, frequency dependent susceptibility

$$\chi(\omega) = \frac{m}{h} = \chi_0 \frac{\alpha + i\omega C_M}{\alpha + i\omega C_H} \quad , \tag{1.52}$$

which can be written as

$$\chi(\omega) = \chi_{ad} + (\chi_0 - \chi_{ad}) \frac{1}{1 + i\omega\tau_{SL}} \quad , \tag{1.53}$$

where the spin-lattice relaxation time $\tau_{SL} = C_H/\alpha$.
Splitting $\chi(\omega)$ into a real and imaginary part, we obtain

$$\chi'(\omega) = \chi_{ad} + (\chi_0 - \chi_{ad}) \frac{1}{1 + \omega^2\tau_{SL}^2} \quad \text{and} \tag{1.54a}$$

$$\chi''(\omega) = (\chi_0 - \chi_{ad}) \frac{\omega\tau_{SL}}{1 + \omega^2\tau_{SL}^2} \quad . \tag{1.54b}$$

The static susceptibility χ_0 is the value of $\chi(\omega)$ at frequencies so low that the spin temperature is constant and does not follow the field variation. χ_{ad} is the value of $\chi(\omega)$ at frequencies where the spin system follows the field variation without exchanging energy with the lattice.

For many salts, the magnetic specific heat in a high temperature approximation can be written as $C_M = b/T^2$. For a substance obeying Curie's law $M = \frac{C}{T}H$, one finds then with the aid of (1.45)

$$C_H = C_M + \frac{CH^2}{T^2} \quad , \tag{1.55}$$

so that

$$\frac{\chi_{ad}}{\chi_0} = \frac{b}{b + CH^2} \quad . \tag{1.56}$$

For a substance obeying Curie-Weiss law

$$M = \frac{C}{T - \Theta} H \ , \quad \text{as} \quad \left(\frac{\partial M}{\partial T_S}\right)_H = -\frac{C}{(T - \Theta)^2} H \quad \text{and} \quad \left(\frac{\partial H}{\partial T_S}\right)_M = \frac{M}{C} = \frac{C}{T - \Theta} H,$$

one finds

$$C_H = C_M + CH^2 \frac{T}{(T - \Theta)^3} \ , \tag{1.57}$$

so that

$$\frac{\chi_{ad}}{\chi_0} = \frac{b}{b + CH^2 (T/T - \Theta)^3} \ . \tag{1.58}$$

The susceptibility in the case of spin-lattice relaxation is given by the Debye formulae, which implies that the spin-lattice relaxation takes place according to an exponential decay. If the spin-spin relaxation also decays exponentially, the susceptibility for the spin-spin relaxation process is given by the Debye formulae as well

$$\chi'(\omega) = \chi'_{bet} + (\chi_{ad} - \chi'_{bet}) \frac{1}{1 + \omega^2 \tau_{SS}^2} \ , \tag{1.59a}$$

$$\chi''(\omega) = (\chi_{ad} - \chi'_{bet}) \frac{\omega \tau_{SS}}{1 + \omega^2 \tau_{SS}^2} \ , \tag{1.59b}$$

in which τ_{SS} is the spin-spin relaxation time.
Combination of equations (1.54a and b) and (1.59a and b) gives

$$\chi'(\omega) = \chi'_{bet} + (\chi_{ad} - \chi'_{bet}) \frac{1}{1 + \omega^2 \tau_{SS}^2} + (\chi_0 - \chi_{ad}) \frac{1}{1 + \omega^2 \tau_{SL}^2}$$

and

$$\chi''(\omega) = (\chi_{ad} - \chi'_{bet}) \frac{\omega \tau_{SS}}{1 + \omega^2 \tau_{SS}^2} + (\chi_0 - \chi_{ad}) \frac{\omega \tau_{SL}}{1 + \omega^2 \tau_{SL}^2} \ . \tag{1.60b}$$

χ'_{bet} is the value of $\chi(\omega)$ at frequencies so high that the spin system is not in thermal equilibrium. χ'_{bet} decays via parallel field resonances in the spin system at the Larmor frequency

$$\omega_L = \frac{g \mu_B H}{\hbar}$$

and twice ω_L.
The whole has been sketched schematically in fig. 1.2.

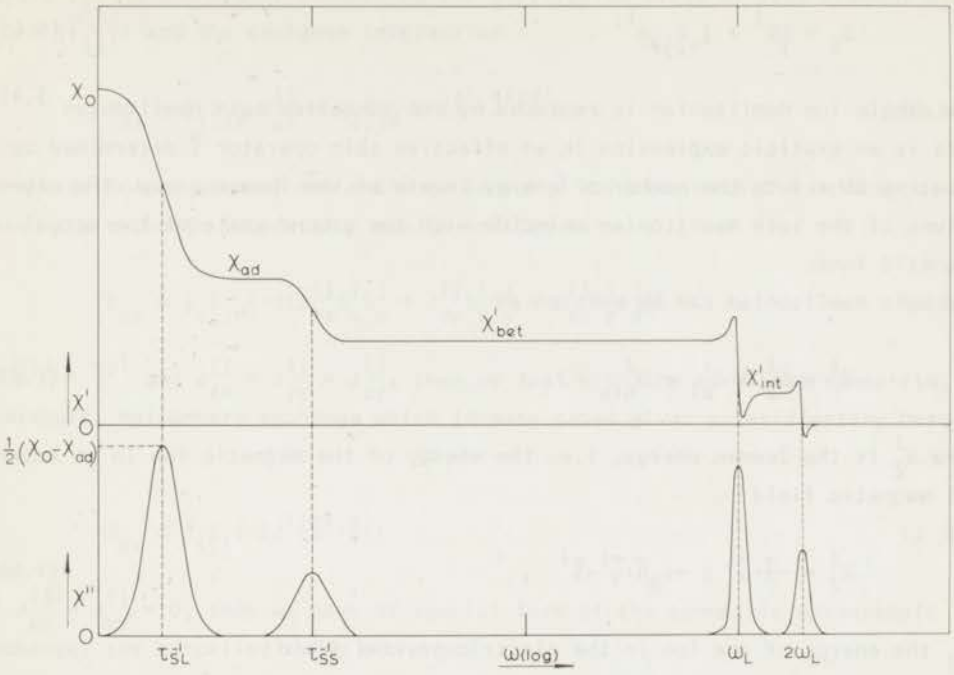

Fig. 1.2 Dispersion and absorption as a function of the frequency for some fixed field $H_z \neq 0$.

1.5 *Quantum statistical description of spin-spin relaxation*

1.5.1 *Hamiltonian of the spin system*

To describe the spin-lattice and the spin-spin relaxation in a paramagnetic crystal one tries to split its Hamiltonian into a Hamiltonian describing the spin system only, a Hamiltonian describing the lattice, and a term for the interaction between both systems,

$$H = H_S + H_L + H_{SL} \quad . \tag{1.61}$$

The subscripts S and L refer resp. to the spin and the lattice systems.

If the spin-lattice relaxation time is much greater than the spin-spin relaxation time (as is often experimentally found), then the spin system is isolated from the lattice during the spin-spin relaxation process. The Hamiltonian for the isolated spin system can be written as a sum of single ion Hamiltonians and a sum of interactions between the single ions

$$H_S = \sum_i H^i + \tfrac{1}{2} \sum_{i,j \neq} H^{ij} \quad . \tag{1.62}$$

The single ion Hamiltonian is replaced by the so-called spin Hamiltonian [3,4]. This is an explicit expression in an effective spin operator $\vec{S}$ determined by equating 2S + 1 to the number of energy levels of the lowest group. The eigenvalues of the spin Hamiltonian coincide with the ground state of the actual magnetic ions.

The spin Hamiltonian can be written as

$$H^i = H^i_Z + H^i_{el} + H^i_{hfs} \quad . \tag{1.63}$$

Here H^i_Z is the Zeeman energy, i.e. the energy of the magnetic ion in an external magnetic field

$$H^i_Z = -\vec{H} \cdot \vec{\mu}^i \equiv +\mu_B \vec{H} \cdot \overline{\overline{g}}^i \cdot \vec{S}^i \quad , \; * \tag{1.64}$$

H^i_{el} the energy of the ion in the electric crystal field

$$H^i_{el} = D^i \{ (S^i_z)^2 - \frac{1}{3} S(S+1) \} + E^i \{ (S^i_x)^2 - (S^i_y)^2 \} + \ldots \quad , \tag{1.65}$$

and H^i_{hfS} the interaction energy between the electron and nuclear spin

$$H^i_{hfS} = \vec{J}^i \cdot \overline{\overline{A}}^i \cdot \vec{S}^i \quad . \tag{1.66}$$

The interactions between the single ions are the dipole dipole interaction

$$H_{dip} = \tfrac{1}{2} \sum_{i,j \neq} H^{ij}_{dip} = \tfrac{1}{2} \mu_B^2 \sum_{i,j \neq} \frac{1}{r^3_{ij}} \{ (\overline{\overline{g}}^i \cdot \vec{S}^i) \cdot (\overline{\overline{g}}^j \cdot \vec{S}^j) - 3 \frac{(\vec{r}_{ij} \cdot \overline{\overline{g}}^i \cdot \vec{S}^i)(\vec{r}_{ij} \cdot \overline{\overline{g}}^j \cdot \vec{S}^j)}{r^2_{ij}} \} \tag{1.67}$$

---

* As definition of the Bohrmagneton we use

$$\mu_B = \frac{|e|}{2 m_e c}$$

(where $\vec{r}_{ij}$ is the vector connecting the equilibrium sites of ions i and j and $r_{ij} = |\vec{r}_{ij}|$) and the exchange interaction

$$H_{ex} = \tfrac{1}{2}\Sigma_{i,j\neq} H_{ex}^{ij} = \tfrac{1}{2}\Sigma_{i,j\neq} (-2\vec{S}^i \cdot \bar{\bar{J}}^{ij} \cdot \vec{S}^j) \quad . \tag{1.68}$$

If the principal axes of the exchange tensor $\bar{\bar{J}}$ coincide with the reference axes, the exchange interaction may be written as

$$H_{ex} = \tfrac{1}{2}\Sigma_{i,j\neq}\{-2(J_{xx}^{ij} S_x^i S_x^j + J_{yy}^{ij} S_y^i S_y^j + J_{zz}^{ij} S_z^i S_z^j)\} \quad . \tag{1.69}$$

If $\bar{\bar{J}}^{ij} = \bar{\bar{J}}^{ji}$ and $J_{xx}^{ij} = J_{yy}^{ij} = J_{zz}^{ij}$, then we deal with the so-called symmetric, isotropic, Heisenberg exchange which in many cases gives a satisfactory description:

$$H_{ex} = \tfrac{1}{2}\Sigma_{i,j} (-2J^{ij} \vec{S}^i \cdot \vec{S}^j) \quad . \tag{1.70}$$

If $J_{xx}^{ij} = J_{yy}^{ij} = 0$, then we have as special form of the symmetric anisotropic exchange, the so-called Ising exchange:

$$H_{ex} = \tfrac{1}{2}\Sigma_{i,j} (-2J^{ij} S_z^i S_z^j) \quad . \tag{1.71}$$

The summation over pairs in the exchange interaction may often be restricted to the nearest neighbours or nearest and next nearest neighbours.

1.5.2 *Decomposition of H_{dip} and H_{ex} into eigenoperators of L_Z*

The greater part of the theories on spin-spin relaxation deals with $S = \frac{1}{2}$ which according to a theorem of Kramers implies $H_{el} = 0$.
The Hamiltonian of the spin system is assumed to consist of a Zeeman term H_Z and an interaction term which is taken to be the sum of a dipole dipole interaction H_{dip} and an isotropic exchange interaction H_{ex}:

$$H = H_Z + H_{int} \equiv H_Z + H_{dip} + H_{ex} \quad . \tag{1.72}$$

For identical ions and the magnetic field applied along one of the principal axis of the g tensor (z axis), the Zeeman term can be written as

$$H_Z = -HM_z = g_z \mu_B H \Sigma_i S_z^i \quad . \tag{1.73}$$

The interaction term H_{int} is decomposed into eigenoperators of the Liouville operator L_Z corresponding to the Zeeman term H_Z, i.e. into operators A satisfying the equation

$$L_Z A \equiv \frac{1}{\hbar}[H_Z, A] = \lambda A \tag{1.74}$$

for some scalar λ.

For that purpose we write out H_{dip} and H_{ex} into $S_0^i \equiv S_z^i$ and the step up and step down operators $S_\pm^i = S_x^i \pm iS_y^i$ in the following way:

$$H_{dip} = H_{-2} + H_{-1} + H_{dip\ 0} + H_1 + H_2 \quad , \tag{1.75}$$

with

$$\begin{aligned} H_{dip\ 0} &= \tfrac{1}{2}\mu_B^2 \sum_{i,j\neq} (C_{00}^{ij} S_0^i S_0^j + C_{+-}^{ij} S_+^i S_-^j) \quad , \\ H_{\pm 1} &= \tfrac{1}{2}\mu_B^2 \sum_{i,j\neq} C_{\pm 0}^{ij} S_\pm^i S_0^j \quad , \text{ and} \\ H_{\pm 2} &= \tfrac{1}{2}\mu_B^2 \sum_{i,j\neq} C_{\pm\pm}^{ij} S_\pm^i S_\pm^j \quad . \end{aligned} \tag{1.76}$$

The C^{ij}'s are functions of the local coordinates and components of the g tensor

$$\begin{aligned} C_{00}^{ij} &= r_{ij}^{-3} g_z^2 (1 - 3\zeta_{ij}^2) \quad , \\ C_{+-}^{ij} &= \tfrac{1}{2} r_{ij}^{-3} \{g_x^2 (1 - 3\xi_{ij}^2) + g_y^2 (1 - 3\eta_{ij}^2)\} \quad , \\ C_{\pm 0}^{ij} &= -3 r_{ij}^{-3} g_z \zeta_{ij} (g_x \xi_{ij} \mp i g_y \eta_{ij}), \text{ and} \\ C_{\pm\pm}^{ij} &= -\tfrac{1}{4} r_{ij}^{-3} \{g_x^2 - g_y^2 - 3(g_x \xi_{ij} \mp i g_y \eta_{ij})\} \quad , \end{aligned} \tag{1.77}$$

in which ξ_{ij}, η_{ij} and ζ_{ij} are the direction cosines.

H_{ex} is written as

$$H_{ex} = \tfrac{1}{2} \sum_{i,j\neq} -2J^{ij} (S_z^i S_z^j + S_+^i S_-^j) \quad . \tag{1.78}$$

Now it is easy to see that

$$L_Z (H_{dip\ 0} + H_{ex}) = 0$$

and

$$L_Z H_k = k \frac{g\mu_B H}{\hbar} H_k \equiv k\omega_L H_k ; \; k = \pm 1, \pm 2. \tag{1.79}$$

$\omega_L \equiv g\mu_B H/\hbar$ is the Larmor frequency.

That part of H_{int} which commutes with H_Z is called the secular part of the interaction, and the remainder the non secular part. The Hamiltonian may thus be written as

$$H = H_Z + H_{sec} + H_{n\,sec} \quad . \tag{1.80}$$

1.5.3 *A formal expression for the relaxation function in a high temperature approximation*

The starting point in theories on spin-spin relaxation is the relaxation function, mostly in a high temperature approximation. Therefore one considers the response of the isolated spin system to a disturbance in the magnetic field applied along the z axis:

$$H(t) = \begin{cases} H + h & \text{for } t < 0 \\ H & \text{for } t > 0 \end{cases}$$

At time $t < 0$, the equilibrium state is described by the stationary density operator

$$\rho(-\infty) = \frac{e^{-\beta H(H + h)}}{\mathrm{Tr}\, e^{-\beta H(H + h)}} \quad , \tag{1.81}$$

in which $H(H + h)$ is the Hamiltonian at time $t < 0$,

$$H(H + h) = -(H + h)M_z + H_{int} \quad , \tag{1.82}$$

and

$$\beta = \frac{1}{kT} \quad .$$

The mean value of the magnetization for $t < 0$ is given by

$$\overline{M_z(t)} = \mathrm{Tr}\, \rho(-\infty) M_z \quad . \tag{1.83}$$

After the disturbance in the magnetic field, $\overline{M_z(t)}$ is given by

$$\overline{M_z(t)} = \mathrm{Tr}\, \rho(-\infty) M_z(t) \quad , \tag{1.84}$$

in which $M_z(t)$ is the Heisenberg operator of M_z,

$$M_z(t) = e^{\frac{i}{\hbar}H(H)t} M_z e^{-\frac{1}{\hbar}H(H)t} \equiv e^{iL(H)t} M_z \quad , \tag{1.85}$$

and $H(H)$ the Hamiltonian for $t > 0$

$$H(H) = -HM_z + H_{int} \quad . \tag{1.86}$$

$L(H)$ is the corresponding Liouville operator.
In a linear approximation in h, and a high temperature approximation, one finds

$$\overline{M_z(t)} = \beta \begin{cases} h\langle\langle M_z^2 \rangle\rangle + H\langle\langle M_z^2 \rangle\rangle & \text{for } t < 0, \\ h\langle\langle M_z M_z(t) + H\langle\langle M_z^2 \rangle\rangle & \text{for } t > 0, \end{cases} \tag{1.87}$$

where we have used the notation

$$\langle\langle A \rangle\rangle = \frac{\mathrm{Tr}\ A}{\mathrm{Tr}\ 1} \quad .$$

As

$$\langle\langle M_z^2 \rangle\rangle = g_z^2 \mu_B^2 \sum_i \langle\langle (S_z^i)^2 \rangle\rangle = N g_z^2 \mu_B^2 \frac{1}{3} S(S+1) \quad , \tag{1.88}$$

we have for the mean value of the magnetization for $t < 0$,

$$\overline{M_z(t)} = N \frac{g_z^2 \mu_B^2 S(S+1)}{3kT} (H + h) \quad , \tag{1.89}$$

by which Curie's constant is determined.
Defining for $t > 0$ the relaxation function by

$$\phi_{zz}(t) = \frac{1}{h} \{\overline{M_z(t)} - \beta H\langle\langle M_z^2 \rangle\rangle\} \quad , \tag{1.90}$$

it follows that

$$\phi_{zz}(t) = \beta\langle\langle M_z M_z(t) \rangle\rangle \quad . \tag{1.91}$$

1.5.4 *A formal expression for the relaxation time in a high temperature approximation*

A formal expression for the spin-spin relaxation time, characterizing the

approach to equilibrium of the isolated spin system after a disturbance in the external magnetic field, has been derived by several authors in different ways [5,6,7,8,9]. One usually starts from a Hamiltonian of the spin system consisting of a Zeeman term H_Z, a dipole dipole term H_{dip}, and an isotropic Heisenberg term H_{ex}:

$$H = H_Z + H_{dip} + H_{ex} = H_Z + H_{sec} + H_{n\,sec} \quad .$$

In analyzing the relaxation function, Mazur and Terwiel [8] distinguished two limiting cases for which the Hamiltonian can be separated into a large unperturbed part and a small perturbation. The first, which they call the weak coupling case, is that for which the secular part of the interaction is much larger than the non secular part. The Zeeman term and the secular part of the interaction constitute the large unperturbed Hamiltonian and the non secular part the small perturbation. The results are valid for all magnetic fields including zero field. The second, which they call the strong coupling case, is that for which the secular part of the interaction is comparable to or weaker than the non secular part. In that case the sum of the Zeeman term and the secular part of the interaction constitute only for a strong external magnetic field a large unperturbed Hamiltonian, and the non secular part can be considered as a small perturbation. The results are thus restricted to large fields.

Weak coupling theory

Using Zwanzig's [10] elegant projection operator technique, M and T derive an exact integral equation for the time derivative of the relaxation function, assuming that after the disturbance in the magnetic field the spin system reaches a new thermodynamic equilibrium for large t.
The relaxation function which they consider is the function defined by (1.90) which in a high temperature approximation is given by

$$\phi_{zz}(t) = \beta \langle\langle M_z M_z(t) \rangle\rangle \quad . \tag{1.91}$$

The limiting value of $\phi_{zz}(t)$ in the limit for large t is different from zero, and thermodynamically one can show that

$$\phi_{zz}(\infty) \equiv \lim_{t\to\infty} \phi_{zz}(t) = \chi_0 - \chi_{ad} = \frac{H^2}{H^2 + \frac{1}{2}H_i^2} \quad , \tag{1.92}$$

where

$$\tfrac{1}{2}H_i^2 \equiv \frac{b_{int}}{C} \equiv \frac{\langle\langle H_{int}^2 \rangle\rangle}{\langle\langle M_z^2 \rangle\rangle} \equiv \frac{\langle\langle H_{int}^2 \rangle\rangle}{kC} \quad . \tag{1.93}$$

The non vanishing part of the relaxation function is taken into account by defining

$$\beta\Omega(t) \equiv \phi_{zz}(t) - i\{\beta^{-1}\phi_{zz}(\infty)\} \equiv \beta\langle\langle \mu\mu(t) \rangle\rangle \quad . \tag{1.94}$$

With the aid of the formalism of Zwanzig, M & T derive the time derivative of $\Omega(t)$

$$\frac{\partial\Omega(t)}{\partial t} = -\int_0^t d\tau G(\tau)\Omega(t - \tau) \quad , \tag{1.95}$$

where the kernel or memory function

$$G(\tau) = \frac{\langle\langle \mu L_{n\ sec} e^{i(L_Z + L_{sec})\tau + i(1 - P_\mu)L_{n\ sec}\tau} L_{n\ sec}\mu \rangle\rangle}{\langle\langle \mu^2 \rangle\rangle} \quad . \tag{1.96}$$

L_Z, L_{sec}, and $L_{n\ sec}$ are the Liouville operators corresponding to H_Z, H_{sec}, and $H_{n\ sec}$ resp. P_μ is a projection operator defined by

$$P_\mu O(t) = \mu \frac{\langle\langle \mu O(t) \rangle\rangle}{\langle\langle \mu^2 \rangle\rangle} \quad , \tag{1.97}$$

with $O(t)$ an arbitrary Heisenberg operator.

In the weak coupling case, the memory function can be written as a sum of damped oscillations

$$G(t) = \frac{H^2 + \tfrac{1}{2}H_{i\ sec}^2}{\tfrac{1}{2}H_{i\ sec}^2} \sum_{k=\pm1,\pm2} e^{ik\omega_L t} G_k(t) \quad , \tag{1.98}$$

with

$$G_k(t) = \frac{g^2\mu_B^2}{\hbar^2} k^2 \frac{\langle\langle H_{-k} e^{iL_{sec}t} H_k \rangle\rangle}{\langle\langle M_z^2 \rangle\rangle} \quad . \tag{1.99}$$

The Fourier transform of the kernel or memory function (called by Verbeek [13] memory spectrum) is given by

$$G(\omega) = \frac{H^2 + \tfrac{1}{2}H_{i\ sec}^2}{\tfrac{1}{2}H_{i\ sec}^2} \sum_{k=\pm1,\pm2} G_k(\omega - k\omega_L) \quad . \tag{1.100}$$

The memory spectrum consists of four lines at frequencies $k\omega_L$, $k = \pm 1, \pm 2$, whose shape does not change if the field is varied. The lines have an intensity

$$\langle\omega^0\rangle_k = \frac{g^2\mu_B^2}{\hbar^2} k^2 \frac{\langle\langle H_k H_{-k}\rangle\rangle}{\langle\langle M_z^2\rangle\rangle} \quad , \tag{1.101}$$

and a second moment

$$\langle\omega^2\rangle_k = \frac{1}{\hbar^2} \frac{\langle\langle [H_{sec}, H_k][H_{-k}, H_{sec}]\rangle\rangle}{\langle\langle H_k H_{-k}\rangle\rangle} \quad . \tag{1.102}$$

The lines are multiplied by a field dependent factor

$$\frac{H^2 + \frac{1}{2}H_{i\ sec}^2}{\frac{1}{2}H_{i\ sec}^2} \quad .$$

The spin-spin relaxation rate τ^{-1} is given by

$$\frac{1}{\tau} = \int_0^\infty dt G(t) = \pi[G(\omega)]_{\omega=0} = \pi \frac{H^2 + \frac{1}{2}H_{i\ sec}^2}{\frac{1}{2}H_{i\ sec}^2} \sum_{k=\pm 1,\pm 2} [G_k(\omega - k\omega_L)]_{\omega=0} \tag{1.103}$$

If a Gaussian line shape is assumed for $G_k(\omega - k\omega_L)$, determined by the moments of zero and second order,

$$G_k(\omega - k\omega_L) = \langle\omega^0\rangle_k \frac{1}{\{2\pi\langle\omega^2\rangle_k\}^{\frac{1}{2}}} \exp\{-\tfrac{1}{2} \frac{(\omega - k\omega_L)^2}{\langle\omega^2\rangle_k}\} \quad , \tag{1.104}$$

then

$$\frac{1}{\tau} = \frac{H^2 + \frac{1}{2}H_{i\ sec}^2}{\frac{1}{2}H_{i\ sec}^2} \left(\frac{1}{\tau_1} + \frac{1}{\tau_2}\right) \quad , \tag{1.105}$$

with

$$\frac{1}{\tau_1} = 2\pi \frac{\langle\langle H_1 H_{-1}\rangle\rangle}{\hbar^2 \frac{1}{3} S(S+1)} \frac{1}{\{2\pi\langle\omega^2\rangle_1\}^{\frac{1}{2}}} \exp\{-\tfrac{1}{2}(\frac{g\mu_B H}{\hbar})^2 \frac{1}{\langle\omega^2\rangle_1}\} \quad , \tag{1.106}$$

$$\frac{1}{\tau_2} = 8\pi \frac{\langle\langle H_2 H_{-2}\rangle\rangle}{\hbar^2 \frac{1}{3} S(S+1)} \frac{1}{\{2\pi\langle\omega^2\rangle_1\}^{\frac{1}{2}}} \exp\{-\tfrac{1}{2}(\frac{2g\mu_B H}{\hbar})^2 \frac{1}{\langle\omega^2\rangle_2}\} \quad , \tag{1.107}$$

and

$$\langle\omega^2\rangle_{1,2} = \frac{1}{\hbar^2} \frac{\langle\langle [H_{sec}, H_{1,2}][H_{-1,-2}, H_{sec}]\rangle\rangle}{\langle\langle H_{1,2}, H_{-1,-2}\rangle\rangle} \quad . \tag{1.108}$$

Strong coupling theory

In the case of strong coupling, the time behaviour of $\Omega(t)$ is investigated by M & T on the basis of an analysis of the Fourier transform of $\Omega(t)$, related to the absorption by

$$\beta\Omega(t) = \frac{\chi''(\omega)}{\pi\omega} \quad . \tag{1.31}$$

For sufficiently large fields, the spectrum of $\Omega(t)$ (called absorption spectrum) consists of five lines centered around 0, $\pm\omega_L$, and $\pm 2\omega_L$.
$\Omega(t)$ itself is given by

$$g(t,H) \equiv \frac{\Omega(t)}{\Omega(0)} = \sum_{k=0,\pm1,\pm2} g_{kk}(t,H) \quad , \tag{1.109}$$

with

$$g_{kk}(t,H) = \frac{\langle\langle H_{-k} e^{iLt} H_k \rangle\rangle}{\langle\langle H_{int}^2 \rangle\rangle} \quad . \tag{1.110}$$

The Liouville operator L in the exponent is the sum of L_Z and L_{int}. For $k \neq 0$, M & T assume that L may be replaced by $L_Z + c_k L_{sec}$, where c_k is a real constant not only of the order unity, but exactly equal to 1, which has been later proven by Verbeek and independently by Terwiel. Thus it is assumed that the real interaction may be replaced by the secular interaction. In that case $g(t,H)$ consists of damped oscillations given by

$$g_{kk}(t,H) = \frac{\langle\langle H_{-k} H_k \rangle\rangle}{\langle\langle H_{int}^2 \rangle\rangle} D_k(t,c_k) e^{ik\omega_L t} \quad , \tag{1.111}$$

where

$D_k(t,c_k)$ is a damping function:

$$D_k(t,c_k) = \frac{\langle\langle H_{-k} e^{iL_{sec}t} H_k \rangle\rangle}{\langle\langle H_k H_{-k} \rangle\rangle} \quad . \tag{Cf. 1.99}$$

$g_{00}(t,H)$ satisfies a similar integral equation as in the weak coupling case (equation 1.95). For sufficiently large fields, the kernel of this integral equation $G^0(t,H)$ consists of four components.

$$G^0(t,H) = \sum_{k=\pm1,\pm2} G^0_{kk}(t,H) \quad , \tag{1.112}$$

with

$$G^0_{kk}(t,H) = \frac{\langle\langle H_{sec} L_{-k} e^{iLt} L_k H_{sec} \rangle\rangle}{\langle\langle H^2_{sec} \rangle\rangle} \quad . \tag{1.113}$$

If the Liouville operator in the exponent is replaced again by $L_Z + d_k L_{sec}$, then the relaxation rate, analogous to the case of weak coupling, is given by

$$\frac{1}{\tau} = \pi [G^0(\omega,H)]_{\omega=0} = \pi \frac{H^2}{\frac{1}{2}H^2_{i\ sec}} \sum_{k=\pm1,\pm2} \frac{g^2\mu_B^2}{\hbar^2} \frac{k^2}{d_k^2} [D_k(\omega - k\omega_L, d_k)]_{\omega=0} \quad . \tag{1.114}$$

M & T show that τ is much larger than the decay time of the damped oscillations. The damped oscillations describe the parallel field resonances and $G^0(t,H)$ the long time relaxation behaviour. If a Gaussian line shape is assumed for $D_k(\omega - k\omega_L, d_k)$, determined by the moments of zero and second order, then

$$\frac{1}{\tau} = \frac{H^2}{\frac{1}{2}H^2_{i\ sec}} \left(\frac{1}{\tau_1} + \frac{1}{\tau_2}\right) \quad , \tag{1.115}$$

with

$$\frac{1}{\tau_1} = 2\pi \frac{1}{d_1^3} \frac{\langle\langle H_1 H_{-1} \rangle\rangle}{\hbar^2 \frac{1}{3} S(S+1)} \frac{1}{\{2\pi \langle\omega^2\rangle_1\}^{\frac{1}{2}}} \exp\left\{-\tfrac{1}{2}\left(\frac{g\mu_B H}{\hbar}\right)^2 \frac{1}{d_1^2 \langle\omega^2\rangle_1}\right\} \quad , \tag{1.116}$$

$$\frac{1}{\tau_2} = 8\pi \frac{1}{d_2^3} \frac{\langle\langle H_2 H_{-2} \rangle\rangle}{\hbar^2 \frac{1}{3} S(S+1)} \frac{1}{\{2\pi \langle\omega^2\rangle_2\}^{\frac{1}{2}}} \exp\left\{-\tfrac{1}{2}\left(\frac{2g\mu_B H}{\hbar}\right)^2 \frac{1}{d_2^2 \langle\omega^2\rangle_2}\right\} \quad , \tag{1.117}$$

and $\langle\omega^2\rangle_{1,2}$ given by equation (1.108).

The result of Mazur and Terwiel in the weak coupling case is the same as that found by Hartman and Anderson, Tjon and Sauermann but differs by the factor $(H^2 + \frac{1}{2}H^2_{i\ sec})/(\frac{1}{2}H^2_{i\ sec})$ from Caspers' result. Therefore, $\tau_1^{-1} + \tau_2^{-1}$ is sometimes abbreviated as τ_C^{-1}.

1.5.5 *Expressions for* $\langle\langle H_0^2 \rangle\rangle$, $\langle\langle H_1 H_{-1} \rangle\rangle$, $\langle\langle H_2 H_{-2} \rangle\rangle$, $\langle\langle H^2_{int} \rangle\rangle$, $\langle\langle [H_0,H_1][H_{-1},H_0] \rangle\rangle$ *and* $\langle\langle [H_0,H_2][H_{-2},H_0] \rangle\rangle$.

If we assume that the Fourier transform of the kernel or memory function consists of Gaussian lines, the relaxation time is given by (1.106) and (1.107) in the case of weak coupling and by (1.116) and (1.117) in the strong coupling case. For the calculation of the relaxation time we need explicit expressions for $\langle\langle H_1 H_{-1} \rangle\rangle$, $\langle\langle H_2 H_{-2} \rangle\rangle$, $\langle\langle [H_0,H_1][H_{-1},H_0] \rangle\rangle$, and $\langle\langle [H_0,H_2][H_{-2},H_0] \rangle\rangle$ in terms of the local coordinates of the crystal lattice and the components of the g tensor. For the calculation of b/C (cf. 1.93) we need an explicit expression for

$\langle\langle H_0^2 \rangle\rangle$. The expressions have been evaluated for an interaction consisting of dipole dipole interaction and isotropic Heisenberg exchange interaction. The results are

$$\langle\langle H_0^2 \rangle\rangle = \frac{1}{18}\mu_B^4 S^2(S+1)^2 \sum_{i,j\neq} \{(c_{00}^{ij})^2 + 2(c_{+-}^{ij})^2\} ,$$

$$\langle\langle H_1 H_{-1} \rangle\rangle = \frac{1}{18}\mu_B^4 S^2(S+1)^2 \sum_{i,j\neq} |c_{+0}^{ij}|^2 ,$$

$$\langle\langle H_2 H_{-2} \rangle\rangle = \frac{2}{9}\mu_B^4 S^2(S+1)^2 \sum_{i,j\neq} |c_{++}^{ij}|^2 ,$$

$$\langle\langle H_{int}^2 \rangle\rangle = \langle\langle H_0^2 \rangle\rangle + 2\langle\langle H_1 H_{-1} \rangle\rangle + 2\langle\langle H_2 H_{-2} \rangle\rangle , \text{ and}$$

$$\langle\langle [H_0, H_1][H_{-1}, H_0] \rangle\rangle = \frac{1}{9}\mu_B^8 S^2(S+1)^2 \times$$

$$\times \Bigg(\frac{2}{3}S(S+1) \sum_{i,j,l\neq} \Big(|c_{+0}^{ij}|^2 \{(c_{00}^{il})^2 + 12(c_{+-}^{il})^2\}$$

$$+ 8|c_{+0}^{ij}|^2 c_{+-}^{il} c_{+-}^{jl}$$

$$+ (c_{00}^{ij}c_{00}^{il} - 2c_{00}^{ij}c_{+-}^{il} + 4c_{+-}^{ij}c_{+-}^{il})(c_{+0}^{ij}c_{-0}^{il} + c_{-0}^{ij}c_{+0}^{il})$$

$$-2(c_{00}^{ij}c_{+-}^{ij} + c_{00}^{ij}c_{+-}^{il} + 2(c_{+-}^{ij})^2 + 2c_{+-}^{ij}c_{+-}^{il})(c_{+0}^{il}c_{-0}^{jl} + c_{-0}^{il}c_{+0}^{jl}) \Big)$$

$$+ \frac{2}{5} \sum_{i,j\neq} \Big(|c_{+0}^{ij}|^2 \{(3S(S+1) - 1)(c_{00}^{ij})^2 - 2(2S+1) + 1)c_{00}^{ij}c_{+-}^{ij}$$

$$+ 10(2S(S+1) - 1)(c_{+-}^{ij})^2\} \Big) \Bigg)$$

$$\langle\langle [H_0, H_2][H_{-2}, H_0] \rangle\rangle = \frac{1}{9}\mu_B^8 S^2(S+1)^2 \times$$

$$\times \Bigg(\frac{4}{3}S(S+1) \sum_{i,j,l\neq} \Big(|c_{++}^{ij}|^2 \{(c_{00}^{il})^2 + (c_{+-}^{il})^2\}$$

$$+ |c_{++}^{ij}|^2 c_{00}^{il} c_{00}^{jl}$$

$$+ \tfrac{1}{2}c_{+-}^{ij}c_{+-}^{il}(c_{++}^{ij}c_{--}^{il} + c_{--}^{ij}c_{++}^{il})$$

$$- (c_{00}^{ij}c_{+-}^{ij} + c_{00}^{jl}c_{+-}^{ij})(c_{++}^{il}c_{--}^{jl} + c_{--}^{il}c_{++}^{jl}) \Big)$$

$$+ \frac{1}{45}(4S(S+1) - 3) \sum_{i,j\neq} \Big(|c_{++}^{ij}|^2 \{(c_{00}^{ij})^2 + 2(c_{+-}^{ij})^2\} \Big) \Bigg) . \quad (1.118)$$

The C^{ij}'s have been defined in section 1.4.2 with one modification:

$$H_0 \equiv H_{dip\ 0} + H_{ex} = \tfrac{1}{2}\mu_B^2 \sum_{i,j\neq} (C_{00}^{ij} S_0^i S_0^j + C_{+-}^{ij} S_+^i S_-^j) \quad ,$$

with

$$C_{00}^{ij} = r_{ij}^{-3} g_z^2 (1 - 3\zeta_{ij}^2) - 2 \frac{J^{ij}}{\mu_B^2} \quad ,$$

and

$$C_{+-}^{ij} = \tfrac{1}{2} r_{ij}^{-3} \{g_x^2 (1 - 3\xi_{ij}^2) + g_y^2 (1 - 3\eta_{ij}^2)\} - 2 \frac{J^{ij}}{\mu_B^2} \quad . \tag{1.119}$$

The summation sign $\sum_{i,j,l\neq}$ means a summation over the three mutually different indices i, j, and l.

The results are written in a form suitable for a computer calculation. Our results are the same as evaluated by Grambow* [11] for an effective spin 1/2 and pure dipole dipole interaction. The results of Caspers for an isotropic g value differ slightly from those of Strombotne and Hahn [12] and both differ in some terms from our results.

In the evaluation of the traces, extensive use has been made of the following expressions for the trace of the product of two, three, and four spin operators:

$$\begin{aligned}
&\langle\langle S_\alpha S_\beta \rangle\rangle = 0 && \text{unless } \alpha + \beta = 0, \text{ where } z \equiv 0,\\
&\langle\langle S_\alpha S_\beta S_\gamma \rangle\rangle = 0 && \text{unless } \alpha + \beta + \gamma = 0,\\
&\langle\langle S_\alpha S_\beta S_\gamma S_\delta \rangle\rangle = 0 && \text{unless } \alpha + \beta + \gamma + \delta = 0,\\
&\langle\langle S_z^2 \rangle\rangle = \frac{1}{3} S(S+1),\\
&\langle\langle S_+ S_- \rangle\rangle = \frac{2}{3} S(S+1),\\
&\langle\langle S_z S_+ S_- \rangle\rangle = -\langle\langle S_z S_- S_+ \rangle\rangle = \frac{1}{3} S(S+1),\\
&\langle\langle S_z^4 \rangle\rangle = \frac{1}{15} S(S+1)\{3S(S+1) - 1\},\\
&\langle\langle S_z^2 S_+ S_- \rangle\rangle = \frac{1}{15} S(S+1)\{2S(S+1) + 1\},\\
&\langle\langle S_z S_+ S_z S_- \rangle\rangle = \frac{2}{15} S(S+1)\{S(S+1) - 2\},\\
&\langle\langle S_+ S_- S_+ S_- \rangle\rangle = \frac{4}{15} S(S+1)\{2S(S+1) + 1\}.
\end{aligned} \tag{1.120}$$

* In formula (22) on page 256 of Grambow's paper, a factor 2 is missing, in formula (25) on page 257 in the first line $R_1^{jk'}$ should be replaced by $D^{jk'}$.

References

1) Van Vleck, J.H., The Theory of Electric and Magnetic Susceptibilities, Oxford University Press (1932).
2) Casimir, H.B.G. and Du Pré, F.K., Physica 5 (1938) 507.
3) Abragam, A. and Pryce, M.H.L., Proc. Roy. Soc. (London) A205 (1951) 135.
4) Bleaney, B. and Stevens, K.W.H., Repts. Progr. Phys. 16 (1953) 108.
5) Caspers, W.J., Physica 25 (1959) 43, 645 26 (1960) 778, 809.
   Caspers, W.J., Theory of Spin Relaxation, Interscience Publ., New York (1964).
6) Hartman, S.R. and Anderson, A.G., Proc. 11th Colloque Ampère, Eindhoven (1962) 157.
   Hartman, S.R., Phys. Rev. 133 (1964) A17.
7) Tjon, J.A., Physica 30 (1964) 1, 1341.
8) Terwiel, R.H. and Mazur, P., Physica 32 (1966) 1813.
   Mazur, P. and Terwiel, R.H., Physica 36 (1967) 289.
9) Sauermann, G., Physica 32 (1966) 2017.
10) Zwanzig, R., Lectures in Theoretical Physics, Vol. III, 106, Interscience Publ., New York (1961).
11) Grambow, I., Z. Physik 257 (1972) 245.
12) Strombotne, R.L. and Hahn, E.L., Phys. Rev. 133 (1964) A1616.
13) Verbeek, P.W., thesis Leiden (1973).

C H A P T E R 2

THE TWIN T BRIDGE FOR MEASURING THE COMPLEX SUSCEPTIBILITY BETWEEN 100 kHz AND 30 MHz

Synopsis

Both components of the complex susceptibility, $\chi = \chi' - j\chi''$ can be measured with the aid of a twin T circuit.

By means of frequency modulation of the signal generator, and phase sensitive detection of the AM demodulated output signal, the generator is locked on the minimum of the twin T bridge, allowing continuous registration of signals proportional to χ' and χ'' as a function of the external magnetic field parallel to the r.f. field.

2.1 *Introduction*

The block diagram of the experimental set-up is given in fig. 2.01.

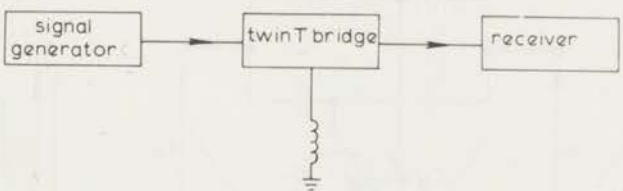

Fig. 2.01 Block diagram of the experimental set-up.

The twin T bridge is a modified General Radio, type 821-A. The generator is a General Radio, model 1003, and the receiver a modified Rhode & Schwartz selective microvoltmeter, type USVH. The twin T bridge forms a notch filter; the attenuation curve in the vicinity of the bridge minimum is symmetric, and a linear function of the frequency (fig. 2.02). The twin T circuit itself is given in fig. 2.03.

The measuring coil L, with a parallel condensor C, forms one branch of the bridge. If the paramagnetic sample with susceptibility $\chi = \chi' - j\chi''$ is

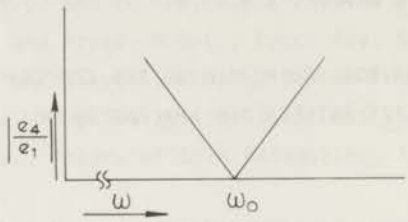

Fig. 2.02 Attenuation curve of the twin T bridge in the vicinity of the bridge minimum. e_1 and e_4 are resp. the input and output voltage, ω_0 is the frequency of the completely balanced bridge.

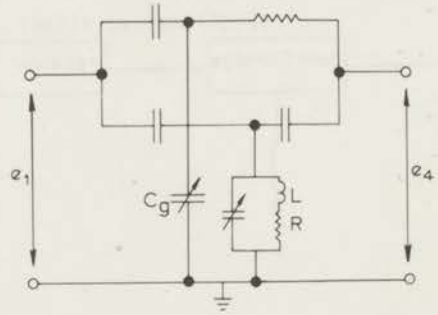

Fig. 2.03 Twin T circuit.

inserted into the coil, with original impedance $Z = R + j\omega L$, the impedance will change to

$$Z_1 = R_1 + j\omega L_1 = R(1 + 4\pi qQ\chi'') + j\omega L(1 + 4\pi q\chi') ,$$

where q denotes the filling factor and Q the quality factor of the coil: $Q = (\omega L/R)$.

From this expression one can see that the change of the inductance of the coil is proportional to χ', and the change of the series resistance of the coil is proportional to χ''. Starting from balanced bridge conditions, Verstelle [1] has given an expression for the output voltage of the bridge due to a small change of L, R and ω.

If we change only ω, and leave L and R unchanged, we obtain curve a of fig. 2.04. If L and R are changed, due to the insertion of the paramagnetic sample into the measuring coil, the output voltage will vary according to curve b of fig. 2.04.

Verstelle has shown that the change in frequency of the bridge minimum and the change in amplitude of the minimum are proportional to χ' and χ'' resp.

If one would try to lock the generator frequency onto the minimum of the completely balanced bridge by means of frequency modulation (FM) (curve a of fig. 2.04), there would be no central frequency component or carrier left in the output voltage of the bridge. To overcome this problem, we disturb the balance of the bridge a little by changing C_g, giving curve c of fig. 2.04. There is now always a carrier in the output signal of the bridge, so we can use this carrier to lock the receiver onto this incoming signal too. In section 2 we will show that the frequency difference between the two bridge minima is still proportional to χ', and the difference in output voltage to χ''.

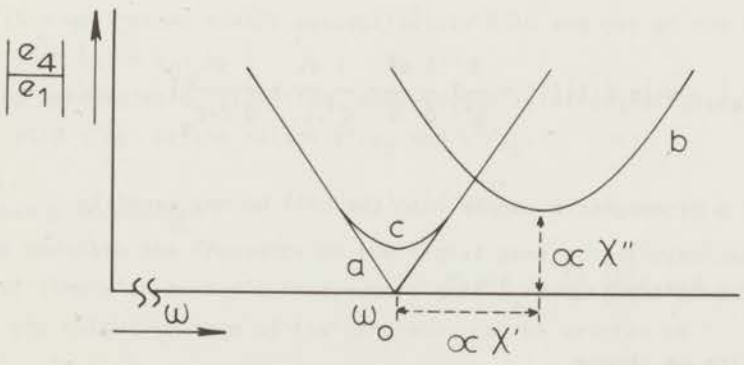

Fig. 2.04 Output voltage of the bridge, starting from balanced bridge conditions:

a. due to a small change of ω,

b. due to the insertion of the paramagnetic sample,

c. due to a small change of C_g.

2.2 *Analysis of the twin T bridge*

For the analysis of the twin T bridge we refer to Verstelle loc.cit. and to fig. 2.03. Starting from a balanced bridge, the output voltage of the bridge e_4 due to a small change of L, R, ω, and C_g is given by

$$e_4 = -e_1 F[2(1 + \frac{1}{Q^2})\frac{d\omega}{\omega_0} + \frac{dL}{L} + \frac{1}{Q^2}\frac{dR}{R} + \frac{1}{Q^2}\frac{dC_g}{C+C_g} +$$

$$+ j(\frac{2}{Q}\frac{d\omega}{\omega_0} + \frac{1}{Q}\frac{dL}{L} - \frac{1}{Q}\frac{dR}{R} + \frac{1}{Q}\frac{dC_g}{C+C_g})] \,, \qquad (2.1)$$

where e_1 is the input voltage, F is a complex factor which is eliminated in the calibration, $Q = (\omega_0 L/R)$, and ω_0 is the frequency of the balanced bridge.

By differentiation of the expression for $|e_4|$ with respect to $d\omega/\omega_0$, we find for the relative frequency variation of the bridge minimum as a function of dL/L, dR/R, and $dC_g/(C+C_g)$:

$$(\frac{d\omega}{\omega_0})_{min} = -\frac{(1 + \frac{2}{Q^2})\frac{dL}{L} + \frac{1}{Q^4}\frac{dR}{R} + (2 + \frac{1}{Q})\frac{1}{Q^2}\frac{dC_g}{C+C_g}}{2[(1 + \frac{1}{Q^2})^2 + \frac{1}{Q^2}]} \,,$$

and for the change in the amplitude of the bridge minimum:

$$|e_4|_{min} = |e_1||F|[(1 + \frac{2}{Q^2})\frac{1}{Q}\frac{dR}{R} - \frac{1}{Q^3}\frac{dL}{L} + \frac{1}{Q}\frac{dC_g}{C+C_g}] \,.$$

If we insert a paramagnetic sample into the coil we may identify

$$\frac{dL}{L} \equiv 4\pi q\chi' \,, \quad \frac{1}{Q}\frac{dR}{R} \equiv 4\pi q\chi'' \,,$$

and in practice we choose

$$\frac{1}{Q}\frac{dC_g}{C+C_g}$$

of the same order of magnitude as $4\pi q\chi''$ in order to stay well within the linearity region of the bridge.

As Q is at least 20 (typical value 50) we have within 1%:

$$\left(\frac{d\omega}{\omega_0}\right)_{min} = -2\pi q\chi' + \frac{1}{Q}\frac{dC_g}{C+C_g} \quad ,$$

$$|e_4|_{min} = |e_1||F|\left[4\pi q\chi'' + \frac{1}{Q}\frac{dC_g}{C+C_g}\right] \quad .$$

During the measurements $\frac{1}{Q}\frac{dC_g}{C+C_g}$ remains unchanged, so we have

$$\Delta\chi' = -\frac{1}{2\pi q}\frac{\Delta\omega}{\omega_0} \quad , \text{ and}$$

$$\Delta\chi'' = \frac{1}{2\pi q}\frac{1}{2|e_1||F|}\Delta|e_4|_{min} \quad .$$

A calibration is required to eliminate the factor $2|e_1||F|$. Starting from a completely balanced bridge, the output voltage is measured as a function of $d\omega$ (with $dL = 0$, $dR = 0$ and $dC_g = 0$).
This gives

$$|e_4|_{cal} = 2|e_1||F|\left(\frac{d\omega}{\omega_0}\right)_{cal} \quad .$$

The only unknown factor in the equations of $\Delta\chi'$ and $\Delta\chi''$ is still the filling factor q. This may be determined at low frequencies and zero field by moving a sample with a well-known static susceptibility into and out of the measuring coil, for then $\Delta\chi' = \chi_0$.
In studying paramagnetic relaxation, however, it is often sufficient to determine the ratio χ''/χ' or the ratios χ'/χ_0 and χ''/χ_0.

2.3 *Frequency modulation*

If we modulate the frequency of the signal generator sinusoidally as a function of time with an audio frequency signal ω_m around the unmodulated value ω_c, the output voltage of the generator can be written as

$$E(t) = A\cos\left(\omega_c t + \frac{\Delta\omega}{\omega_m}\sin\omega_m t\right),$$

with $\frac{\Delta\omega}{\omega_m} = \beta$, the modulation index.

Using the trigonometric formula for $\cos(\alpha+\beta)$ we may write

$$E(t) = A[\cos\omega_c t\cos(\beta\sin\omega_m t) - \sin\omega_c t\sin(\beta\sin\omega_m t)] \ .$$

$\cos(\beta\sin\omega_m t)$ and $\sin(\beta\sin\omega_m t)$ can both be expanded in Fourier series, whose coefficients are Bessel functions of the first kind with argument β (e.g. [3,4,5]):

$$\cos(\beta\sin\omega_m t) = J_0(\beta) + 2\sum_{n=1}^{\infty} J_{2n}(\beta)\cos 2n\omega_m t \ ,$$

$$\sin(\beta\sin\omega_m t) = 2\sum_{n=0}^{\infty} J_{2n+1}(\beta)\sin(2n+1)\omega_m t \ ,$$

with

$$J_0(\beta) = 1 - (\tfrac{\beta}{2})^2 + \tfrac{1}{4}(\tfrac{\beta}{2})^4 - \ldots \ ,$$

$$J_1(\beta) = \tfrac{\beta}{2} - \tfrac{1}{2}(\tfrac{\beta}{2})^3 + \tfrac{1}{12}(\tfrac{\beta}{2})^5 - \ldots \ ,$$

$$J_2(\beta) = \tfrac{1}{2}(\tfrac{\beta}{2})^2 - \tfrac{1}{6}(\tfrac{\beta}{2})^4 + \tfrac{1}{48}(\tfrac{\beta}{2})^6 - \ldots \ ,$$

If the modulation index $\beta < 0.04$, the amplitude of the higher order sidebands $J_n(\beta)$ with $n > 1$ is smaller than 1% of the amplitude of $J_1(\beta)$, so that we may write in good approximation

$$E(t) = A[\cos\omega_c t + \tfrac{\beta}{2}\cos(\omega_c + \omega_m)t - \tfrac{\beta}{2}\cos(\omega_c - \omega_m)t] \ .$$

The amplitude spectrum of the FM wave consists of a carrier at ω_c and two sidebands at a distance ω_m on each side of the carrier. The amplitude spectrum has been sketched in fig. 2.05a, and the phasor representation is given in fig. 2.05b.

If we compare this expression with the expression for an amplitude modulated wave (AM), the latter differs only in the sign of the low frequency sideband.
The phasor representation of an AM wave is given in fig. 2.05c.

2.4 *Description of the measuring system*

The complete block diagram of the measuring system is given in fig. 2.06. For small $d\omega$ and dC_g (with $dL = 0$ and $dR = 0$), expression (2.1) for e_4 reduces in a $1/Q^2$ approximation to

$$e_4 = -e_1 F[2\frac{d\omega}{\omega_0} + j(\frac{2}{Q}\frac{d\omega}{\omega_0} + \frac{1}{Q}\frac{dC_g}{C + C_g})] \ .$$

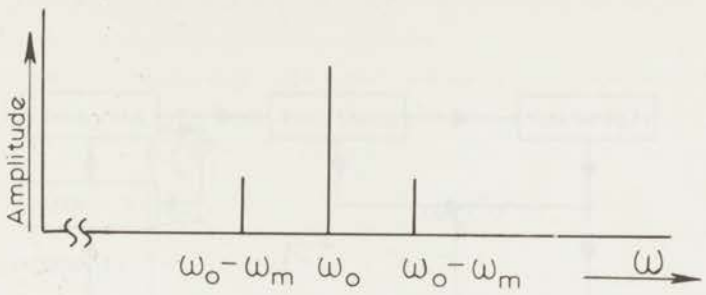

Fig. 2.05a Amplitude spectrum of the FM signal.

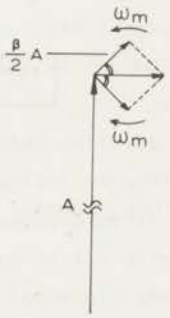

Fig. 2.05b Phasor representation of the FM signal.

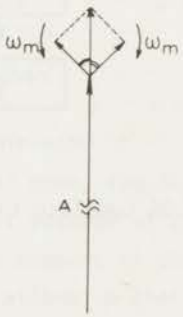

Fig. 2.05c Phasor representation of an AM signal.

If arg F varies but little with the frequency around ω_0, the corresponding amplitude characteristic is as sketched in fig. 2.02, and the phase characteristic as sketched in fig. 2.07. If the carrier frequency ω_c equals ω_0, both first order sidebands of the FM wave are attenuated and shifted in phase to the same extent, but in opposite direction with respect to the carrier, so that no AM component will result (fig. 2.08). If, however, the carrier frequency ω_c is different from ω_0, e.g. $\omega_c > \omega_0$, then the upper sideband of the FM wave is attenuated less than the lower sideband, and the phase shifts are different, so that an AM component results (fig. 2.08c). In the output signal of the bridge,

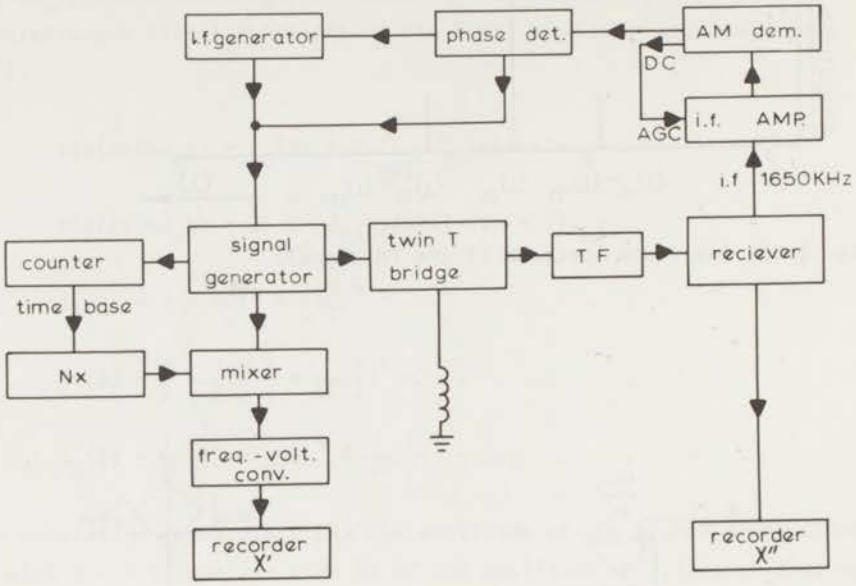

Fig. 2.06 Complete block diagram of the measuring system.

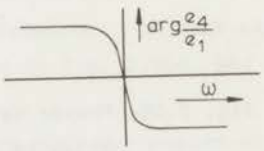

Fig. 2.07 Phase characteristic of e_4/e_1.

the sidebands are partially of FM nature and partially of AM nature.

In the receiver, the incoming signal is mixed with a local oscillator signal with preservation of amplitude as well as phase information. The intermediate frequency signal (i.f.) is then amplified and finally amplitude demodulated. The resulting AM component is amplified and fed to the phase sensitive detector, which uses the modulating audio frequency signal as reference signal. With the DC output of the phase sensitive detector, the radio frequency (r.f.)

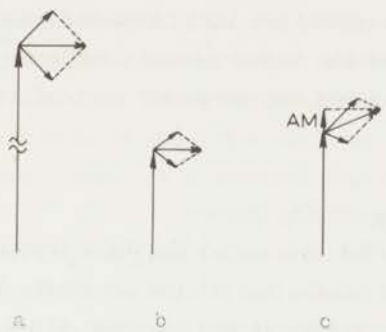

Fig. 2.08 Phasor representation of the signal:

a. at the bridge input,

b. at the bridge output if the carrier frequency ω_c equals the frequency of the bridge minimum ω_0,

c. at the bridge output if $\omega_c \neq \omega_0$.

generator is locked onto the frequency of the bridge minimum.

Since the selective voltmeter operates in a linear mode, the DC output of the amplitude demodulator is proportional to the output voltage of the bridge, and therefore can be fed directly to the recorder as a measure of the variation of χ''. In order to record the very small relative variations in the frequency of the bridge minimum caused by the χ' of the sample, the frequency of the signal generator is mixed with a multiple of the 100 kHz time base of the counter. The low frequency (l.f.) output of the mixer in the range of 1-5 kHz is converted to a DC signal by means of a one shot type frequency to voltage converter. The counter is used to adjust the frequency of the General Radio generator to a value in the neighbourhood of the desired multiple of 100 kHz. Typical measuring frequencies were 100, 200, 300, 500, 700 kHz, 1 MHz, 1.5, 2, 4, 8, 16 and 30 MHz for which we used three different coils because of the limited range in frequency in which the bridge could be balanced with each coil. At the lower frequencies an external variable C_g in the range of 0-5000 pF was needed to balance the bridge. In order to suffice with three coils, we used at 1, 1.5, and 16 MHz an extra condensor in series with the coil, and at 2 MHz an extra coil in series with the measuring coil. At 30 MHz, an extra $\frac{\lambda}{2}$ coaxial cable in series with the coil was needed to balance the bridge. As FM modulation

frequencies we used four fixed frequencies at 500, 1100, 2000 and 3000 Hz. The modulation index was adjusted so that the sidebands just exceeded the noise of the amplitude demodulator of the receiver. The sensitivity of the bridge can be shown to be maximum when the imaginary part of the output admittance of the bridge is tuned out and with no resistive load connected to the output terminals of the bridge. Therefore we used the highest input impedance of the receiver (500 kΩ parallel to 20 pF) and tuned the imaginary part of the admittance with a set of coils (TF).

2.5 *Practical aspects of the measuring system*

The measuring coil is located in a metal can in a cryostat and connected by means of a coaxial conductor to the top of the cryostat. The coil is wound on a rexolite tube, in which a Faraday screen has been fixed, to prevent dielectric effects caused by movements of the sample, because these would be indistinguishable from magnetic effects.

The metal can is filled with helium gas providing a good thermal contact with the bath. The temperature within the can is measured with a calibrated Germanium thermometer mounted close to the coil. The metal can and coil contain solder points. The commonly used solders become superconductive at liquid helium temperatures. If the external magnetic field is increased, the superconductivity is suppressed, resulting in a varying impedance in series with the coil. To minimize this effect, we have kept the number of solder points as low as possible, and have used solders which are not superconducting at liquid helium temperatures, i.e. zinc-cadmium solder with a melting point of 265°C and bismuth-cadmium solder with a melting point of 140°C.

The overall sensitivity is mainly determined by the sensitivity of the bridge (given by the slope of curve a in fig. 2.04), the filling factor q of the coil, and the sensitivity of the detectors for χ' and χ''.

It is limited, however, by other factors such as frequency noise of the signal generator, detector noise, the high frequency isolation between in- and output of the bridge (better than 120 db), mechanical vibrations in the coaxial conductor from the coil to the top of the cryostat, and especially at higher frequencies by the effect of thermal drift in the impedance of the coaxial conductor which then forms a relatively large part of the measuring coil circuit impedance. The sensitivity of the bridge is slightly frequency dependent, and varies between $0.5 \times 10^{-6}/2\pi$ Hz^{-1} at low frequencies to $10^{-6}/2\pi$ Hz^{-1} at high frequencies. The filling factor q of the coils was about 0.12 in the frequency range from 100-700 kHz and 0.042 between 4 and 8 MHz. At 1, 1.5, and 16 MHz,

the filling factor was greater than 0.12 and 0.042 resp., due to the condensor in series with the coil, and at 2 and 30 MHz correspondingly smaller than 0.042. The frequency stability of the signal generator during a measurement lasting a few minutes was about 0.1 ppm. The sensitivity of the detector was such that a frequency shift of about 0.1 Hz in the bridge minimum could be detected. A voltage variation of 0.05 μV at the output terminals of the bridge could be detected by the χ'' detector. These factors, together with the limitations, lead to an overall sensitivity of about 2×10^{-7} for χ' as well as for χ''. The sensitivity of a single measurement at a constant field (fig. 2.09a and c) was about a factor 10 higher.

As an illustration, we give a complete set of measurements of a single crystal $CoCs_3Cl_5$ with the tetragonal axis parallel to the mutually parallel r.f. and static field at a measuring frequency of 16 MHz and at a temperature of 3.06 K (fig. 2.09 a, b, c, d and e). First χ' is measured in relative units in zero field and as a function of the external field. Then χ'' is measured in relative units in zero field, and as a function of the static field too, and finally the units of χ'' are calibrated in the units of χ'. In the evaluation of the measurements, a correction is taken into account for the thermal drift. At about 600 Oe one sees the remaining influence of superconductive solder junctions. As long as we stay within the linearity of the bridge, the effect is not serious, because it is the same for the two positions of the sample. At 3758 Oe, proton resonance in the coil holder is noticed which we used as a calibration of the magnetic field (fig. 2.10).

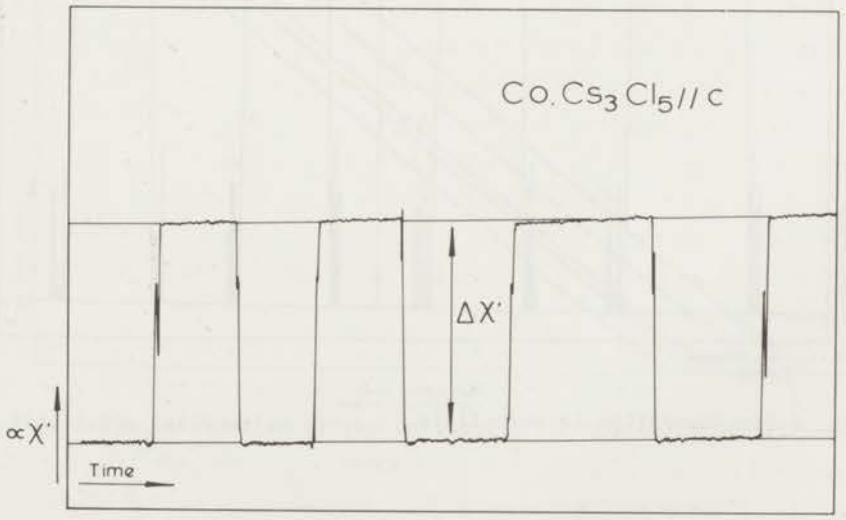

Fig. 2.09a Dispersion in zero field.

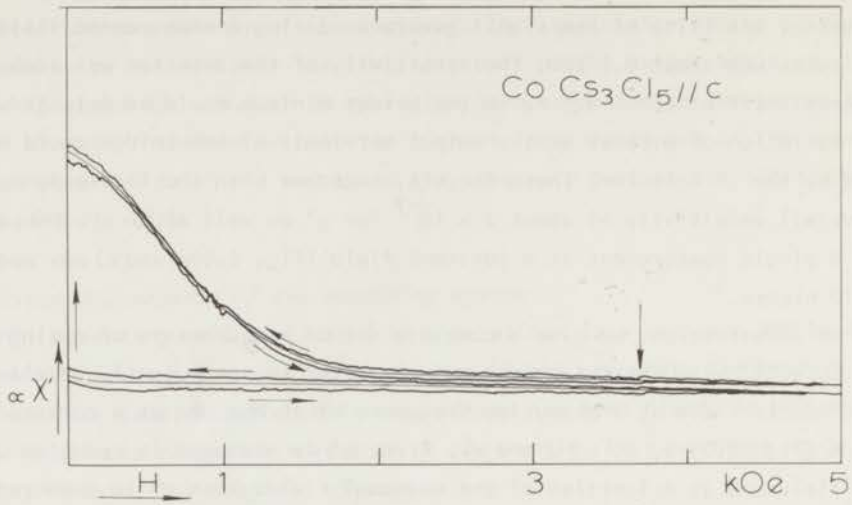

Fig. 2.09b Dispersion as a function of the external magnetic field.

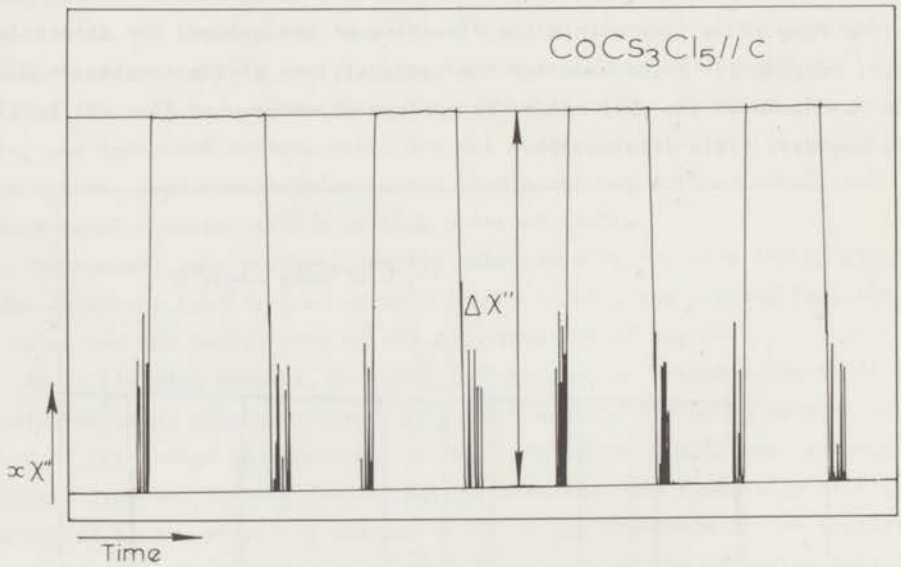

Fig. 2.09c Absorption in zero field.

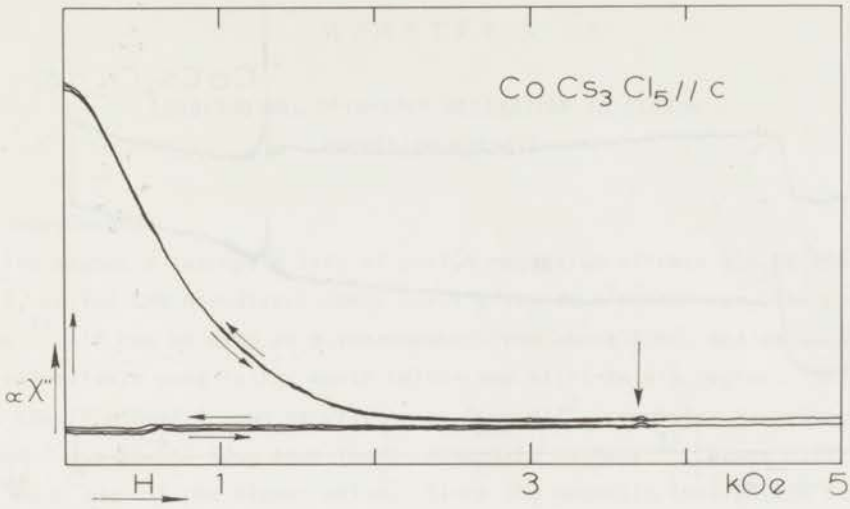

Fig. 2.09d Absorption as a function of the external magnetic field.

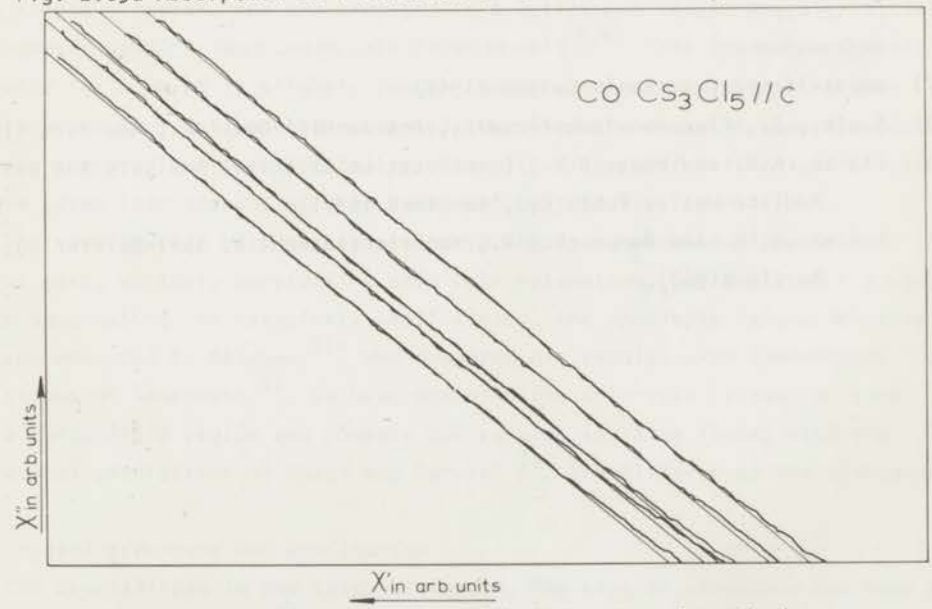

Fig. 2.09e Calibration of the units of χ'' in the units of χ'.

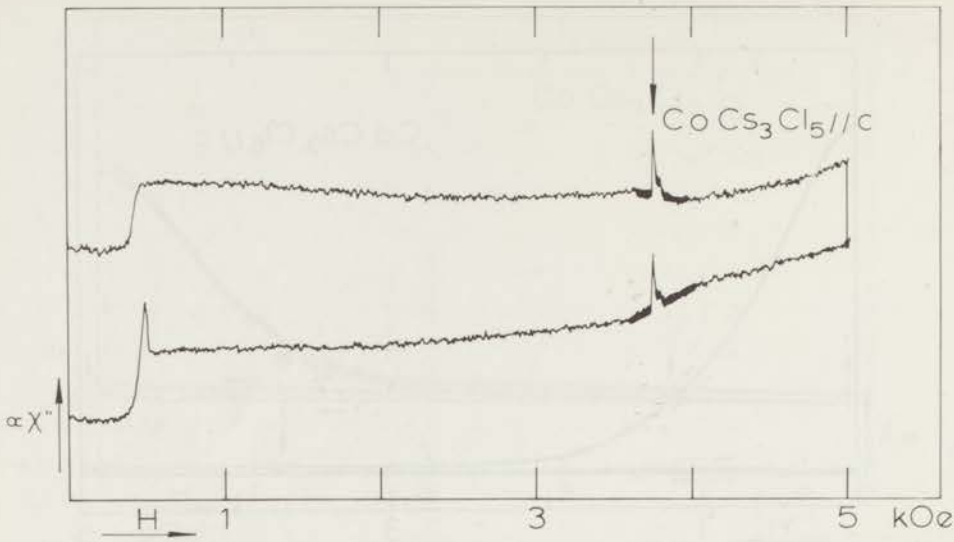

Fig. 2.10 Calibration of the magnetic field.

References

1) Verstelle, J.C., thesis Leiden (1962).

2) Seeley, S., Electron Tube Circuits, McGraw-Hill Book Cy., New York (1958).

3) Clarke, K.K. and Hess, D.T., Communication Circuits: Analysis and Design, Addison-Wesley Publ. Cy., New York (1971).

4) Steinbuch, K. and Rupprecht, W., Nachrichtentechnik, Springer-Verlag, Berlin (1967).

CHAPTER 3

LONGITUDINAL SPIN-SPIN RELAXATION IN CERIUM MAGNESIUM NITRATE

3.1 *Introduction*

The magnetic susceptibility of cerium magnesium nitrate ($Ce_2Mg_3(No_3)\cdot 24\ H_2O$, called CMN hereafter) obeys Curie's law down to the very low temperatures [1]. It can be used as a thermometer from about 2 mK, and as such it has been extensively used in the centi-Kelvin and milli-Kelvin region. The magnetic specific heat C_M can be written as $C_M = b/T^2$, where for b, values between 4.2 and $7.5 \times 10^{-6} K^2$ have been found. According to Mess [2], above 0.15 K one must make use of the higher values. Since the magnetic interaction between the cerium ions in CMN consists of only the dipole-dipole interaction (Ce has no hyperfyne splitting), and the magnetic equivalent cerium ions have a well-known simple g factor, and are arranged in a well-known simple Bravais lattice, the magnetic specific heat can be calculated as well [3,4]. This leads to a theoretical value for b which is slightly larger than the values measured at higher temperatures. At 1.3 K we have accurately measured the magnetic specific heat and have compared our experimental results with a computer calculation where we have taken into account a large number of neighbours.

The secular part of the interaction in CMN is comparable with the non-secular part, so that, considering spin-spin relaxation, one deals with a case of strong coupling. In relatively small fields, the spin-spin relaxation time has been measured by Grambow [5], who compared his results with theoretical predictions of Sauermann [6]. We have measured the spin-spin relaxation time over a large field region and compare our results in large fields with the theoretical predictions of Mazur and Terwiel [7]. The differences are discussed.

3.2 *Crystal structure and Hamiltonian*

CMN crystallizes in the trigonal system. The crystal structure has been determined by Zalkin et al. [8]. The Ce^{3+} ions constitute a simple rhombohedral lattice, the long diagonal of the rhombohedron coincides with the trigonal axis of the crystal. If the crystal is described by the alternative hexagonal unit cell, the dimensions are

$a = 11.004 \pm 0.006$ Å, and

$c = 34.592 \pm 0.012$ Å,

where the c axis of the cell is parallel to the trigonal axis of the crystal (fig. 3.01).

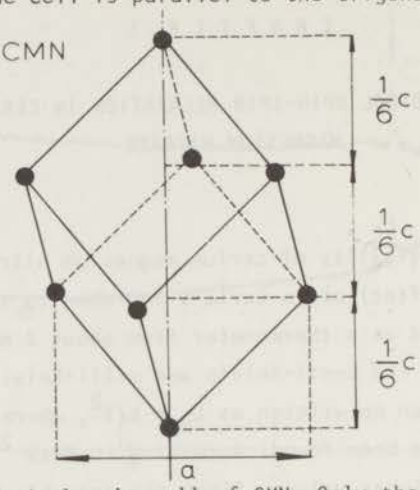

Fig. 3.01 Rhombohedral unit cell of CMN. Only the Ce^{3+} ions have been drawn.

The $^2F_{5/2}$ ground state of the cerium ion is split by the crystal field into three Kramer doublets. The splitting, Δ/k, between the lowest two doublets is approximately 35 K, so that effectively at liquid helium temperatures only the lowest lying doublet is populated, and we are concerned with an effective spin $\frac{1}{2}$. The splitting of the lowest doublet is described by an anisotropic g factor:

g perpendicular the trigonal axis $g_\perp = 1.84$, and

g parallel the trigonal axis $g_{//} = 0.024$.

We have only dipole-dipole interaction in CMN, so that for an external magnetic field perpendicular to the trigonal axis, the isolated spin system has the following Hamiltonian:

$$H = H_z + H_{dip} = H_z + H_{sec} + H_{n\,sec} ,$$

with

$$H_z = g\,\mu_B H \Sigma_i S_z^i \quad .$$

In section 3.4 we shall show that the secular part of the interaction is comparable with the non-secular part, so that we have a strong coupling case for spin-spin relaxation. In strong external magnetic fields, we therefore compare our experimental results with the theoretical predictions of Mazur and Terwiel (section 3.4.2).

3.3 *Experiment*

Both the components of the complex susceptibility $\chi = \chi' - i\chi''$ of a single crystal CMN have been measured with the aid of the twin T bridge, described in chapter 2. The mutually parallel r.f. and static fields were perpendicular to the trigonal axis. To eliminate the influence of the spin-lattice relaxation, the measurements were performed at 1.3 K. Fixed frequencies between 200 kHz and 30 MHz were used and χ' and χ'' were recorded directly as a function of the external magnetic field up to 500 Oe. Both components become vanishingly small at higher fields.

3.3.1 *b/C value and the ratio χ'_{bet}/χ_{ad}.*

The real part of the complex susceptibility is given by

$$\chi'(\omega) = \chi'_{bet} + (\chi_{ad} - \chi'_{bet})\frac{1}{1 + \omega^2\tau_{SS}^2} + (\chi_0 - \chi_{ad})\frac{1}{1 + \omega^2\tau_{SL}^2} \quad . \tag{1.60a}$$

The frequencies equal to the inverse of the spin-lattice and spin-spin relaxation time will be called spin-lattice resp. spin-spin relaxation rate. The ratio χ'_{bet}/χ_{ad} will be abbreviated as α.

In CMN, the spin-lattice and spin-spin relaxation rates are well separated in frequency. In that case, $\chi'(\omega)$ reaches the value χ_{ad} for frequencies in the range between these two rates, and the b/C-value can be derived from the adiabatic susceptibility χ_{ad} according to

$$\frac{b}{C} = \frac{H^2}{\chi_0/\chi_{ad} - 1} \qquad \text{(see formula 1.56)}$$

At fields for which $H^2 >> \frac{b}{C}$, this becomes

$$\frac{b}{C} = \frac{\chi_{ad}}{\chi_0} H^2 \quad .$$

$\chi'(\omega)$ equals χ'_{bet} for frequencies $\omega >> \tau_{SS}^{-1}$.

For $H^2 >> b/C$, $\alpha b/C$ can then be derived from χ'_{bet} by

$$\alpha\frac{b}{C} = \frac{\chi'_{bet}}{\chi_0} H^2 \quad .$$

Starting from the situation $\tau_{SL}^{-1} << \omega << \tau_{SS}^{-1}$, an increase of the static field

will reduce the spin-spin relaxation rate in such a way that the situation $\omega >> \tau_{SS}^{-1}$ is reached. At different fixed frequencies, χ' has been measured as a function of the external magnetic field up to 500 Oe. A typical graph of $H^2/(\chi_0/\chi' - 1)$ is given in fig. 3.02.

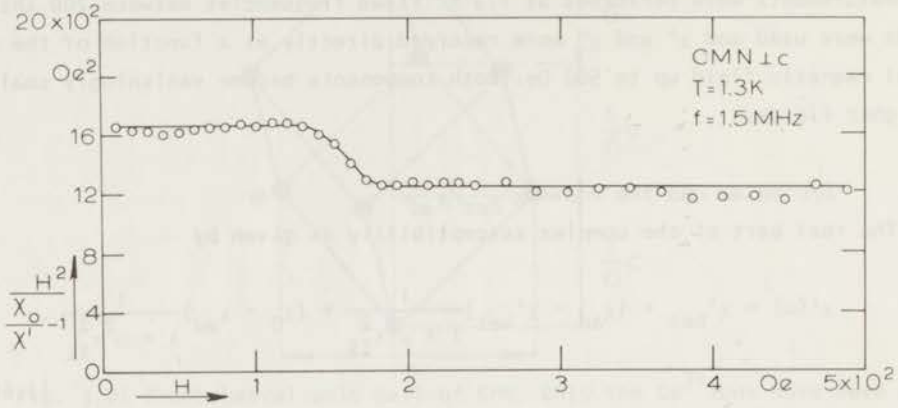

Fig. 3.02 Typical graph of $H^2/(\chi_0/\chi' - 1)$ versus H in CMN $\perp$ c axis as derived from from a measurement at 1.3 K and 1.5 MHz. The lines have been drawn through the experimental values.

The result of about twenty measurements is

$$b/C = 1615 \pm 20 \text{ Oe}^2$$

and

$$\alpha = \chi'_{bet}/\chi_{ad} = 0.72 \pm 0.04 \ .$$

3.3.2 *Spin-spin relaxation time*

The imaginary part of the susceptibility is given by

$$\chi''(\omega) = (\chi_{ad} - \chi'_{bet})\frac{\omega\tau_{SS}}{1 + \omega^2\tau_{SS}^2} + (\chi_0 - \chi_{ad})\frac{\omega\tau_{SL}}{1 + \omega^2\tau_{SL}^2} \ . \qquad (1.60b)$$

At frequencies around the spin-spin relaxation rate,

$$\frac{\chi''}{\chi_{ad}} = (1 - \frac{\chi'_{bet}}{\chi_{ad}})\ \frac{\omega\tau_{SS}}{1 + \omega^2\tau_{SS}^2} \ .$$

Starting, for a fixed frequency ω, from $\tau_{SS}^{-1} > \omega$ in zero field, τ_{SS}^{-1} becomes $< \omega$

in high fields. The function $\omega\tau_{SS}/(1 + \omega^2\tau_{SS}^2)$ reaches its maximum value $\frac{1}{2}$ at the field for which $\omega = \tau_{SS}^{-1}$. If for this field $H_{max}^2 >> b/c$, then in the neighbourhood of this field χ'_{bet}/χ_{ad} is constant, and the maximum of χ''/χ_{ad} coincides with that of $\omega\tau_{SS}/(1 + \omega^2\tau_{SS}^2)$. The maximum value of χ''/χ_{ad} is $\frac{1}{2}(1 - \chi'_{bet}/\chi_{ad})$. Some graphs of χ''/χ_{ad} versus H at different frequencies are given in fig. 3.03

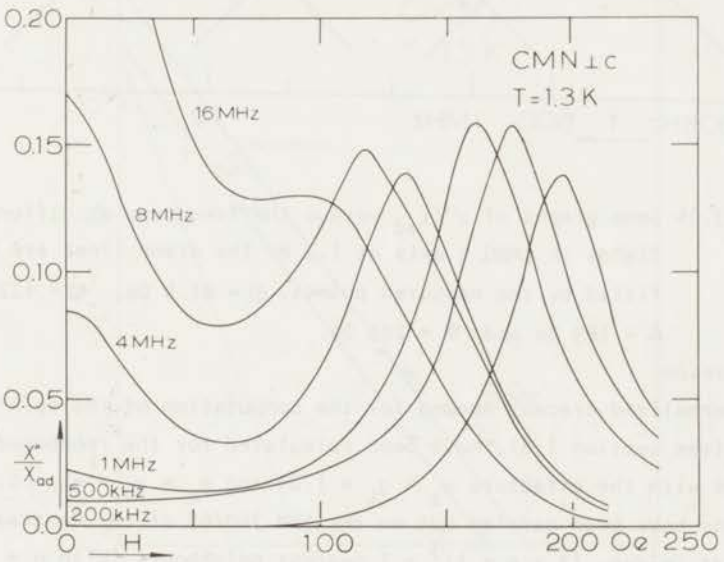

Fig. 3.03 Some graphs of χ''/χ_{ad} versus H at different fixed frequencies in CMN⊥ c axis at 1.3 K.

and some graphs of χ''/χ_{ad} versus the frequency f on a double logarithmic scale at different fields in fig. 3.04. In the latter figure, we see that the experimental values can be fitted by Debye curves, which implies that the spin-spin relaxation process takes place according to a single exponential decay. The graph of $\tau_{SS}^{-1}\chi_{ad}/\chi_0$ on a logarithmic scale versus H^2 is given in fig. 3.05. From the absorption measurements we conclude that

$$\alpha = \chi'_{bet}/\chi_{ad} = 0.67 \pm 0.02 \ .$$

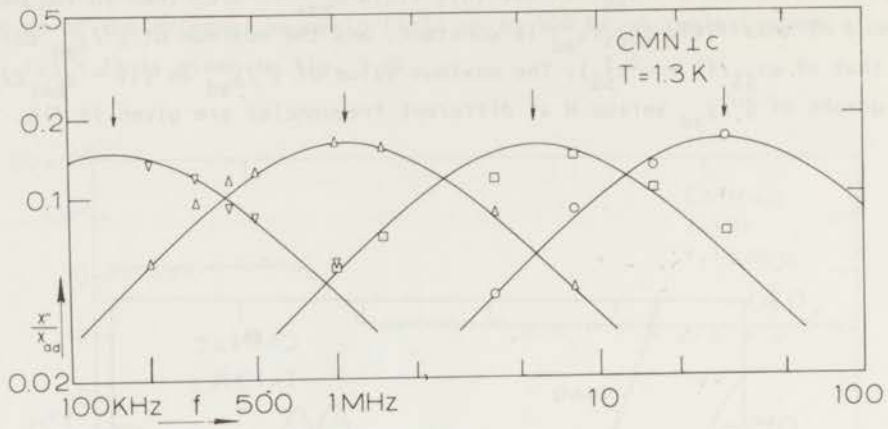

Fig. 3.04 Some graphs of χ''/χ_{ad} versus the frequency at different fixed fields in CMN⊥ c axis at 1.3 K. The drawn lines are Debye curves fitted by the measured points. ⊙ = 81.4 Oe, ⊡ = 122 Oe, △ = 163 Oe and ▽ = 203 Oe.

3.4 *Discussion*

The normalized traces, needed for the computation of the spin-spin relaxation time (see section 1.6), have been calculated for the rhombohedral unit cell of CMN with the g-factors $g_z = g_\perp = 1.84$ and $g_x = g_y = g_{//} = 0.024$. The calculations have been carried out on the IBM 360/65 of the Centraal Reken Instituut at Leiden. $(2 \times n + 1)^3 - 1$ nearest neighbours (with $n = 3$) have been taken into account. The results for N (Avogadro's number) times the contribution per magnetic ion are given in table 1.

Table 1

$\langle\langle H_0^2 \rangle\rangle$	30.5×10^{-15} erg^2
$\langle\langle H_1 H_{-1} \rangle\rangle$	17.0×10^{-15} erg^2
$\langle\langle H_2 H_{-2} \rangle\rangle$	5.09×10^{-15} erg^2
$\langle\langle H_{dip}^2 \rangle\rangle$	74.8×10^{-15} erg^2
$\langle\langle [H_0, H_1][H_{-1}, H_0] \rangle\rangle$	81.9×10^{-51} erg^4
$\langle\langle [H_0, H_2][H_{-2}, H_0] \rangle\rangle$	48.6×10^{-51} erg^4

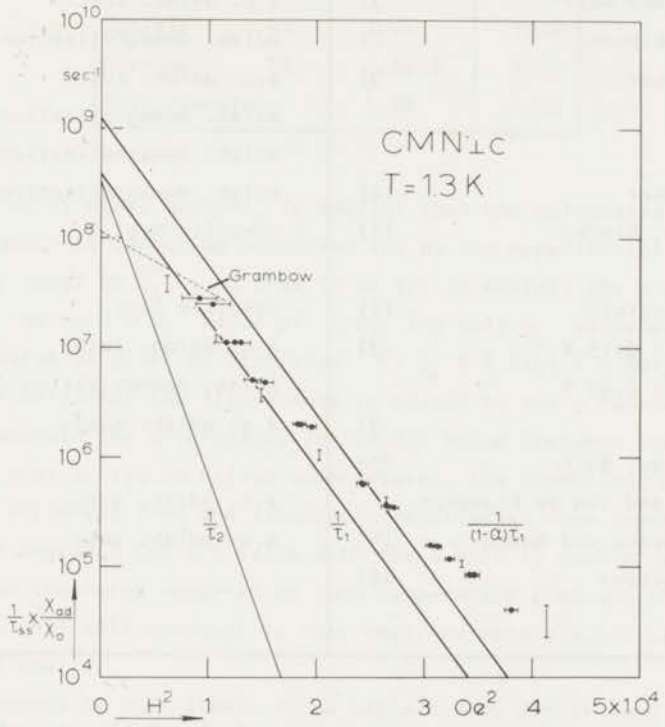

Fig. 3.05 $\tau_{SS}^{-1}\ \chi_{ad}/\chi_0$ versus H^2 in CMN⊥ c axis at 1.3 K. Horizontal bars correspond with spin-spin relaxation times determined from the maximum of χ''/χ_{ad} versus H (ω constant), and vertical bars with spin-spin relaxation times determined from the maximum of χ''/χ_{ad} versus ω (H constant). Full lines are theoretical curves, the dotted line represents the experimental results of Grambow.

3.4.1 *b/C value and the ratio* $\chi'_{bet}/\chi_{ad} = \alpha$

In the literature, b/C values are given between 1100 and 2000 Oe^2. A list of b/C values has been compiled by Mess [2]. The list has been supplemented and is given in table 2.

Table 2

Experimentalists		Method	$\frac{b}{C}$ Oe^2
Cooke, Duffus and Wolf	3)	a.c. adiab. susc.	1767
Daniels and Robinson	1)	adiab. demagnetization	1676
Hudson and Kaeser	9)	a.c. adiab. susc.	1650
		adiab. demagnetization	1440
		adiab. demagnetization	1545
Hudson and Kaeser	10)	adiab. demagnetization	1508
Abel, Anderson, Black,	11)	specific heat	1100
and Wheatley			1519
Abraham and Eckstein	12)	specific heat	1100
Mess T > 0.15 K	2)	a.c. adiab. susc.	1623
T < 0.02 K		adiab. magnetization	1257
Grambow	5)	a.c. adiab. susc.	1656
Flokstra, Verhey, Bots	13)		
Van der Marel and Van de Klundert		a.c. adiab. susc.	1571
Abraham, Ketterson and Roach	14)	a.c. adiab. susc.	1613
Hudson and Pfeiffer	15)		1597
This research			1615

The following conversion factors have been used: R = 8.317 erg mole^{-1}deg^{-1} and C = 3.176 x 10^{-4}erg deg mole^{-1}Oe^{-2}, which gives R/C = 2.619 x 10^{4}Oe^{2}deg^{-2}. Mess [2] has already noted that b/C has a constant value 1257 Oe^2 below 20 mK and increases to another constant value 1623 Oe^2 above 0.15 K. Theoretically, b/C is given by formula (1.93)

$$\frac{b}{C} = \frac{\langle\langle H_{int}^2 \rangle\rangle}{\langle\langle M_z^2 \rangle\rangle} = \frac{\langle\langle H_{int}^2 \rangle\rangle}{N \frac{1}{3} g_z^2 \mu_B^2 S(S+1)} ,$$

where it is assumed that the substance obeys Curie's law. This is certainly the case for CMN at liquid helium temperatures. The calculated b/C value, together with the calculated values of other authors, is given in table 3.
The b/C value measured by us, just as the most recent and probably most accurate

Table 3

Authors	$g_\perp$ used	$\frac{b}{C}(Oe^2)$
Cooke et al. 3)	1.84	1767
Daniels 4)	1.84	1728
Grambow 5)	1.8264	1735
This research	1.84	1706

values reported by other authors, is smaller than the calculated one. This discrepancy of about 5% cannot be accounted for by the experimental uncertainties. b/C is proportional to $g_\perp^{-2}$, so that if we try to explain the discrepancy by the g factor, we need a $g_\perp$ value of 1.89. The only $g_\perp$ value different from 1.84 is the value as given by Stapleton [16]. $g_\perp = 1.8264 \pm 0.0013$, so that it is not very likely that the discrepancy is caused by the g factor. Another possibility to explain the discrepancy in the b/C value (between theory and experiment) is that at liquid helium temperatures, the dimensions of the unit cell are slightly different from the dimensions reported at room temperature. If we calculate for instance the b/C value with the a axis 1% smaller and the c axis 2% larger than the value reported at room temperature (leaving the volume of the hexagonal unit cell constant in this way), we obtain a b/C value of 1684 Oe^2 thus 1.3% smaller.

So the discrepancy is most likely to be explained by either some unknown deformation of the crystal or by some unknown interaction term which then has to give a negative total contribution to b/C.

From the dispersion measurements, we conclude that $\alpha = 0.72 \pm 0.04$ and from the absorption measurements that $\alpha = 0.67 \pm 0.02$. Theoretically, α is given by

$$\alpha = \frac{\chi'_{bet}}{\chi_{ad}} = \frac{\langle\langle H_{int}^2 \rangle\rangle - \langle\langle H_0^2 \rangle\rangle}{\langle\langle H_{int}^2 \rangle\rangle} = 0.60 \ .$$

The discrepancy of about 15% cannot be accounted for by the inaccuracy in the measurements, and the same arguments as given above for b/C apply in this case even more strongly.

3.4.2 *Spin-spin relaxation time*

If the Fourier spectrum of the kernel $G^{\circ}(t,H)$ in the case of strong coupling consists of Gaussian lines, then the relaxation time is given by (see section 1.5)

$$\frac{1}{\tau_{SS}} = \frac{H^2}{\frac{1}{2}H_{i\ sec}^2}\left(\frac{1}{\tau_1} + \frac{1}{\tau_2}\right) = \frac{1}{1-\alpha}\frac{H^2}{\frac{1}{2}H_i^2}\left(\frac{1}{\tau_1} + \frac{1}{\tau_2}\right) \tag{1.115}$$

with

$$\frac{1}{\tau_1} = \frac{2\pi << H_1 H_{-1} >>}{d_1^3 \hbar^2 \frac{1}{3}S(S+1)} \frac{1}{\{2\pi<\omega^2>_1\}^{\frac{1}{2}}} \exp\{-\tfrac{1}{2}(\frac{g\mu_B H}{\hbar})^2 \frac{1}{d_1^2<\omega^2>_1}\}\ , \tag{1.116}$$

$$\frac{1}{\tau_2} = \frac{2\pi << H_2 H_{-2} >>}{d_2^3 \hbar^2 \frac{1}{3}S(S+1)} \frac{1}{\{2\pi<\omega^2>_2\}^{\frac{1}{2}}} \exp\{-\tfrac{1}{2}(\frac{2g\mu_B H}{\hbar})^2 \frac{1}{d_2^2<\omega^2>_2}\}\ , \tag{1.117}$$

and

$$<\omega^2>_{1,2} = \frac{1}{\hbar^2}\frac{<<[H_0,H_{1,2}][H_{-1,-2},H_0]>>}{<<H_{1,2},H_{-1,-2}>>}\ . \tag{1.108}$$

If we write

$$\frac{1}{\tau_1} = \frac{1}{d_1^3}\frac{1}{\tau_1(0)}\exp(-\frac{H^2}{d_1^2\gamma_1}) \quad \text{and}$$

$$\frac{1}{\tau_2} = \frac{1}{d_2^3}\frac{1}{\tau_2(0)}\exp(-\frac{H^2}{d_2^2\gamma})\ ,$$

then substitution of the numerical values of table 1 gives the values of table 4, in which the values calculated by Grambow have been given as well.
From the table, one sees that the values for τ_2 are in good agreement, but that the value of Grambow for γ_1, is a factor $(\frac{3}{2})^2$ larger than our value, and that the value of Grambow for $\tau_1(0)$ is a factor $\frac{3}{2}$ larger than our value. This indicates that the value of Grambow for $<\omega^2>_1$ is a factor $\frac{3}{2}$ larger than our value.

The theoretical curves $1/\tau_1$ and $1/\tau_2$ for $d_1 = d_2 = 1$ are drawn in fig. 3.05.

Grambow compares his results at relatively low fields with theoretical predictions of Sauermann.

Table 4

	Grambow	This research
$\tau_1(0)$	3.9×10^{-9} sec	2.55×10^{-9} sec
$\tau_2(0)$	3.0×10^{-9} ssec	3.02×10^{-9} sec
γ_1	7225 Oe^2	3270 Oe^2
γ_2	1521 Oe^2	1620 Oe^2

$$\frac{1}{\tau'_{SS}} = (1 - \alpha) \frac{H^2 + \frac{1}{2}H_i^2}{\frac{1}{2}H_i^2} \left(\frac{1}{\tau'_1} + \frac{1}{\tau'_2}\right) ,$$

where

$\tau'_1 = \tau_1$ for $d_1 = 1$ and

$\tau'_2 = \tau_2$ for $d_1 = 1$.

In large fields, for which $H^2 >> \frac{1}{2}H_i^2$, one finds a discrepancy of a factor $(1 - \alpha)^2$ between Sauermann's result and that of Mazur and Terwiel for $d_1 = d_2 = 1$.

In order to compare our experimental results with the theory of Mazur and Terwiel, the theoretical curves τ_1^{-1} and τ_2^{-1} should be shifted upwards to obtain $(1 - \alpha)^{-1}\tau^{-1}$ and $(1 - \alpha)\tau_2^{-1}$ (fig. 3.05). If d_1 roughly equals d_2, the experimental results should be compared with $(1 - \alpha)^{-1}\tau_1^{-1}$ only. Looking at fig. 3.05, one sees that for $d_1 \simeq 1$, this gives indeed a more or less reasonable description. As the experimental points cannot be fitted by a straight line, we cannot determine d_1 more precisely.

In conclusion, we may say that the line in the memory spectrum, $G^\circ(\omega,H)$ at ω_L is roughly Gaussian. The broadening is of the order of the secular interaction, as is proposed as a working hypothesis by Mazur and Terwiel. In order to make a comparison between our results and the theory of Sauermann as used by Grambow, the theoretical curves τ_1^{-1} and τ_2^{-1} should be shifted downwards to obtain $(1 - \alpha)\tau_1^{-1}$ and $(1 - \alpha)\tau_2^{-1}$. The experimental results at high magnetic fields should be compared with $(1 - \alpha)\tau_1^{-1}$ and this is less in agreement with the experiments.

References

1) Daniels, J.M. and Robinson, F.N.H., Phil. Mag. 44 (1953) 630.

2) Mess, K.W., thesis, Leiden 1969.
Mess, K.W., Lubbers, J., Niesen, L. and Huiskamp, W.J., Physica 41 (1969) 260.

3) Cooke, A.H., Duffus, H.J. and Wolf, W.P., Phil. Mag. 44 (1953) 623.

4) Daniels, J.M., Proc. Phys. Soc. 66 (1953) 673.

5) Grambow, J., Z. Physik 257 (1972) 245.

6) Sauermann, G., Physica 32 (1966) 2017.

7) Mazur, P. and Terwiel, R.H., Physica 36 (1967) 289.

8) Zalkin, A., Forrester, J.D. and Templeton, D.H., J. Chem. Phys. 39 (1963) 2881.

9) Hudson, R.P., Kaeser, R.S. and Radford, H.E., VII Int. Conf. on Low Temp. Phys., Toronto 1960, p. 100.

10) Hudson, R.P. and Kaeser, R.S., Physics 3 (1967) 95.

11) Abel, W.R., Anderson, A.C., Black, W.C. and Wheatley, J.C., Physics 1 (1965) 337; Phys. Rev. 147 (1966) 111.
Wheatley, J.C., Ann. Acad. Sci. Fennicae A210 (1966) 15.

12) Abraham, B.M. and Eckstein, Y., Phys. Rev. Letters 20 (1968) 649.

13) Flokstra, J., Verhey, W.A., Bots, G.J.C., Van der Marel, L.C. and Van de Klundert, L.J.M., Phys. Letters 40A (1972) 363.

14) Abraham, B.M., Ketterson, J.B. and Roach, P.R., Phys. Rev. B6 (1972) 4675.

15) Hudson, R.P. and Pfeiffer, E.R., in Proc. of the European Phys. Soc. Low Temp. Physics Conf. Freudenstadt, Germany (unpublished).

16) Stapleton, H.J., Private communication in Ruby, R.H., Benoit, H. and Jeffries, C.D., Phys. Rev. 127 (1962) 51.

CHAPTER 4

SPIN-LATTICE RELAXATION IN CMN

4.1 *Introduction*

Since 1961 many experiments have been reported on spin-lattice relaxation in CMN, first by Finn, Orbach and Wolf [1], using the Casimir-du Pré method and later on amongst others by Leifson and Jeffries [2], and Ruby, Benoit, and Jeffries [3], using the microwave transient method. Practically all experiments have been carried out in relatively low fields (up to 5 kOe). Recently Breur [4] has done measurements at 1.4 K and 1.7 K in magnetic fields from 4.7 kOe up to 47 kOe. The over-all data in relatively low fields can be described by the sum of a bottlenecked direct process and an Orbach process.

$$\frac{1}{\tau} = A\coth^2\left(\frac{g\mu_B H}{2kT}\right) + B\exp\left(-\frac{\Delta}{kT}\right) \quad , \tag{4.01}$$

with $\frac{\Delta}{k} \simeq 34$ K.
The factor A in the bottlenecked direct process is proportional to H^2, and the field dependence of B is given by the Brons-Van Vleck [5] formula.

$$B(H) = B(\infty)\,\frac{H^2 + \mu' \tfrac{1}{2}H_i^2}{H^2 + \tfrac{1}{2}H_i^2} \quad . \tag{4.02}$$

Hoffmann and Sapp [6] have calculated $\mu' = 2.2$, and we have measured $\frac{1}{2}H_i^2 = b/C = 1706\ \mathrm{Oe}^2$, thus for fields above a few hundred Oersteds we expect B to be field independent. Experimentally however, we have found B to be field dependent up to high fields.

We have measured the field dependency of the spin-lattice relaxation time in the liquid helium range with the aid of three different types of equipment. In the frequency range from 30 MHz down to 100 kHz, we used the twin T-bridge described in chapter 2, from 100 kHz to 2 kHz we used the bridge designed by De Vries [7], and from 2 kHz to 10 Hz a direct measurement apparatus which will be published by Soeteman [8].

The use of the latter two pieces of low frequency equipment has been kindly put at our disposal by Dr. van Duyneveldt and his group in our laboratory. In

the low frequency region, the measurements were performed in magnetic fields up to 34 kOe; at higher frequencies the magnetic field was restricted to 5 kOe.

4.2 *Experimental results*

The observed spin-lattice relaxation time as a function of the magnetic field at eight different temperatures is shown in fig. 4.01. At 4.22 K and 3.97 K we found in low fields (up to 500 Oe) that the relaxation process can be described by two relaxation times

$$\frac{\chi'}{\chi_0} = 1 - F + F\left(\frac{a}{1 + \omega^2\tau_1^2} + \frac{1 - a}{1 + \omega^2\tau_2^2}\right) , \tag{4.03a}$$

$$\frac{\chi''}{\chi_0} = F\left(\frac{a}{1 + \omega^2\tau_1^2} + \frac{1 - a}{1 + \omega^2\tau_2^2}\right) , \tag{4.03b}$$

or in complex notation

$$\frac{\chi}{\chi_0} = 1 - F + F\left(\frac{a}{1 + i\omega\tau_1} + \frac{1 - a}{1 + i\omega\tau_2}\right) . \tag{4.04}$$

As an illustration the measured values of χ''/χ_0 at 4.22 K are plotted in fig. 4.02 as a function of the frequency (on a logarithmic scale) at different fields.

From a computer analysis to fit the measured data to the formulae given above, values for τ_1 and τ_2 are found as plotted in fig. 4.01, together with values for F, Fa and F(1-a) (fig. 4.03). The same procedure has been followed for the data at 3.97 K.

4.3 *Discussion*

For a description of the relaxation process at 4.22 K and 3.97 K, we can use the simple thermodynamic model of fig. 4.04, which has been used in the same context by Gorter et al. [9], Van der Marel [10], and Stoneham [11]. The model consists of three systems, each of which is in internal equilibrium: the spin system, the phonons responsible for spin-lattice relaxation (phonons on speaking terms), and the bath, which is also thought to contain the rest of the phonon system and has an infinite heat capacity. If we suppose that the energy transfer between the systems is proportional to the temperature difference, and we make use of the first law of thermodynamics for the spin system, the energy balances for the spin and phonon system can be written as:

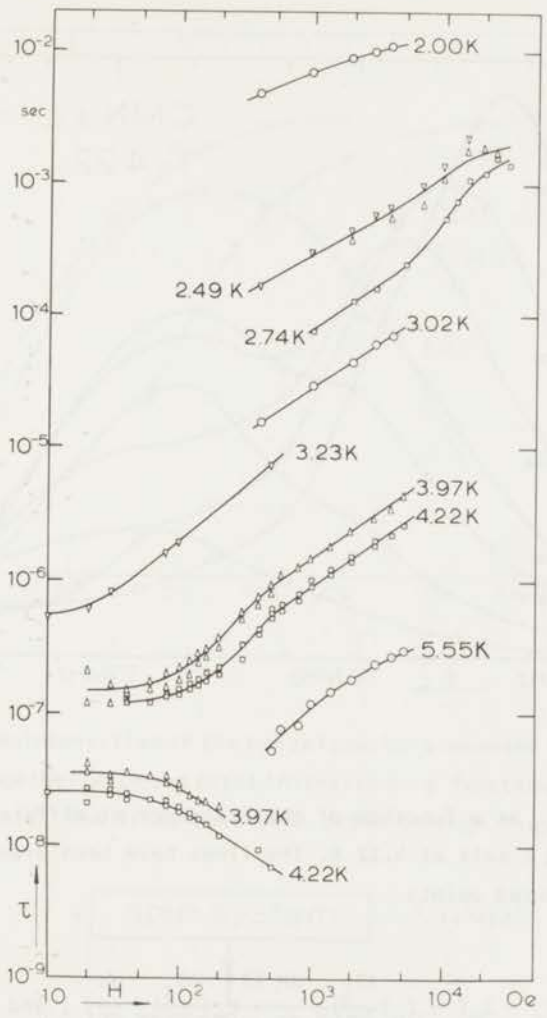

Fig. 4.01 Spin-lattice relaxation time of CMN⊥ c axis as a function of the magnetic field at different temperatures. The lines have been drawn through the measured points.

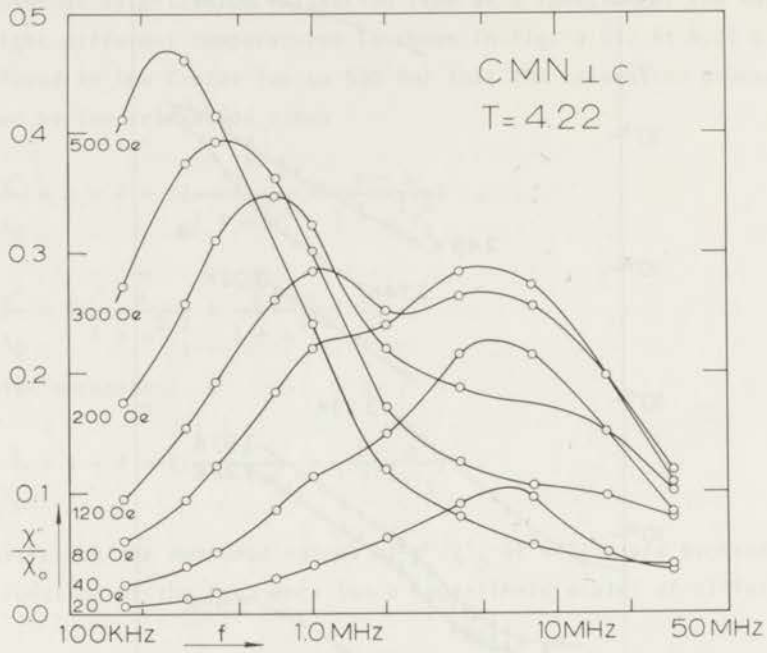

Fig. 4.02 χ''/χ_0 as a function of the frequency at different low fields in CMN$\perp$ c axis at 4.22 K. The lines have been drawn through the measured points.

$$\frac{dQ}{dt} = -\alpha(T_S - T_P) = C_H\left(\frac{\partial T_S}{\partial M}\right)_H \frac{dM}{dt} + C_M\left(\frac{\partial T_S}{\partial H}\right)_M \frac{dH}{dt} \quad , \text{ and} \tag{4.05}$$

$$C_P \frac{dT_P}{dt} = \alpha(T_S - T_P) - \beta(T_P - T_B) \ . \tag{4.06}$$

For a total field consisting of a constant part and a small oscillating part, we may write in a linear approximation.

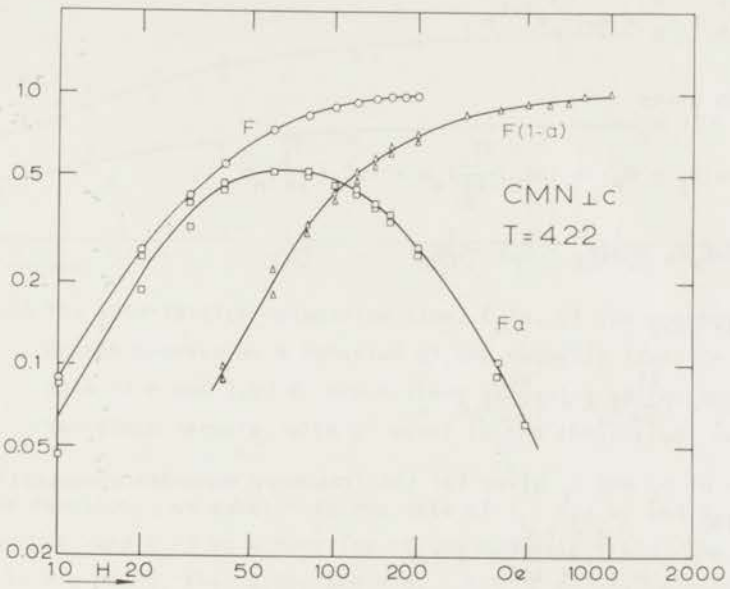

Fig. 4.03 The intensities of the two relaxation processes in CMN⊥ c axis at 4.22 K, together with the total intensity as a function of the magnetic field. The lines have been drawn through the calculated values.

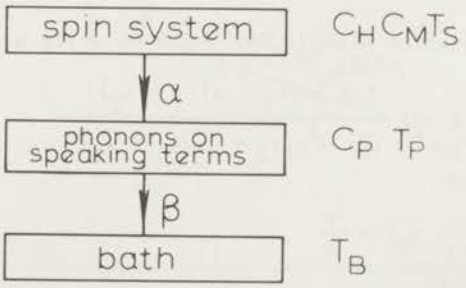

Fig. 4.04 Thermodynamic model for the description of the relaxation in CMN⊥ c axis at 4.22 K and 3.97 K.

$$
\begin{aligned}
H &= H_0 + \mathrm{Re}(he^{i\omega t}) \quad , \\
M &= M_0 + \mathrm{Re}(me^{i\omega t}) \quad , \\
T_S &= T_B + \mathrm{Re}(\Theta_S e^{i\omega t}) \quad , \\
T_P &= T_B + \mathrm{Re}(\Theta_P e^{i\omega t}) \quad .
\end{aligned} \tag{4.07}
$$

Substitution gives

$$
-\alpha(\Theta_S - \Theta_P) = i\omega C_H \left(\frac{\partial T_S}{\partial M}\right)_H m + i\omega C_M \left(\frac{\partial T_S}{\partial H}\right)_M h \quad , \tag{4.08}
$$

$$
i\omega C_P \Theta_P = \alpha(\Theta_S - \Theta_P) - \beta\Theta_P . \tag{4.09}
$$

On the other hand

$$
\Theta_S = \left(\frac{\partial T_S}{\partial M}\right)_H m + \left(\frac{\partial T_S}{\partial H}\right)_M h \quad . \tag{4.10}
$$

Elimination of Θ_S and Θ_P gives for the frequency dependence susceptibility (see ref. 10)

$$
\frac{\chi}{\chi_0} = \frac{\alpha \dfrac{\beta + i\omega C_P}{\alpha + \beta + i\omega C_P} + i\omega C_M}{\alpha \dfrac{\beta + i\omega C_P}{\alpha + \beta + i\omega C_P} + i\omega C_H} \quad , \tag{4.11}
$$

which can be written as

$$
\frac{\chi}{\chi_0} = 1 - F + F \frac{1 + i\omega \dfrac{C_P}{\beta}}{1 - \omega^2 \dfrac{C_H}{\alpha}\dfrac{C_P}{\beta} + i\omega\left[\left(\dfrac{1}{\alpha} + \dfrac{1}{\beta}\right) C_H + \dfrac{C_P}{\beta}\right]} \tag{4.12}
$$

Identifying this equation with (4.04) which we write as

$$
\frac{\chi}{\chi_0} = 1 - F + F \frac{1 + i\omega\{\tau_1 - a(\tau_1 - \tau_2)\}}{1 - \omega^2 \tau_1 \tau_2 + i\omega(\tau_1 + \tau_2)} \quad , \tag{4.13}
$$

gives

$$
\begin{aligned}
\tau_1 - a(\tau_1 - \tau_2) &= \frac{C_P}{\beta} \quad , \\
\tau_1 \tau_2 &= \frac{C_H}{\alpha}\frac{C_P}{\beta} \quad , \\
\tau_1 + \tau_2 &= \left(\frac{1}{\alpha} + \frac{1}{\beta}\right) C_H + \frac{C_P}{\beta} \quad .
\end{aligned} \tag{4.14}
$$

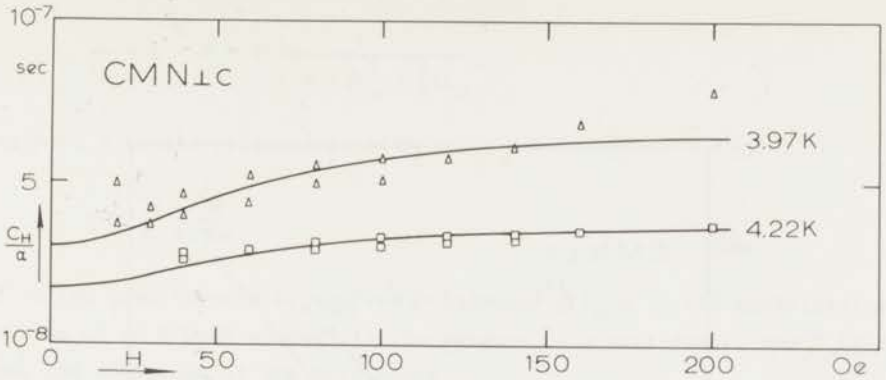

Fig. 4.05 The spin-lattice relaxation time, C_H/α, of the non-bottlenecked Orbach process as a function of the magnetic field in CMN $\perp$ c axis at 4.22 K and 3.97 K. Drawn lines according to the Brons-Van Vleck formula, with μ' equal to the theoretical value 2.2.

In these equations, we substitute the data of τ_1, τ_2, a, and C_H, and we obtain C_H/α, C_P/β, and C_H/β as a function of the magnetic field. The results are plotted in fig. 4.05, fig. 4.06, and fig. 4.07. C_H/α can be described by

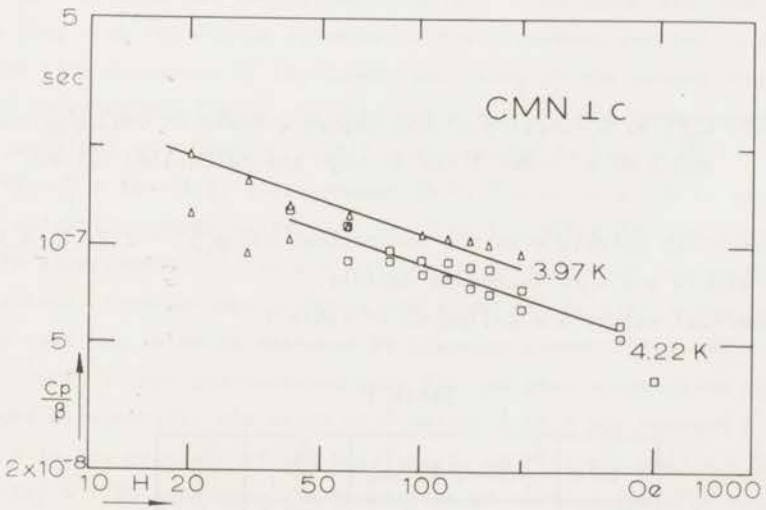

Fig. 4.06 C_P/β as a function of the magnetic field in CMN $\perp$ c axis at 4.22 K and 3.97 K. Drawn lines through the calculated values.

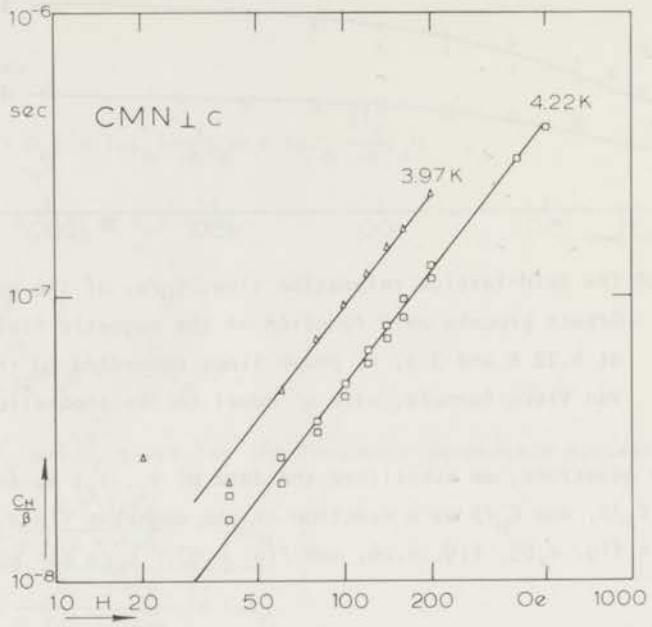

Fig. 4.07 C_H/β as a function of the magnetic field in CMN ⊥ c axis at 4.22 K and 3.97 K. Drawn lines through the calculated values.

the Brons-Van Vleck formula with the theoretical value $\mu' = 2.2$. C_P/β is found to decrease slowly and C_H/β increases rapidly.

The numerical values are collected in table I.

Table I

T in K	$\frac{C_H}{\alpha}(H=\infty)$ in sec	$\frac{C_P}{\beta}$	$\frac{C_H}{\beta}$
4.22	3.8×10^{-8}	$\propto H^{-0.3}$	$\propto H^{1.3}$
3.97	6.7×10^{-8}	$\propto H^{-0.3}$	$\propto H^{1.3}$

For fields H >> 500 Oe, we have $\omega C_p/\beta \ll 1$, and formula (4.12) transforms into

$$\frac{\chi}{\chi_0} = 1 - F + F \frac{1}{1 + i\omega(\frac{1}{\alpha} + \frac{1}{\beta})C_H} \quad . \tag{4.15}$$

So we have a single relaxation, with

$$\tau = \frac{C_H}{\alpha} + \frac{C_H}{\beta} \quad .$$

This is the same formula as derived by Stoneham[11]. C_H/α is the spin-lattice relaxation time of an Orbach process in the absence of a bottleneck, and C_H/β describes the influence of the bottleneck.

The two temperatures at which we were able to determine a value of C_H/α are too close together to derive a value for B as well as for Δ in the absence of a bottleneck.
With $\frac{\Delta}{k}$ = 35 K, we find $B_{Orb.} = 1.0 \times 10^{11}\ sec^{-1}$.

If we extrapolate the field dependence of C_H/β measured in low fields to high fields, we expect $\tau \propto H^{1.3}$. Above 2 K we found a practically temperature independent field dependence of τ: $\tau \propto H^{0.7}$, which indicates that C_H/β increases less rapidly as a function of H in large fields.

A possible explanation of the field dependence of the phonon bottleneck in the Orbach process has been given by Gill [12]. He associates the phonon relaxation time with the finite lifetime of the broadened excited levels. This relaxation time decreases if the Zeeman splitting of the ground doublet is reduced. In intermediate fields, he predicts $\tau \propto H^{0.5}$. The temperature dependence of τ^{-1} described by formula (4.01) and sketched in fig. 4.08.

We find $\frac{\Delta}{k}$ = 35 ± 1 K, just between 34 K, the value given by earlier paramagnetic relaxation experiments, and 36.25 K, the value derived from infrared absorption experiments [16]. At 2 K we see the influence of the bottlenecked direct process. From our measurements, we could not determine the value of A, but if we take the value as measured by Breur on concentrated CMN $A = 3.4 \times 10^{-2} H^2 sec^{-1} kOe^{-2}$, then the measured data fit the theoretical line quite well. (The slight curvature in the graph of $\frac{1}{\tau}$ versus $\frac{1}{T}$ at 4 kOe between 2.5 and 2 K.)

For B in the presence of the bottleneck, we find $B(1\ kOe) = 4.3 \times 10^9 sec^{-1}$ and $B(4\ kOe) = 1.80 \times 10^9 sec^{-1}$. A comparison of our results with results obtained by other authors is given in table 2.

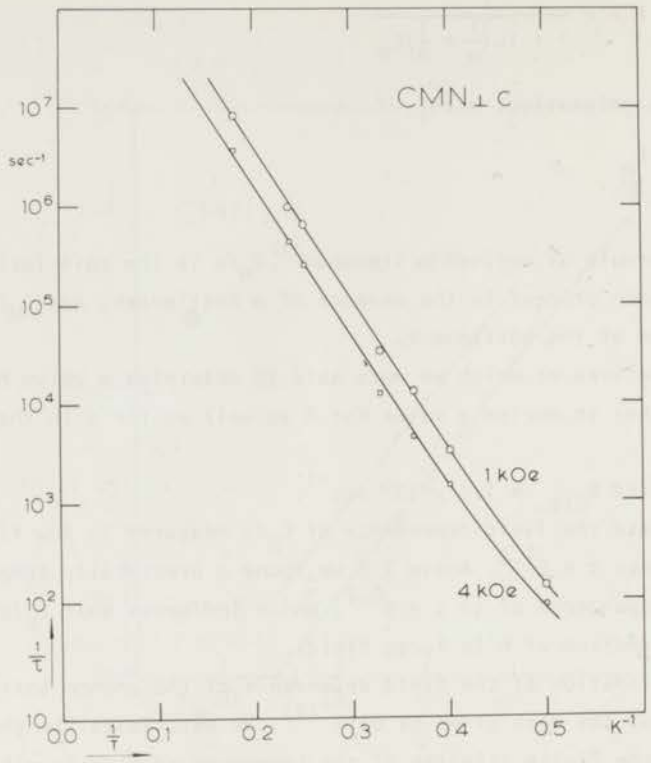

Fig. 4.08 $1/\tau$ versus $1/T$ in CMN⊥ c axis at 1 and 4 kOe.

Table 2

authors	method	Δ/k(K)	B(10^9 sec^{-1})
Finn et al. [1]	Casimir and du Pré	34	5 (1 kOe)
Cowen and Kaplan [13]	spin-echo	34	1.7
Hudson and Kaeser [14]	Casimir and du Pré	36.27	62.7(50 Oe)
Hudson and Mangum [15]	Casimir and du Pré	34.0 ±0.5	2.8(900 Oe)
Ruby et al. [3]	pulsed microwave	34	2.7(3.8 kOe)
Thornley [16]	infrared absorption	36.25±0.4	
Breur [4]	pulsed field		3.6
Giauque et al. [17]	specific heat	35.5 ±0.5	
This research	Casimir and du Pré	35 ±1	4.3 1 kOe
	thermod. model		100

4.4 Conclusion

At 4.22 K and 3.97 K we have observed that the relaxation process can be described by two relaxation times which correspond with the two times that follow from a simple thermodynamic model. From the measured values of the relaxation times and the intensities, we derived values for the non-bottlenecked Orbach relaxation time C_H/α, and the phonon relaxation time C_P/β and C_H/β. For large fields, the two step relaxation process transforms into a single relaxation, with $\tau = C_H/\alpha + C_H/\beta$. The values derived from our measurements are in good agreement with results obtained by other authors.

References

1) Finn, C.B.P., Orbach, R. and Wolf, W.P., Proc. Phys. Soc. (London) 77 (1961) 261.
2) Leifson, O.S. and Jeffries, C.D., Phys. Rev. 122 (1961) 1781.
3) Ruby, R.H., Benoit, H. and Jeffries, C.D., Phys. Rev. 124 (1962) 51.
4) Breur, W., thesis Amsterdam (1973).
5) Brons, F., thesis Groningen (1938).
6) Hoffmann, J.T. and Sapp, R.C., J. App. Phys. 39 (1968) 837.
7) De Vries, A.J. and Livius, J.W.M., Commun. Kamerlingh Onnes Lab., Leiden No. 349a; Appl. sci. Res. 17 (1967) 31.
8) Soeteman, J., thesis, to be published.
9) Gorter, C.J., Van der Marel, L.C. and Bölger, B., Physica 21 (1955) 103.
10) Van der Marel, L.C., thesis Leiden (1958).
11) Stoneham, A.M., Proc. Phys. Soc. 86 (1965) 1163.
12) Jill, J.C., J. Phys. C: Solid State Phys., 6 (1973) 109.
13) Cowen, J.A. and Kaplan, D.E., Phys. Rev. 124 (1961) 1098.
14) Hudson, R.P. and Kaeser, R.S., Nuovo Cimento 19 (1961) 1275.
15) Hudson, R.P. and Mangum, B.W., Nuovo Cimento 23 (1962) 1133.
16) Thornley, J.H.M., Phys. Rev. 132 (1963) 1492.
17) Giauque, W.F., Fisher, R.A., Hornung, E.W. and Brodale, G.E., J. Chem. Phys. 58 (1973) 2621.

CHAPTER 5

EXPONENTIAL TEMPERATURE DEPENDENCE OF THE LONGITUDINAL SPIN-SPIN RELAXATION TIME IN $CoCs_3Cl_5$ AND $CoCs_3Br_5$

Synopsis

The magnetic specific heat and longitudinal spin-spin relaxation time of single crystals of $CoCs_3Cl_5$ and $CoCs_3Br_5$ has been studied in the liquid helium and liquid hydrogen temperature regions. The complex susceptibility $\chi = \chi' - i\chi''$ along the tetragonal axes has been determined as a function of the external magnetic field up to 5 kOe with the aid of a twin T bridge.

The observed magnetic specific heat in the chloride can be described by $b/C = (550\ Oe)^2$ and $\Theta = -0.31$ K, and in the bromide by $b/C = (1070\ Oe)^2$ and $|\Theta| < 0.05$ K.

In both salts, the spin-spin relaxation time depends exponentially on the temperature, i.e. $\tau \propto \exp(\Delta/kT)$, with Δ equal to the splitting between the two Kramers doublets.

An explanation of the exponential temperature dependence is given.

5.1 *Introduction*

At liquid helium temperatures mainly the lowest Kramers doublets in $CoCs_3Cl_5$ and $CoCs_3Br_5$ are populated. This doublet is described by a very anisotropic g value with $g_\perp = 0$. Hence the non secular part of the interaction is much smaller than the secular part, and we expect weak coupling properties. If we consider only the lowest doublet, the non secular part is actually zero (section 5.5.1), therefore one may expect influence of the occupation of the upper doublet on the spin-spin relaxation process.

$CoCs_3Cl_5$ and $CoCs_3Br_5$, although crystallographic isomorphous, are magnetically inequivalent [1,2]. The b/C values as determined from the magnetic specific heat are considerably different, and both differ from values determined from the adiabatic susceptibility. This was reason enough for us to measure b/C once more. The difference in magnetic behaviour of $CoCs_3Cl_5$ and $CoCs_3Br_5$ is reflected in the relaxation times, which below 2.5 K show a quite different field behaviour.

5.2 *Crystal structure and Hamiltonian*

The crystal structure of $CoCs_3Cl_5$ has been determined by Powell and Wells [3], and in more detail by Figgis et al. [4]. The unit cell, containing four molecules $CoCs_3Cl_5$, is tetragonal and has the dimensions

$$a = 9.219 \pm 0.05 \text{ Å} \quad \text{and}$$
$$c = 14.554 \pm 0.07 \text{ Å} \ .$$

As far as the cobalt ions are concerned, a primitive orthorhombic unit cell can be constructed from the tetragonal unit cell, which then has the dimensions (fig. 5.01)

$$\tfrac{1}{2}a\sqrt{2} = 6.519 \text{ Å} \quad \text{and}$$
$$\frac{c}{2} = 7.277 \text{ Å} \ .$$

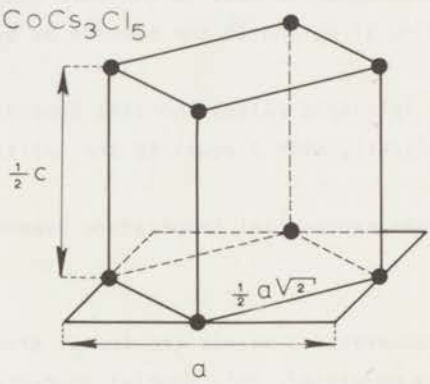

Fig. 5.01 Primitive orthorhombic unit cell of $CoCs_3Cl_5$. Only the Co^{2+} ions have been drawn.

$CoCs_3Br_5$ is isomorphous with $CoCs_3Cl_5$. The dimensions of its tetragonal unit cell are

$$a = 9.619 \pm 0.003 \text{ Å} \quad \text{and}$$
$$c = 15.163 \pm 0.003 \text{ Å} \ ,$$

from which for the dimensions of the orthorhombic unit cell follows:

$$\tfrac{1}{2}a\sqrt{2} = 6.801 \text{ Å} \quad \text{and}$$
$$\frac{c}{2} = 7.582 \text{ Å} \ .$$

The $^4F_{9/2}$ groundstate of the free cobalt ion is split in a tetrahedral

crystal field into an orbital singlet and two triplets, the singlet being lowest. The fourfold spin degeneracy is removed by a tetragonal distortion, resulting in two Kramers doublets. The two doublets can be described with S = 3/2 and by the following spin Hamiltonian

$$H^i = g_{//}\mu_B H_2 S_z^i + g\,\mu_B(H_x S_x^i + H_y S_y^i) + D\{(S_2^i)^2 - \frac{1}{3}S(S+1)\}\,, \quad (5.01)$$

where hyperfine interactions have been neglected. The z axis is chosen along the tetragonal axis of the crystal (c axis), giving the $S_z = \pm 3/2$ doublet as the lowest. The experimental values for the energy distance between the two Kramers doublets and g factors are given in table 1 [5].

Table 1

	$\frac{2D}{k}$(K)	$g_{//}$	$g_{\perp}$	$g'_{//}$	$g'_{\perp}$
$CoCs_3Cl_5$	- 12.4 ± 1%	2.40	2.30	7.20	0
$CoCs_3Br_5$	- 15.4 ± 2%	2.24	2.32	7.26	0

The value of 2D/k indicates that in the liquid helium temperature range, the population of the lower doublet $S_z = \pm 3/2$ is very much larger than the population of the upper doublet. Only the lowest doublet may be described by an effective spin S' = 1/2 and a very anisotropic g' value, which is given in table 1 as well.

The Hamiltonian for the whole spin system consists of the sum of Hamiltonians of the single ions and of interaction Hamiltonians between the single ions. These are the dipole dipole interaction,

$$H_{dip} = \tfrac{1}{2}\mu_B^2 \sum_{i,j\neq} \frac{1}{r_{ij}^3}\{(\overline{\overline{g}}^i\cdot\vec{S}^i)\cdot(\overline{\overline{g}}^j\cdot\vec{S}^j) - 3\,\frac{(\vec{r}_{ij}\cdot\overline{\overline{g}}^i\cdot\vec{S}^i)(\vec{r}_{ij}\cdot\overline{\overline{g}}^j\cdot\vec{S}^j)}{r_{ij}^2}\}\,, \quad (1.67)$$

and the isotropic Heisenberg exchange interaction

$$H_{ex} = \tfrac{1}{2}\sum_{i,j\neq} -2J\vec{S}^i\cdot\vec{S}^j \quad (1.70)$$

At very low temperatures, we have

$$H'_{dip} = \tfrac{1}{2}\mu_B^2 g_{//}^2 \sum_{i,j\neq} \frac{1}{r_{ij}^3}(1 - 3\zeta_{ij}^2)(S_z^i)'(S_z^j)' \quad , \tag{5.02}$$

(in which ζ_{ij} is the direction cosine with respect to the z axis), and an anisotropic Ising exchange:

$$H'_{ex} = -\tfrac{1}{2}\frac{J'}{S^2}\sum_{i,j\neq}(S_z^i)'(S_z^j)' \quad , \tag{5.03}$$

with $J' = 9/2\ J$ [6].

Van Stapele et al. [7] have measured the exchange interaction between Co^{2+} pairs in $ZnCs_3Cl_5$. They have found that the exchange interaction between two nearest-neighbour cobalt ions in the a-b plane is antiferromagnetic, with $J/k = -0.0204$ K, and that the exchange between two nearest-neighbour cobalt ions along the c axis is ferromagnetic, with $J/k = 0.0154$ K.

5.3 *Preparation of the crystals*

Blöte has prepared for us crystals of $CoCs_3Br_5$ and $CoCs_3Cl_5$ by slow evaporation of an aqueous solution of $CoCs_3Br_5$ and $CoCs_3Cl_5$, with supersaturation necessary in the latter case.

At our request, van den Broek had an analysis performed of a typical sample of $CoCs_3Br_5$ at the Philips Research Laboratories, Eindhoven, Netherlands. Special attention has been given to metal ion impurities. The result of the spectrochemical analysis is given in table 2.

Table 2

$CoCs_3Br_5$	Co	Cu	Mn	Ni	Fe	Cr
weight %	5.5	0.003	< 0.002	< 0.005	< 0.006	< 0.002

From table 2 one can conclude that the sample was rather pure; only a trace of copper could be detected. One may expect that this does not influence the spin-spin relaxation.

5.4 *Experiment*

Both the components of the susceptibility χ' and χ'' of single crystals $CoCs_3Cl_5$ and $CoCs_3Br_5$ have been measured with the aid of the twin T bridge, described in chapter 2. Small crystals of about 500 mg were used, and the

crystals were oriented with the tetragonal axis (c axis) parallel to the mutually parallel radiofrequency and static fields. The measurements were performed in the liquid hydrogen and liquid helium temperature range. We used fixed frequencies between 100 kHz and 30 MHz, and χ' and χ'' were registered directly as a function of the external magnetic field up to 5 kOe.

5.4.1 *b/C values*

The static susceptibility of $CoCs_3Cl_5$ and $CoCs_3Br_5$ at liquid helium temperatures can be described by a Curie-Weiss law

$$\chi_0 = \frac{C}{T - \Theta} ,$$

with a small negative Θ [2,5]. The adiabatic susceptibility for salts obeying a Curie-Weiss law is given by (1.58)

$$\frac{\chi_{ad}}{\chi_0} = \frac{b}{b + CH^2(T/T - \Theta)^3} .$$

The b/C value can be computed from the adiabatic susceptibility according to

$$\frac{b}{C} = \frac{H^2}{\chi_0/\chi_{ad} - 1} \left(\frac{T}{T - \Theta}\right)^3 . \qquad (5.04)$$

Defining

$$\left(\frac{b}{C}\right)_{exp} = \frac{H^2}{\chi_0/\chi_{ad} - 1} , \qquad (5.05)$$

it follows that

$$\left(\frac{b}{C}\right)_{th} = \left(\frac{b}{C}\right)_{exp} \left(\frac{T}{T - \Theta}\right)^3 , \qquad (5.06)$$

where we have added the subscript th to b/C in order to distinguish it from $(b/C)_{exp}$.

The real part of the frequency dependent susceptibility is given by

$$\chi'(\omega) = \chi'_{bet} + (\chi_{ad} - \chi'_{bet}) \frac{1}{1 + \omega^2\tau_{SS}^2} + (\chi_0 - \chi_{ad}) \frac{1}{1 + \omega^2\tau_{SL}^2} . \qquad (1.60a)$$

At liquid helium temperatures, the spin-lattice relaxation process in $CoCs_3Cl_5$ and $CoCs_3Br_5$ is much slower than the spin-spin relaxation process [2,8].

$\chi'(\omega)$ equals χ_{ad} at frequencies between the spin-lattice and spin-spin relaxation rate ($\tau_{SL}^{-1} << \omega << \tau_{SS}^{-1}$).

5.4.2 *b/C value of $CoCs_3Cl_5$*

Experimental b/C values have been derived from χ_{ad} according to formula (5.05). Starting, at a fixed frequency ω, from the situation in which $\chi'(\omega) = \chi_{ad}$, the relaxation rate decreases if the magnetic field increases. Spin-spin relaxation takes place, and finally $\chi'(\omega)$ becomes χ'_{bet}. We have measured χ' as a function of the external magnetic field up to 5 kOe, using different fixed frequencies. A typical graph of $H^2/(\chi_0/\chi' - 1)$ (for $\tau_{SL}^{-1} << \omega << \tau_{SS}^{-1}$ equal to $(b/C)_{exp}$) is given in fig. 5.02.

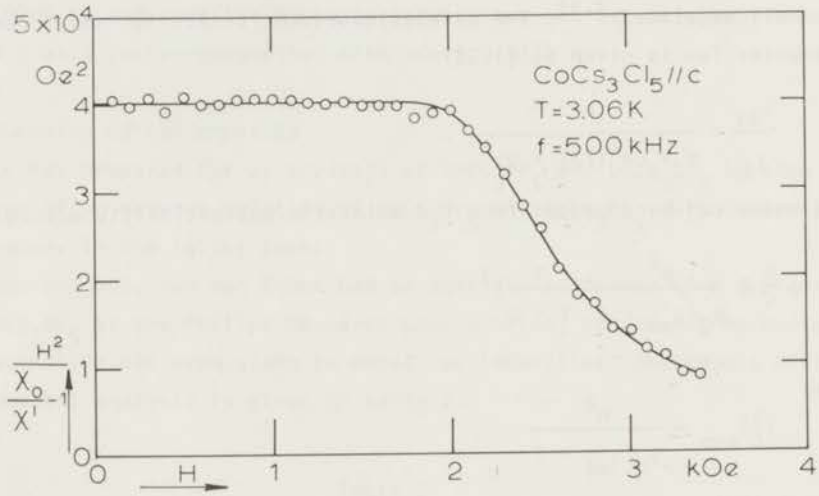

Fig. 5.02 Typical graph of $H^2/(\chi_0/\chi' - 1)$ versus H in $CoCs_3Cl_5$ // c axis, derived from a measurement at 3.06 K and 500 kHz. The line has been drawn through the experimental values.

The experimental values of b/C at liquid helium temperatures are collected in table 3.

According to formula (5.06) a graph of $(b/C)_{exp}^{1/3}$ versus 1/T should show a straight line. Indeed, the experimental values can be fitted by a straight line (fig. 5.03), determined by $b/C = (550\ Oe)^2$ and $\theta = -0.31$ K. If one calculates $(b/C)_{exp}$ using these values, the difference between the experimentally found values and the calculated values is less than 2%.

Table 3

T(K)	$(b/C)_{exp}(10^4 Oe^2)$
4.22	37.88
3.56	38.36
3.06	39.60
2.17	45.52
1.76	49.00

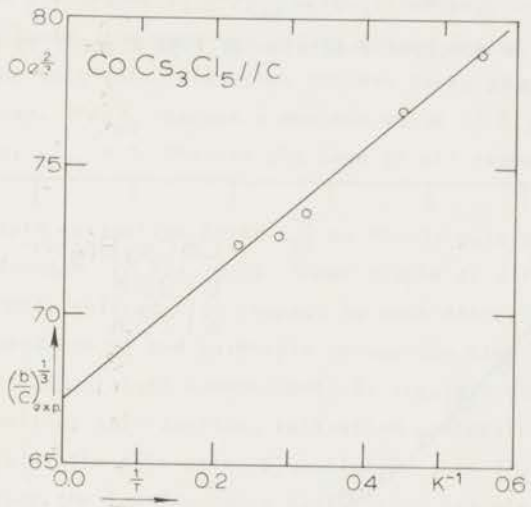

Fig. 5.03 Temperature dependence of $(b/C)_{exp}$ in $CoCs_3Cl_5$ // c axis. The drawn line corresponds to $(b/C)_{th} = (550\ Oe)^2$ and $\theta = -0.31$ K.

5.4.3 *b/C value of $CoCs_3Br_5$*

Above 2 K in the liquid helium range, the experimental b/C value is constant within the experimental accuracy of a few percent and is equal to $(1070\ Oe)^2$. Below 2 K, our measuring frequencies were too high to measure χ_{ad} directly. We could only measure the high frequency tail of the spin-spin relaxation process. At 1.98 K and 1.75 K, $\tau_{SS}^{-1}\ \chi_{ad}/\chi_0$ and χ_{ad}/χ_0 have been determined as follows. For $\omega\tau >> 1$ (see section 5.4.4)

$$\frac{\chi''}{\chi_{ad}} = \frac{1}{\omega\tau_{SS}} \quad , \tag{5.07}$$

so that

$$\omega\frac{\chi''}{\chi_0} = \omega\frac{\chi''}{\chi_{ad}}\frac{\chi_{ad}}{\chi_0} = \frac{1}{\tau_{SS}}\frac{\chi_{ad}}{\chi_0} \quad . \tag{5.08}$$

On the other hand, for all frequencies

$$\omega\frac{\chi'}{\chi''} = \frac{1}{\tau_{SS}} \quad , \tag{5.09}$$

so that

$$\frac{\chi_{ad}}{\chi_0} = \frac{\chi''}{\chi_0} \times \frac{\chi''}{\chi'} \quad . \tag{5.10}$$

From our measurements, we conclude that also at 1.98 K and 1.75 K b/C is equal to $(1070\ \text{Oe})^2$ (fig. 5.04).

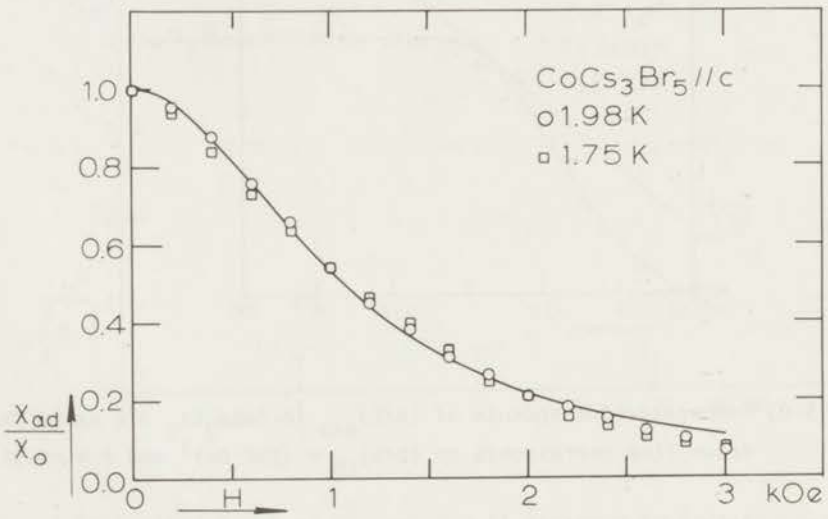

Fig. 5.04 χ_{ad}/χ_0 versus H in $CoCs_3Cl_5$ // c axis at 1.98 K and 1.75 K. The drawn line is a theoretical one for $b/C = (1070\ \text{Oe})^2$.

5.4.4 *Spin-spin relaxation times*

The imaginary part of the frequency dependent susceptibility is given by

$$\chi''(\omega) = (\chi_{ad} - \chi'_{bet})\frac{\omega\tau_{SS}}{1+\omega^2\tau_{SS}^2} + (\chi_0 - \chi_{ad})\frac{\omega\tau_{SL}}{1+\omega^2\tau_{SL}^2} \quad . \tag{1.60b}$$

In the region of spin-spin relaxation,

$$\frac{\chi''}{\chi_{ad}} = (1 - \frac{\chi'_{bet}}{\chi_{ad}}) \frac{\omega\tau_{SS}}{1 + \omega^2\tau_{SS}^2} \qquad \text{is valid.} \tag{5.11}$$

The maximum value of χ''/χ_{ad} is 0.5 $(1 - \chi'_{bet}/\chi_{ad})$ and this is reached for $\omega = \tau_{SS}^{-1}$.

5.4.5 *Spin-spin relaxation time in $CoCs_3Cl_5$*

The spin-spin relaxation times at liquid helium temperatures have been determined from the graphs of χ''/χ_{ad} versus frequency on a double logarithmic scale. At each field, the observed values can be fitted by a Debye curve, which implies that the spin-spin relaxation process takes place according to a single exponential decay. χ''/χ_{ad} reaches a maximum value of 0.5 at all field strengths, which means that $\chi'_{bet} = 0$. This is the case at all temperatures in the liquid helium range.

The spin-spin relaxation rates τ_{SS}^{-1} as found, multiplied by χ_{ad}/χ_0, have been plotted versus H^2 in fig. 5.05. These graphs at different temperatures are at first sight only shifted with respect to each other. This indicates the same temperature dependence of the spin-spin relaxation time for all fields, as χ_{ad}/χ_0 is almost temperature independent. At liquid hydrogen temperatures, spin-spin, as well as spin-lattice, relaxation was measured as a function of the magnetic field. The spin-spin relaxation in zero field was so fast that we could only measure the low frequency tail χ''/χ_0. Assuming that in the liquid hydrogen temperature region the spin-spin relaxation process is exponential as well, we determined the spin-spin relaxation time from this low frequency tail.

The temperature dependence of the spin-spin relaxation time is given in fig. 5.06, where we have plotted the relaxation rate τ_{SS}^{-1} on a logarithmic scale versus the inverse temperature T^{-1}, in zero field and for 2 kOe. From this figure it is evident that the temperature dependence of the relaxation time can be described by

$$\frac{1}{\tau_{SS}} = \frac{1}{\tau_{SS}(T = \infty)} \exp(-\Delta/kT) \quad . \tag{5.12}$$

The values of Δ and $\tau_{SS}^{-1}(T = \infty)$ are given in table 4.

5.4.6 *Spin-spin relaxation time in $CoCs_3Br_5$*

On account of the exceptional field dependence of χ''/χ_{ad} in this salt at temperatures below 2.5 K, the spin-spin relaxation times have been determined from the graphs of χ''/χ_0 versus the frequency. For all fields it is possible to

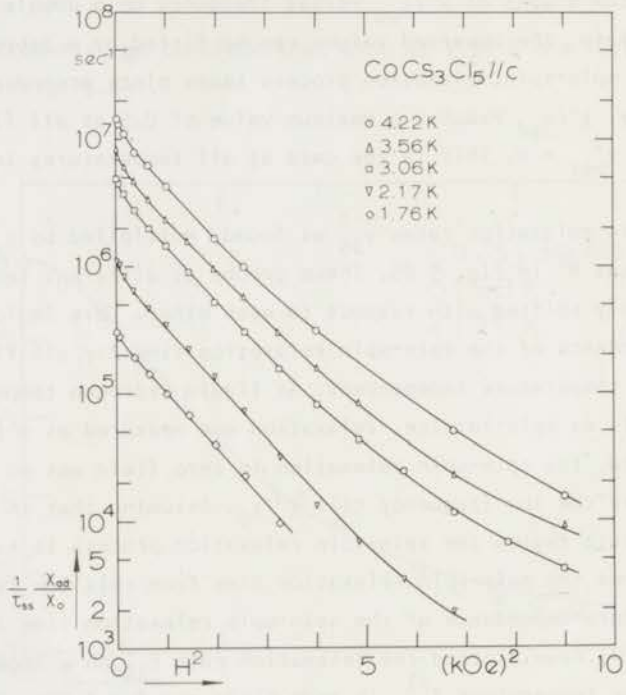

Fig. 5.05 $\tau_{SS}^{-1}\ \chi_{ad}/\chi_0$ versus H^2 in $CoCs_3Cl_5$ // c axis in the liquid helium range. Drawn lines through the experimental values.

fit the experimental results by Debye curves, so we deal with an exponential spin-spin relaxation process. χ'_{bet} is found to be zero. The maximum value of χ''/χ_0 was used to determine b/C in an alternative way. The graphs of $\tau_{SS}^{-1}\ \chi_{ad}/\chi_0$ versus H^2 in the liquid helium range are given in fig. 5.07.

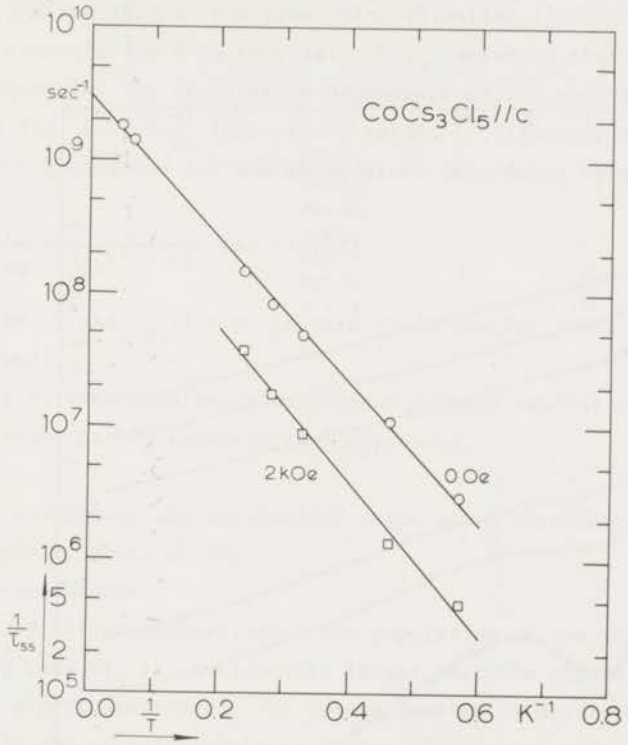

Fig. 5.06 Exponential temperature dependence of the spin-spin relaxation rate in $CoCs_3Cl_5$// c axis in zero field and for 2 kOe.

Table 4

	Δ/k(K)	$\tau_{SS}^{-1}(T=\infty)$ in sec^{-1}	field
$CoCs_3Cl_5$	12.4	3.0×10^9	0 Oe
	13.3	7.8×10^8	2 kOe
$CoCs_3Br_5$	15.4	2.2×10^9	0 Oe
	15.4	1.0×10^9	3 kOe

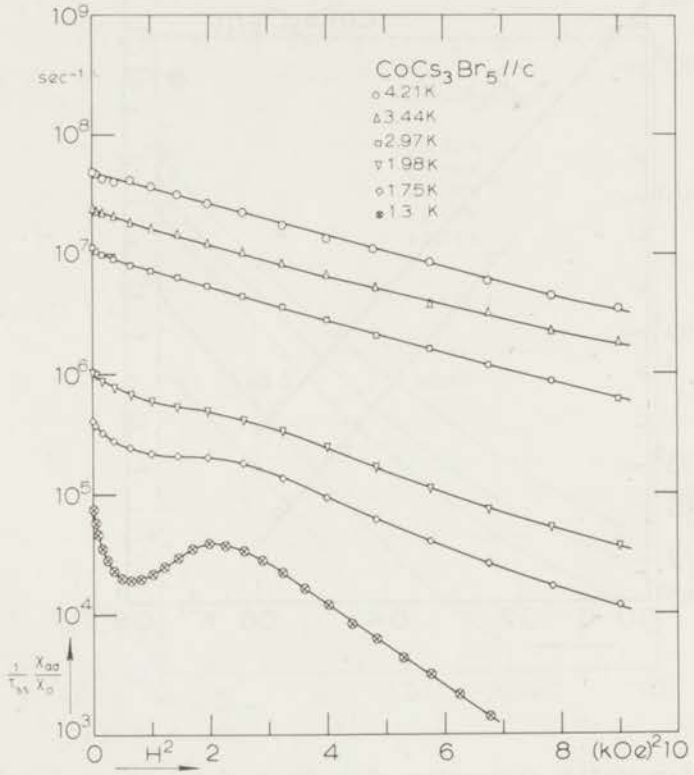

Fig. 5.07 $\tau_{SS}^{-1}\ \chi_{ad}/\chi_0$ versus H^2 in $CoCs_3Br_5$ // c axis in the liquid helium range. Drawn lines through the experimental values.

At the highest temperatures, 4.21 K, 3.44 K, and 2.97 K, the graphs of $\tau_{SS}^{-1}\ \chi_{ad}/\chi_0$ have the same shape, which indicates the same temperature dependence of the spin-spin relaxation time for all fields. The graphs of $\tau_{SS}^{-1}\ \chi_{ad}/\chi_0$ at the

lowest three temperatures (1.98 K, 1.75 K, and 1.3 K) are clearly different. As mentioned before, below 2 K we could only measure the high frequency tail of the spin-spin relaxation process, and consequently $\tau_{SS}^{-1}\ \chi_{ad}/\chi_0$ has been determined in the way as described in section 5.4.3. The absolute accuracy in the determination of $\tau_{SS}^{-1}\ \chi_{ad}/\chi_0$ in this way is not very high (especially at 1.3 K), but the relative accuracy is nevertheless a few percent.

At 20.3 K and 15.3 K, the spin-spin relaxation time in zero field has been determined from the low frequency tail χ''/χ_0, assuming that χ''/χ_0 is described by a Debye formula. The temperature dependence of the spin-spin relaxation time is given in fig. 5.08 (τ_{SS}^{-1} logarithmic versus T^{-1} linear). From this figure, it is evident that above 2 K the temperature dependence is exponential

$$\frac{1}{\tau_{SS}} = \frac{1}{\tau_{SS}(T = \infty)}\ \exp\ (-\Delta/kT)\quad . \tag{5.12}$$

The values of Δ and $\tau_{SS}^{-1}(T = \infty)$ in zero field and for 3 kOe are given in table 4 as well.

Below 2 K, the temperature dependence becomes smaller and the spin-spin relaxation might become temperature independent.

5.5 *Theory concerning the exponential temperature dependence of the spin-spin relaxation time*

5.5.1 *Introduction*

At liquid helium temperatures, the population of the lowest doublet in $CoCs_3Cl_5$ and $CoCs_3Br_5$ is considerably larger than the population of the upper doublet, as already mentioned. The lowest doublet is described by an effective spin S' = 1/2 and an anisotropic g' factor of which $g_\perp' = 0$. Such a description implies a fully secular dipole dipole interaction, and consequently, one might expect weak coupling theory to be applicable. For the dynamical spin-spin relaxation process however, we cannot restrict ourselves to the lowest doublet only. This may be seen in the following way. If we neglect the upper doublet and consider the relaxation rates τ_1^{-1} and τ_2^{-1} of the lowest doublet, then these are proportional to the non secular contributions $\langle\langle H_1' H_{-1}' \rangle\rangle^{\frac{1}{2}}$ and $\langle\langle H_2' H_{-2}' \rangle\rangle^{\frac{1}{2}}$ (formulae (1.106) and (1.107)). $\langle\langle H_1' H_{-1}' \rangle\rangle$ and $\langle\langle H_2' H_{-2}' \rangle\rangle$ are given by formulae (1.118), in which $(C_{\pm 0}^{ij})'$ and $(C_{\pm\pm}^{ij})'$ are given by formulae (1.77). For $g_x' = g_y' = g_\perp' = 0$ they all vanish. The relaxation rates τ_1^{-1} and τ_2^{-1} become zero as well, which means an infinitely long spin-spin relaxation time (or no spin-spin relaxation process at all). This remains true for all higher order processes which could cause relaxation in the ground doublet without taking into account

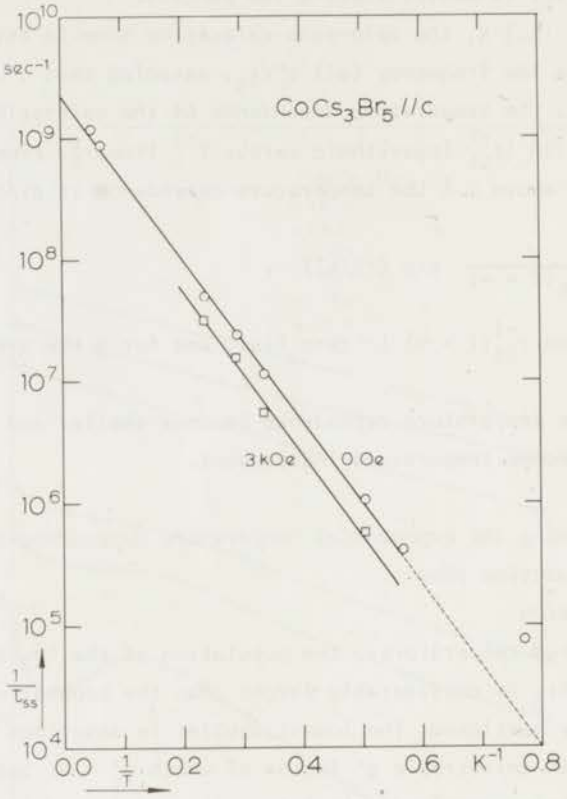

Fig. 5.08 Exponential temperature dependence of the spin-spin relaxation rate in $CoCs_3Br_5$ // c axis in zero field and for 3 kOe.

the higher levels. Thus we have to involve the upper doublet, even at very low temperatures. Both doublets are described by S = 3/2.

For an analysis of the spin-spin relaxation time we cannot make use of the theory as given in section 1.5, which was restricted to S = 1/2, and where a high temperature approximation was used as a starting point. Verbeek [9], in the theoretical part of his thesis, did not proceed from a high temperature

approximation, and we shall use his notation in this part of the thesis.

5.5.2 *Decomposition of H_{int} into common eigenoperators of L_Z and L_{el}*

In the theory of spin-spin relaxation for S = 1/2, the non secular part of the interaction $H_{n\,sec}$ is treated as a small perturbation to a large unperturbed Hamiltonian consisting of the Zeeman term H_Z and the secular part of the interaction H_{sec}. For that purpose, H_{int} is decomposed into eigenoperators of the Liouville Zeeman operator (section 1.5.2). Here the large unperturbed Hamiltonian is chosen to consist of the Zeeman term H_Z, the electric field term H_{el}, and the secular part of the interaction H_{sec}, and we decompose H_{int} into common eigenoperators of $L_Z \equiv \sum_i L_Z^i$ and $L_{el} \equiv \sum_i L_{el}^i$, where L_Z^i and L_{el}^i are the Liouville operators of a single ion. So we decompose H_{int} into eigenoperators A, satisfying the equations

$$L_Z A \equiv \frac{1}{\hbar}[H_Z, A] = \lambda A \qquad \text{and}$$

$$L_{el} A \equiv \frac{1}{\hbar}[H_{el}, A] = \mu A \quad , \tag{5.13}$$

for λ and μ scalars.

Common single spin eigenoperators of the single ion Liouville operators L_Z^i and L_{el}^i are $S_z^i (\equiv S_0^i)$ and the operators $A_{\alpha\beta}^i$; the latter correspond in the S_z-representation to the 4 x 4 matrices $(A_{\alpha\beta}^i)$, of which only the element $A_{\alpha\beta} = 1$, and all other elements are equal to zero.
For instance

$$(A_{12}^i) = \begin{pmatrix} 0 & 1 & 0 & 0 \\ 0 & 0 & 0 & 0 \\ 0 & 0 & 0 & 0 \\ 0 & 0 & 0 & 0 \end{pmatrix} \quad . \tag{5.14}$$

The eigenvalues of the sum $L_Z + L_{el}$ may be deduced from the equation

$$(L_Z + L_{el}) A_{\alpha\beta}^i \equiv \frac{1}{\hbar}[(H_Z + H_{el}), A_{\alpha\beta}^i] = \lambda_{\alpha\beta} A_{\alpha\beta}^i \quad ,$$

with

$$\lambda_{\alpha\beta} = \frac{1}{\hbar}(\varepsilon_\alpha - \varepsilon_\beta) \quad (\alpha,\beta = 1,2,3 \text{ and } 4)$$

and

$$\varepsilon_1 = \frac{3}{2} g_z \mu_B H + D \quad ,$$

$$\varepsilon_2 = \frac{1}{2} g_z \mu_B H - D \quad ,$$

$$\varepsilon_3 = -\frac{1}{2} g_z \mu_B H - D \quad , \qquad \text{and}$$
$$\varepsilon_4 = -\frac{3}{2} g_z \mu_B H + D \quad . \tag{5.15}$$

We do not need all eigenoperators $A^i_{\alpha\beta}$ to express H_{dip}. More complicated eigenoperators of the sum $L_Z + L_{el}$ are the two-spin operators $A^i_{\alpha\beta}A^j_{\gamma\delta}$, $i \neq j$ and $\alpha,\beta,\gamma,\delta = 1,2,3,4$, with

$$(L_Z + L_{el})A^i_{\alpha\beta}A^j_{\gamma\delta} = (\lambda_{\alpha\beta} + \lambda_{\gamma\delta})A^i_{\alpha\beta}A^j_{\gamma\delta} \quad . \tag{5.16}$$

The decomposition of H_{int} into two-spin eigenoperators of L_Z alone, constructed from the single spin eigenoperators S^i_+, S^i_- and S^i_0, is well known and given in section 1.5.2.
If we write S^i_+ and S^i_- as a combination of $A^i_{\alpha\beta}$'s,

$$S^i_+ = S^i_x + iS^i_y = \sqrt{3}\, A^i_{12} + 2A^i_{23} + \sqrt{3}\, A^i_{34} \qquad \text{and}$$
$$S^i_- = S^i_x - iS^i_y = \sqrt{3}\, A^i_{21} + 2A^i_{32} + \sqrt{3}\, A^i_{43} \quad , \tag{5.17}$$

then we automatically obtain the desired decomposition of H_{int} into the common eigenoperators $A^i_{\alpha\beta}A^j_{\gamma\delta}$.
The decomposition reads:

$$H_{int} = \sum_{p,q} H_{pq} \quad , \qquad \begin{matrix} p = -2,\ 0,\ 2 \\ q = -2,\ -1,\ 0,\ 1,\ 2, \end{matrix}$$

with

$$H_{00} = \tfrac{1}{2}\mu_B^2 \sum_{i,j\neq} [C^{ij}_{00} S^i_0 S^j_0 + C^{ij}_{+-}(3A^i_{12}A^j_{21} + 4A^i_{23}A^j_{32} + 3A^i_{34}A^j_{43})] \quad ,$$

$$H_{10} = \tfrac{1}{2}\mu_B^2 \sum_{i,j\neq} [C^{ij}_{+0} 2A^i_{23} S^j_0] \quad ,$$

$$H_{20} = \tfrac{1}{2}\mu_B^2 \sum_{i,j\neq} [C^{ij}_{++}(6A^i_{12}A^j_{34} + 4A^i_{23}A^j_{23})] \quad ,$$

$$H_{02} = \tfrac{1}{2}\mu_B^2 \sum_{i,j\neq} [C^{ij}_{+-}(2\sqrt{3}A^i_{12}A^j_{32} + 2\sqrt{3}A^i_{23}A^j_{43}) + C^{ij}_{++}A^i_{23}A^j_{43}] \quad ,$$

$$H_{04} = \tfrac{1}{2}\mu_B^2 \sum_{i,j\neq} [C^{ij}_{+-} 3A^i_{12}A^j_{43}] \quad ,$$

$$H_{12} = \tfrac{1}{2}\mu_B^2 \sum_{i,j\neq} [C^{ij}_{+0}\sqrt{3}A^i_{12} S^j_0] \quad ,$$

$$H_{1-2} = \tfrac{1}{2}\mu_B^2 \sum_{i,j\neq} [C^{ij}_{+0}\sqrt{3}A^i_{34}S^j_0] \quad ,$$

$$H_{22} = \tfrac{1}{2}\mu_B^2 \sum_{i,j\neq} [C^{ij}_{++}4\sqrt{3}A^i_{12}A^j_{23}] \quad ,$$

$$H_{2-2} = \tfrac{1}{2}\mu_B^2 \sum_{i,j\neq} [C^{ij}_{++}4\sqrt{3}A^i_{23}A^j_{34}] \quad ,$$

$$H_{24} = \tfrac{1}{2}\mu_B^2 \sum_{i,j\neq} [C^{ij}_{++}3A^i_{12}A^j_{12}] \quad \text{and}$$

$$H_{2-4} = \tfrac{1}{2}\mu_B^2 \sum_{i,j\neq} [C^{ij}_{++}3A^i_{34}A^j_{34}] \quad . \tag{5.18}$$

The H_{pq}'s have the following property

$$H_{pq} = (H_{-p-q})^{\dagger} \quad . \tag{5.19}$$

Therefore it is sufficient to give only half the number of terms. The meaning of the symbols p and q is explained by the eigenvalue equation:

$$(L_Z + L_{el})H_{pq} = (p\omega_L + q\,\frac{2D}{\hbar})H_{pq} \equiv \omega_{pq}H_{pq} \quad , \tag{5.20}$$

with $\omega_L = \dfrac{g_z\mu_B H}{\hbar}$, the Larmor frequency.

5.5.3 *The relaxation function without a high temperature approximation*

A formal expression of the relaxation function without making use of a high temperature approximation has been derived by Kubo [10]

$$\phi_{zz}(t,\vec{H}) = \beta(M_z, e^{iLt}M_z) \quad ,$$

in which the scalar product in operator space is defined by

$$(A,B) = \frac{1}{\beta}\int_0^{\beta} d\lambda \mathrm{Tr}\rho e^{\lambda H}A^{\dagger}e^{-\lambda H}B$$

$$= \frac{1}{\beta}\int_0^{\beta} d\lambda \mathrm{Tr}\rho(e^{\hbar\lambda L}A^{\dagger})B \quad ,$$

with $\beta = \dfrac{1}{kT}$

and $$\rho = \frac{e^{-\beta H}}{\mathrm{Tr}\, e^{-\beta H}} \quad . \tag{5.21}$$

In a high temperature approximation, the scalar product changes into

$$(A,B) = \frac{\mathrm{Tr} A^{\dagger} B}{\mathrm{Tr} I} = \langle\langle A^{\dagger} B \rangle\rangle \quad , \tag{5.22}$$

so that in that case we obtain for the relaxation function

$$\phi_{zz}(t,\vec{H}) = \beta \langle\langle M_z e^{iLt} M_z \rangle\rangle \quad . \tag{5.23}$$

The non vanishing part of the relaxation function in the limit for large t is taken into account as follows. The time average of the relaxation function, defined by

$$\overline{\phi}_{zz}(\vec{H}) \equiv \lim_{T\to\infty} \frac{1}{T} \int_0^T \phi_{zz}(t,\vec{H})\, dt \tag{5.24}$$

exists and is equal to [9]

$$\overline{\phi}_{zz}(\vec{H}) = \beta \{ (P_I M_z, P_I M_z) + (P_{H'} M_z, P_{H'} M_z) \} \quad , \tag{5.25}$$

where I = identity operator and $H' = H - P_I H$.
The projection operator P is defined by

$$P_A B = \frac{(A,B)}{(A,A)} A \quad . \tag{5.26}$$

The function which will be studied is

$$\Phi(t,\vec{H}) = \phi_{zz}(t,\vec{H}) - \overline{\phi}_{zz}(\vec{H}) \quad . \tag{5.27}$$

5.5.4 *The absorption spectrum*

At high temperatures $CoCs_3Cl_5$ and $CoCs_3Br_5$ possess a nearly isotropic g-tensor and Heisenberg exchange interaction. We can tell little about weak or strong coupling properties a priori. Hence we try to extend the method as given by Mazur and Terwiel for S = 1/2 in a high temperature approximation to the present case, without using the high temperature approximation as starting point. The function which will be studied can be written as

$$\Phi(t,\vec{H}) = \beta \{ (1 - P_I - P_{H'}) M_z, e^{iLt} (1 - P_I - P_{H'}) M_z \} \quad . \tag{5.28}$$

in the simple S = 1/2 case, when $H = H_Z + H_{int}$, this may be written as

$$\Phi(t,\vec{H}) = \beta H^{-2}\{(1 - P_I - P_{H'})H_Z, e^{iLt}(1 - P_I - P_{H'})H_Z\}$$

$$= \beta H^{-2}\{(1 - P_I - P_{H'})H_{int}, e^{iLt}(1 - P_I - P_{H'})H_{int}\} \quad , \quad (5.29)$$

which allows a simple analysis.
In the present case however, $H = H_Z + H_{el} + H_{int}$, so that only

$$\{(1 - P_I - P_{H'})(H_Z + H_{el}), e^{iLt}(1 - P_I - P_{H'})(H_Z + H_{el})\}$$

is still easy to analyse.
As we may expect that

$$\{(1-P_I-P_{H'})H_Z, e^{iLt}(1-P_I-P_{H'})H_Z\}, \quad \{(1-P_I-P_{H'})H_{el}, e^{iLt}(1-P_I-P_{H'})H_{el}\} ,$$

and the cross terms are equally complicated, an analysis of

$$\{(1 - P_I - P_{H'})M_z, e^{iLt}(1 - P_I - P_{H'})M_z\}$$

cannot be obtained in this way.
The strength of the analysis of

$$\{(1 - P_I - P_{H'})H_{int}, e^{iLt}(1 - P_I - P_{H'})H_{int}\}$$

lies in the fact that the replacement of L by L_Z and L_{el} in the exponent of the scalar product and in the projection operator does not completely destroy the dynamics of this function. The same can be said about the second derivative of $\Phi(t,\vec{H})$

$$\frac{\partial^2}{\partial t^2}\Phi(t,\vec{H}) = \frac{\partial^2}{\partial t^2}\phi_{zz}(t,\vec{H}) = -\beta(LM_z, e^{iLt}LM_z) \quad , \quad (5.30)$$

which moreover shows no complications due to the presence of $\overline{\phi}_{zz}(\vec{H})$.
The second time derivative can also be written as

$$\frac{\partial^2}{\partial t^2}\Phi(t,\vec{H}) = -\int_{-\infty}^{+\infty} d\omega e^{i\omega t} \frac{\omega\chi''(\omega)}{\pi} \quad . \quad (1.38)$$

Hence the Fourier spectrum of $(LM_z, e^{iLt}LM_z)$ equals $\frac{\omega\chi''(\omega)}{\pi}$.

5.5.5 *Analysis of the second time derivative of* $\Phi(t,\vec{H})$

Using the decomposition $H_{int} = \sum_{p,q} H_{pq}$, $p = -2,0,2$ $q = -2,-1,0,1,2,$ (5.18)

we have

$$\beta(LM_z, e^{iLt}LM_z) = \beta H^{-2}(L_z H_{int}, e^{iLt}L_z H_{int})$$

$$= \frac{\beta g_z^2 \mu_B^2}{\hbar^2} \sum_{p,q,r,s} p^2 (H_{pq}, e^{iLt} H_{2s}) \quad . \tag{5.31}$$

Now we make the approximation in which H is replaced by $H_z + H_{el}$. Following Verbeek, this approximation will be called the zero interaction approximation. In the zero interaction approximation not only is L Hermitean, i.e. $(A,LB) = (LA,B)$ but also $L_z + L_{el}$ becomes Hermitean:

$$(A,(L_z + L_{el})B)_{H_z+H_{el}} = ((L_z + L_{el})A,B)_{H_z+H_{el}} \quad .^{*} \tag{5.32}$$

Eigenoperators of $L_z + L_{el}$ belonging to different sets of eigenvalues become orthogonal, i.e. $(H_{pq},H_{rs})_{H_z+H_{el}} = 0$ for $p,q \neq r,s$.
In the zero interaction approximation, only the autocorrelation terms remain. Thus

$$\beta(LM_z, e^{iLt}LM_z) \rightarrow \beta \frac{g_z^2 \mu_B^2}{\hbar} \sum_{p,q} (H_{pq}, e^{i(L_z+L_{el})t} H_{pq})_{H_z+H_{el}} .$$

The autocorrelation terms are undamped oscillations

$$\beta \frac{g_z^2 \mu_B^2}{\hbar^2} p^2 (H_{pq}, e^{i(L_z+L_{el})} H_{pq})_{H_z+H_{el}} = \beta \frac{g_z^2 \mu_B^2}{\hbar^2} p^2 (H_{pq}, H_{pq})_{H_z+H_{el}} e^{i\omega_{pq}t}. \tag{5.33}$$

In the zero interaction approximation, apart from the zero frequency band, $\frac{\omega\chi''(\omega)}{\pi}$ consists of sixteen δ-lines at frequencies ω_{pq} ($p = -2,-1,1,2$ and $q = -2,-1,0,1,2$).

$\frac{\omega\chi''(\omega)}{\pi} = \omega^2 \times \frac{\chi''(\omega)}{\pi\omega}$. The absorption spectrum $\frac{\chi''(\omega)}{\pi\omega}$,

apart from the region around $\omega = 0$, can be constructed by dividing $\omega\chi''(\omega)/\pi$ by ω^2. As $\omega\chi''(\omega)/\pi$ consists of δ-lines it is sufficient to divide each δ-line by the square of its own center frequency. The intensities of the δ-lines of the absorption spectrum are thus given by

---

* The index $H_z + H_{el}$ indicates that in the scalar product H has been replaced by $H_z + H_{el}$ as well.

$$J_{pq} = \beta \frac{g_z^2 \mu_B^2 p^2}{\hbar^2 \omega_{pq}^2} (H_{pq}, H_{pq})_{H_Z + H_{el}} \quad . \tag{5.34}$$

Explicit expressions for these are given in table 5. The absorption spectrum is symmetric around $\omega = 0$, and so we need to give only half the number of terms. We want to compare the intensities of the absorption lines in the liquid helium range with χ_{ad}, being the total intensity of the absorption spectrum, including the zero frequency band. At liquid helium temperatures, we may neglect $e^{\beta D}$ relative to $e^{-\beta D}$ and 1, and for fields of a few kOe we may neglect $g_z \mu_B H$ relative to D. The expressions for the intensities, using these approximations, are also given in table 5. Finally are mentioned in table 5 the numerical values of the intensities of the δ-lines of $CoCs_3Cl_5$ at a temperature of 3 K and for a magnetic field of 2 kOe. For that purpose, we have performed a computer calculation of the sums $\sum_{i,j\neq} |c_{+0}^{ij}|^2$ and $\sum_{i,j\neq} |c_{++}^{ij}|^2$ for the primitive orthorhombic unit cell of $CoCs_3Cl_5$. The results for N (Avogadro's number) times the contribution per magnetic ion (including the interaction with 742 neighbours) are

$$\sum_{i,j\neq} |c_{+0}^{ij}|^2 = 6.62 \times 10^{67} \quad \text{and} \quad \sum_{i,j\neq} |c_{++}^{ij}|^2 = 9.88 \times 10^{69}.$$

Formally the temperature dependence of χ_{ad} is given by [9]

$$\chi_{ad_{zz}} = \beta((1 - P_I - P_{H'})M_z, (1 - P_I - P_{H'})M_z) \quad , \tag{5.35}$$

but a straightforward calculation for low temperatures is tedious. On the other hand the influence of the temperature on χ_{ad} is described by the thermodynamical relation

$$\frac{\chi_{ad}}{\chi_0} = \frac{b}{b + CH^2(T/T - \Theta)^3} \quad , \tag{1.58}$$

in which for the chloride $b/C = (550\ \text{Oe})^2$, $C = 4.99$ erg K Oe^{-2} and $\Theta = -0.31$ K. With the aid of these data, we calculate for a temperature of 3 K and a field of 2 kOe: $\chi_{ad} = 6.1 \times 10^{-2}$.

Hence a comparison of χ_{ad} and the non zero frequency part of the absorption spectrum teaches us that the non zero frequency part constitutes a negligible part of the total intensity. As a matter of fact, all intensity is contained in the zero frequency band. This confirms the experimental results that in the low frequency (relaxation) region, $\chi''(\omega)$ attains the maximum value $1/2\ \chi_{ad}$. This intensity distribution has led us to an important conjecture about

Table 5

Explicit expressions for the intensities of the absorption spectrum

$$J_{10} = \frac{g^2\mu_B^6 4e^{-\beta\varepsilon_3}(1-e^{-h\beta\omega_{10}})}{4\hbar^3\omega_{10}^3} \sum_{i,j\neq} \frac{Tr\, e^{-\beta H_j}(s_0^j)}{Tr\, e^{-\beta H_i} Tr\, e^{-\beta H_j}} |c_{+0}^{ij}|^2$$

$$J_{20} = \frac{g^2\mu_B^6 4(36e^{-\beta(\varepsilon_2+\varepsilon_4)}+32e^{-\beta 2\varepsilon_3})(1-e^{-h\beta\omega_{20}})}{4\hbar^3\omega_{20}^3} \sum_{i,j\neq} \frac{|c_{++}^{ij}|^2}{Tr\, e^{-\beta H_i} Tr\, e^{-\beta H_j}}$$

$$J_{11} = \frac{g^2\mu_B^6 3e^{-\beta\varepsilon_2}(1-e^{-h\beta\omega_{11}})}{4\hbar^3\omega_{11}^3} \sum_{i,j\neq} \frac{Tr\, e^{-\beta H_j}(s_0^j)^2}{Tr\, e^{-\beta H_i} Tr\, e^{-\beta H_j}} |c_{+0}^{ij}|^2$$

$$J_{1-1} = \frac{g^2\mu_B^6 3e^{-\beta\varepsilon_4}(1-e^{-h\beta\omega_{1-1}})}{4\hbar^3\omega_{1-1}^3} \sum_{i,j\neq} \frac{Tr\, e^{-\beta H_j}(s_0^j)^2}{Tr\, e^{-\beta H_i} Tr\, e^{-\beta H_j}} |c_{+0}^{ij}|^2$$

$$J_{21} = \frac{g^2\mu_B^6 4x48e^{-\beta(\varepsilon_2+\varepsilon_3)}(1-e^{-h\beta\omega_{21}})}{4\hbar^3\omega_{21}^3} \sum_{i,j\neq} \frac{|c_{++}^{ij}|^2}{Tr\, e^{-\beta H_i} Tr\, e^{-\beta H_j}}$$

$$J_{2-1} = \frac{g^2\mu_B^6 4x48e^{-\beta(\varepsilon_3+\varepsilon_4)}(1-e^{-h\beta\omega_{2-1}})}{4\hbar^3\omega_{2-1}^3} \sum_{i,j\neq} \frac{|c_{++}^{ij}|^2}{Tr\, e^{-\beta H_i} Tr\, e^{-\beta H_j}}$$

$$J_{22} = \frac{g^2\mu_B^6 4x18e^{-\beta 2\varepsilon_2}(1-e^{-h\beta\omega_{22}})}{4\hbar^3\omega_{22}^3} \sum_{i,j\neq} \frac{|c_{++}^{ij}|^2}{Tr\, e^{-\beta H_i} Tr\, e^{-\beta H_j}}$$

$$J_{2-2} = \frac{g^2\mu_B^6 4x18e^{-\beta 2\varepsilon_4}(1-e^{-h\beta\omega_{2-2}})}{4\hbar^3\omega_{2-2}^3} \sum_{i,j\neq} \frac{|c_{++}^{ij}|^2}{Tr\, e^{-\beta H_i} Tr\, e^{-\beta H_j}}$$

Table 5 continued

Approximate values	$\times \frac{(\text{center freq.})^2}{\beta}$
$J_{10} \approx \frac{9\, g^2 \mu_B^6 \beta e^{\beta 2D}}{8\, (g\mu_B H)^2} \sum_{i,j\neq} \lvert C_{+0}^{ij} \rvert^2 = 5.3 \times 10^{-6}$	4.5×10^{-54}
$J_{20} \approx \frac{9\, g^2 \mu_B^6 \beta e^{\beta 2D}}{(2g\mu_B H)^2} \sum_{i,j\neq} \lvert C_{++}^{ij} \rvert^2 = 1.6 \times 10^{-3}$	3.3×10^{-52}
$J_{11} \approx \frac{27\, g^2 \mu_B^6}{32\, (2\lvert D \rvert)^3} \sum_{i,j\neq} \lvert C_{+0}^{ij} \rvert^2 = 5.1 \times 10^{-9}$	8.5×10^{-68}
$J_{1-1} \approx \frac{27\, g^2 \mu_B^6}{32\, (2\lvert D \rvert)^3} \sum_{i,j\neq} \lvert C_{+0}^{ij} \rvert^2 = 5.1 \times 10^{-9}$	8.5×10^{-68}
$J_{21} \approx \frac{12\, g^2 \mu_B^6 e^{\beta 2D}}{(2\lvert D \rvert)^3} \sum_{i,j\neq} \lvert C_{++}^{ij} \rvert^2 = 1.7 \times 10^{-7}$	2.8×10^{-66}
$J_{2-1} \approx \frac{12\, g^2 \mu_B^6 e^{\beta 2D}}{(2\lvert D \rvert)^3} \sum_{i,j\neq} \lvert C_{++}^{ij} \rvert^2 = 1.7 \times 10^{-7}$	2.8×10^{-66}
$J_{22} \approx \frac{9\, g^2 \mu_B^6}{2\, (4\lvert D \rvert)^3} \sum_{i,j\neq} \lvert C_{++}^{ij} \rvert^2 = 5.1 \times 10^{-7}$	1.1×10^{-66}
$J_{2-2} \approx \frac{9\, g^2 \mu_B^6}{2\, (4\lvert D \rvert)^3} \sum_{i,j\neq} \lvert C_{++}^{ij} \rvert^2 = 5.1 \times 10^{-7}$	1.1×10^{-66}

the relaxation rate in the low frequency region, to be used in the next section.

In chapter 3 on the spin-spin relaxation in CMN, it was shown that in the case of strong coupling, the discrepancy between the predictions of Mazur and Terwiel, and those of Sauermann, mainly consists of a factor $(1 - \alpha)^2$ for the relaxation rate in large fields. This is probably due to the fact that Sauermann essentially applies the weak coupling approach to the strong coupling case, and one may doubt whether this procedure is justified. However, as in the present case $(1 - \alpha)^2 \simeq 1$, such a discrepancy is not to be expected, and we may use with some confidence the Sauermann approach. *In other words: for the validity of the weak coupling limit, the relative small intensity of the parallel field absorption lines at $\omega \neq 0$ might be crucial, rather than the weakness of the non secular part of the interaction.* The weak coupling limit may thus be sanctioned here through a proper choice of the temperature. This is in accordance with the intuitive approach, as given in the introductory section 5.5.1, on account of which we expect weak coupling properties.

For a small but finite interaction strength, we may expect that the absorption lines are still narrow, with approximately the same intensities as given in table 5, and correspondingly we may expect narrow lines for the Fourier spectrum $(LM_z, e^{iLt}LM_z)$. For a sufficiently strong field, we may hope that the overlap of the lines (and thus the contribution of cross-correlation terms) is still negligible.

5.5.6 *Low frequency region*

Up to now the low frequency region could not be considered. The conjectured applicability of the weak coupling approximation allows us to study the relaxation behaviour by means of the kernel or memory function $(LM_z, e^{iLt}LM_z)(A,A)^{-1}$ in the integral equation:

$$\frac{\partial \Phi(t,H)}{\partial t} = - \int_0^t \frac{(LM_z, e^{iLt}LM_z)}{(A,A)} \Phi(t - \tau, \vec{H}) d\tau \quad . \tag{5.36}$$

Here, $\Phi(t,\vec{H})$ is the relaxation function after deducting the non vanishing part of the relaxation function in the limit for large t,

$$\Phi(t,\vec{H}) = \phi_{zz}(t,\vec{H}) - \overline{\phi}_{zz}(\vec{H}) \quad , \tag{5.27}$$

and

$$(A,A) = ((1 - P_I - P_{H'})M_z, (1 - P_I - P_{H'})M_z) = \beta^{-1}\chi_{ad} \quad ^{9)} \quad . \tag{5.28}$$

In this presentation of the integral equation, the high temperature approximation has not been used.

The derivation of the relaxation rate in the weak coupling approximation, as given by Terwiel and Mazur for high temperatures and spin 1/2 systems, can easily be adapted to cover the present situation. $(\pi\tau_{SS})^{-1}$ is given by the zero frequency value of the memory spectrum (Fourier transform of the memory function). In the weak coupling approximation, the memory function is proportional to $(\mathcal{L}M_z, e^{i(\mathcal{L}_Z+\mathcal{L}_{el}+\mathcal{L}_{sec})t}\mathcal{L}M_z)$, which has the same zero interaction approximation, as was derived for $\beta^{-1}\partial^2\Phi(t,H)/\partial t^2$ in the preceding section. Hence with weak coupling and zero interaction, the memory spectrum is also seen to consist of sixteen narrow lines at frequencies ω_{pq}. The sum of the low frequency tails of these lines at $\omega = 0$ divided by χ_{ad} gives $(\pi\tau_{SS})^{-1}$. The intensities of these lines are obtained by multiplying the intensities of the absorption lines by the square of the center frequency and dividing them by β. The numerical values for the intensities of the narrow lines of the memory spectrum (in the same approximation as used earlier in table 5) have also been added to the table. Assuming that all lines have a width of the same order of magnitude, the relaxation rate is almost exclusively determined by the lines of the memory spectrum at $\pm\omega_{10} \equiv \pm\omega_L$ and $\pm\omega_{20} \equiv \pm 2\omega_L$ (see table 5). The lines at $\pm\omega_L$ are caused by $\Delta m = \pm 1$ transitions in the upper doublet. The lines at $\pm 2\omega_L$ are caused by the $\Delta m = \pm 2$ transitions between the upper and lower doublet, as schematically given in fig. 5.09.

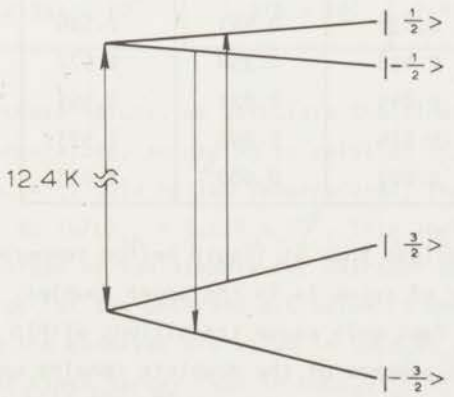

Fig. 5.09 $\Delta m = -2$ transition in $CoCs_3Cl_5$ // c axis.

The intensities of these four lines are proportional to $e^{2\beta D}$ (Cf. J_{10} and J_{20} in table 5). Assuming the width of these lines to be roughly temperature independent in the liquid helium region, one obtains for the temperature dependence of the relaxation rate

$$\frac{1}{\tau} \propto \frac{e^{2\beta D}}{\beta^{-1}\chi_{ad}} .$$

For temperatures a few times larger than $-\Theta$, χ_{ad} is proportional to T^{-1}, so that we arrive at the observed exponential temperature dependence of the spin-spin relaxation time:

$$\tau^{-1} \propto e^{2\beta D} .$$

5.6 *Discussion*

5.6.1 *b/C values*

The ratio of the occupation numbers of the upper and lowest doublets n_u/n_l in $CoCs_3Cl_5$ and $CoCs_3Br_5$ is given by the Boltzman factor, exp (2D/kT). For the values of 2D as given in table 1, this ratio has been calculated for a few temperatures in the liquid hydrogen and helium ranges (table 6).

Table 6

T(K)	n_u/n_l		final b/C
	chloride	bromide	chloride
20	0.538	0.463	2.506
15	0.438	0.358	2.572
4	0.045	0.021	2.953
3	0.016	0.006	2.993
2	0.002	0.000^5	3.013

From the table, one can conclude that at liquid helium temperatures, only a few percent of the total number of spins is in the upper doublet. With our radio frequency field, we can in fact only cause transitions within the doublets. So the ratio of the occupation numbers of the doublets remains unchanged. The splitting of the lower doublet is about 0.5×10^{-4} $Oe^{-1}K^{-1}$ (of the upper doublet a factor 3 smaller), so that for a field up to a few kOe, above 2 K, the temperature is large compared to the splittings, and we may apply for each doublet

a high temperature approximation. The total b/C value for temperatures high compared to the splittings but small compared to $|2D|/k$ is thus given by

$$b/C = n_u/(n_u + n_l)(b/C)_u + n_l/(n_u + n_l)(b/C)_l \quad , \tag{5.29}$$

in which $(b/C)_u$ is the b/C value of the upper doublet,

and $(b/C)_l$ is the b/C value of the lowest doublet.

The b/C value of each doublet consists of a contribution of the dipole dipole interaction, a contribution of the exchange interaction, and a dipole exchange cross term.

The values of b_{dip}/C for the upper and lowest doublets in $CoCs_3Cl_5$ and $CoCs_3Br_5$ have been calculated on the computer. $(2n + 1)^3 - 1$ neighbours (with $n = 3$) have been taken into account, and the results are given in table 7. In the same table we have given the values of $(b/C)_u$ and $(b/C)_l$. For the upper doublet we have used an isotropic Heisenberg exchange with $J/k = -0.0204$ K in the a-b plane and $J/k = 0.0154$ along the c axis. For the lowest doublet we have used as well in the a-b plane as along the c axis an anisotropic Ising exchange with $J'/k = 9/2\ J/k$ (Cf. section 5.4.1).

Table 7

	$b_{dip}/C(0e^2)$		$b_{tot}/C(0e^2)$	
	upper doublet	lower doublet	upper doublet	lower doublet
$CoCs_3Cl_5$ // cas	2.971×10^4	6.789×10^4	1.557×10^5	3.016×10^5
$CoCs_3Br_5$ // cas	2.351×10^4	5.375×10^4	1.472×10^5	2.680×10^5

With the aid of these values, we calculate the final b/C value in $CoCs_3Cl_5$ as a function of temperature, according to relation (5.29). The values have been added to table 6. At liquid helium temperatures, the value is nearly constant, and almost equal to $(b/C)_{th} = 3.025 \times 10^5$. This implies that the exchange constants as reported by Van Stapele for pairs of cobalt ions in $ZnCs_3Cl_5$ give a good description for the observed b/C value in undiluted $CoCs_3Cl_5$ as well.

To describe the observed b/C value in $CoCs_3Br_5$, the exchange constants should be several times larger than in $CoCs_3Cl_5$. If we assume that the different exchange constants are enlarged with the same factor, then we should take $J'/k = -0.27$ K ($J/k = 0.060$ K) in the a-b plane and $J'/k = 0.20$ K ($J/k = +0.044$ K) along the c axis.

In table 8 we compare our results with results obtained by other experimentalists.

Table 8

Experimentalist	Method	(b/C) (Oe^2) $CoCs_3Cl_5$	(b/C) (Oe^2) $CoCs_3Br_5$
Wielinga et al.	specific heat	4.00×10^4	6.50×10^5
Mess	adiab. susc	3.28×10^5	1.199×10^6 *
This research	adiab. susc.	3.025×10^5	
	from relax.times	3.025×10^5	1.144×10^6

From the table it is to be seen that the agreement between the adiabatic susceptibility measurements is fairly good (within 8% in the chloride and 5% in the bromide). The b/C value determined from specific heat measurements, however, is in $CoCs_3Cl_5$ considerably larger and in $CoCs_3Br_5$ considerably smaller. The Θ derived from our b/C measurements in $CoCs_3Cl_5$ (-0.31 K) is somewhat smaller than the value reported by Mess (-0.24 K). Recent measurements of the adiabatic susceptibility in this salt by Van Duyneveldt lead to a somewhat smaller Θ as well (Θ = -0.35 K).

5.6.2 *Spin-spin relaxation times*

In section 5.5 we have given an explanation of the observed exponential temperature dependence of the spin-spin relaxation time. The field dependence of $\tau_{SS}^{-1} \chi_{ad}/\chi_0$ in $CoCs_3Cl_5$ can be characterized by straight lines at all temperatures in the liquid helium region, and in $CoCs_3Br_5$ at the higher liquid helium temperatures. This indicates that we observe the shift of only one line of the memory spectrum as the magnetic field is increased. On account of the intensity as given in table 5, it is probably the line at $2\omega_L$. The width of this line is characterized by the square root of the slope of the straight lines of $\tau_{SS}^{-1} \chi_{ad}/\chi_0$ versus H^2. The roots are about 1000 Oe in $CoCs_3Cl_5$ and 1800 Oe in $CoCs_3Br_5$. As we expect, the widths are of the same order of magnitude as the secular interaction, which is greater in the bromide than in the chloride (550 Oe in $CoCs_3Cl_5$ and 1070 Oe in $CoCs_3Br_5$).

The field dependence of $\tau_{SS}^{-1} \chi_{ad}/\chi_0$ in $CoCs_3Br_5$ below 2.5 K is totally

* A reanalysis of the measurements of D.A. Curtis and A.J. Van Duyneveldt learns that Mess should have given this value.

different from that in the bromide above 2.5 K and from the field dependence of the chloride in the whole helium range. This confirms the different magnetic behaviour of these salts at very low temperatures.

References

1) Wielinga, R.F., thesis Leiden (1968).
Wielinga, R.F., Blöte, H.W.J., Roest, J.A. and Huiskamp, W.J., Physica 34 (1967) 223.
2) Mess, K.W., thesis Leiden (1969).
Mess, K.W., Lagendijk, E., Curtis, D.A. and Huiskamp, W.J., Physica 24 (1967) 126.
3) Powell, H.M. and Wells, A.F., J. Chem. Phys. Soc. (1935) 359.
4) Figgis, B.N., Gerloch, M. and Mason, R., Acta Cryst. 17 (1964) 506.
5) Van Stapele, R.P., Beljers, H.G., Bongers, P.F. and Zijlstra, H., J. Chem. Phys. 44 (1966) 3719.
6) Domb, C. and Miedema, A.R., Progr. low Temp. Phys. IV, ed. C.J. Gorter, North Holland Publ. Comp. Amsterdam (1964) 296.
7) Van Stapele, R.P., Henning, J.C.M., Hardeman, G.E.G. and Bongers, P.F., Phys. Rev. 150 (1966) 310.
8) Roest, J.A., thesis Leiden (1972).
9) Verbeek, P.W., thesis Leiden (1973).
10) Kubo, R., J. Phys. Soc. Japan 12 (1957) 570.

CHAPTER 6

LONGITUDINAL SPIN-SPIN RELAXATION IN COPPER BENZENE SULPHONATE HEXAHYDRATE

Synopsis

The b/C value and longitudinal spin-spin relaxation time of single crystals of $Cu(C_6H_5SO_3)_2 \cdot 6H_2O$ in the direction of the magnetic axes have been determined as a function of the external magnetic field up to 3 kOe.

Comparison of the calculated b/C value, taking into account the dipole dipole interaction, together with an estimate of the hyperfine interaction, indicates a considerable exchange interaction. The experimental results are therefore compared with the weak coupling theory.

6.1 *Introduction*

Single crystals of copper benzene sulphonate hexahydrate (to be called CBS) grow in light-blue plates parallel to the b-c plane. The g tensor, magnetic axes and line widths have been determined by Zimmerman et al. [1]. They report a considerable exchange narrowed Lorentzian resonance line in the b axis, as opposed to a Gaussian line in the c axis.

We have measured the b/C values and the longitudinal spin-spin relaxation times. In section 3 we will show that the secular part of the interaction is much larger than the non secular part. An analysis of the results, on the basis of the weak coupling theory, is made difficult by the presence of inequivalent copper ions, twinning in the crystal and hyperfine interactions.

6.2 *Crystal structure, g values and Hamiltonian*

To our knowledge, the crystal structure of CBS has not been determined. However, we expect $Cu(C_6H_5SO_3)_2 \cdot 6H_2O$ to be isomorphous to Zn - and $Mg(C_6H_5SO_3)_2 \cdot 6H_2O$. The latter structures have been determined by Broomhead and Nicol [2]. The monoclinic unit cell contains two molecules Zn-, Mg-, or in our case Cu-benzene sulphonate hexahydrate. On the basis of the morphological description of CBS as given by Groth [3], one can derive the following dimensions for the unit cell (fig. 6.01) [1]: a = 23.1 Å, b = 6.32 Å, c = 7.04 Å and $\beta = 93°22'$.

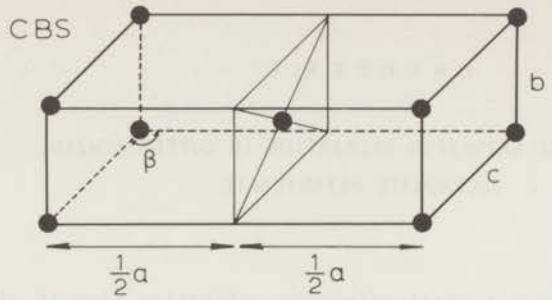

Fig. 6.01 Monoclinic unit cell of CBS. Only the Cu^{2+} ions have been drawn.

The measurements of Zimmerman et al. show that the copper ions in the unit cell, the corner ion (0,0,0) and the body centered ion $(\frac{1}{2},\frac{1}{2},\frac{1}{2})$, are not equivalent and that twinning occurs on a submicroscopic scale. This leads to four g tensors with different orientations.

The magnetic axes (principal axes of the static susceptibility tensor) appear to be the crystalline b and c axis and the a' axis, perpendicular to the b-c plane.

Besides dipole dipole interaction, we expect in CBS exchange and hyperfine interaction. For the magnetic field parallel to one of the magnetic axes, the isolated spin system has the following Hamiltonian

$$H = H_Z + H_{dip} + H_{ex} + H_{hfs} \ ,$$

with

$$H_Z = g\mu_B H \Sigma_i S_z^i \quad . \tag{6.01}$$

The exchange and hyperfine interaction in this salt are unknown. At most we can give an estimate of the hyperfine interaction from comparable copper salts.

6.3 *Experiment*

With the aid of the twin T bridge of chapter 2, χ' and χ'' of CBS have been measured as a function of the magnetic field up to 3 kOe. At higher fields both components become vanishingly small.

The measurements have been performed with the radio frequency and static field parallel to the magnetic axes of the crystal. No temperature dependence was observed at liquid hydrogen and liquid helium temperatures.

The frequencies were chosen between 1 and 30 MHz.

6.3.1 *b/C values*

The spin-lattice relaxation time in CBS at 20 K is of the order of magnitude of 10^{-4} sec and increases if the temperature is lowered. The spin-spin relaxation time is of the order of magnitude of 10^{-8} sec, so that the region of spin-spin relaxation is well separated from the region of spin-lattice relaxation at these temperatures.

$\chi'(\omega)$ becomes χ_{ad} for frequencies $\tau_{SL}^{-1} << \omega << \tau_{SS}^{-1}$.
The ratio χ_{ad}/χ_0 is given by

$$\frac{\chi_{ad}}{\chi_0} = \frac{b}{b + CH^2} \quad . \tag{1.56}$$

The values of b/C have been determined from the slope of the straight lines of χ_0/χ_{ad} versus H^2.
The results are given in table 1.

Table 1

	b/C(10^5 $0e^2$)	g	(b/C) g^2 in 10^5 $0e^2$	χ'_{bet}/χ_{ad}
a' axis	4.9	2.167	23.0	0.2
b axis	4.9	2.148	22.6	0.16
c axis	4.1	2.323	22.1	0.1

b is isotropic and C is proportional to g^2 (formula 1.93), so that b/C is proportional to g^{-2}. Therefore we have added to table 1 the g values in the direction of the magnetic axes (ref. 1) and the product (b/C) g^2. This product is found to be constant within a few percent.

6.3.2 *Spin-spin relaxation times*

If the spin-lattice and the spin-spin relaxation processes do not influence each other (such as is the case), the latter process is described by

$$\frac{\chi''}{\chi_{ad}} = (1 - \frac{\chi'_{bet}}{\chi_{ad}}) \frac{\omega\tau_{SS}}{1 + \omega^2\tau_{SS}^2} \quad .$$

The graphs of χ''/χ_{ad} versus the frequency can be fitted by Debye curves for all fields up to 3 kOe, for the a' axis as well as the b and c axis.

The spin-spin relaxation time has been determined from the frequency for

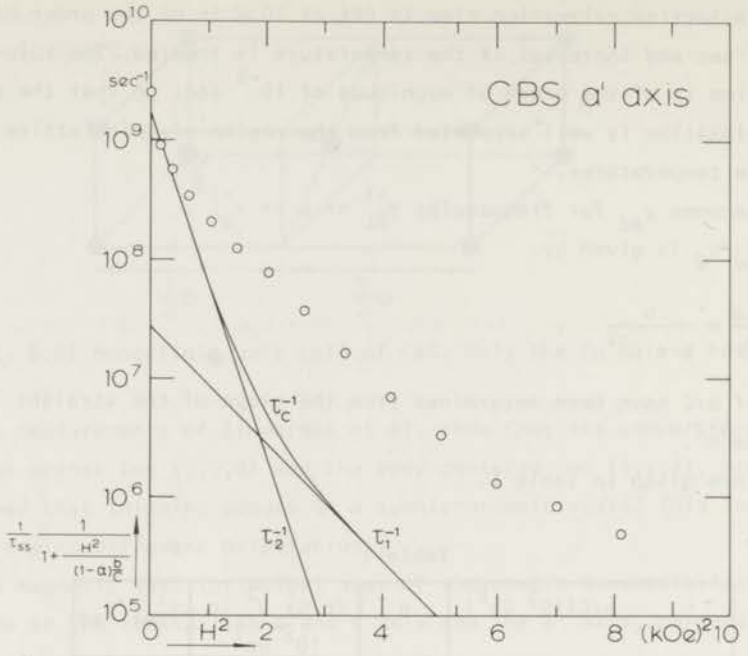

Fig. 6.02a

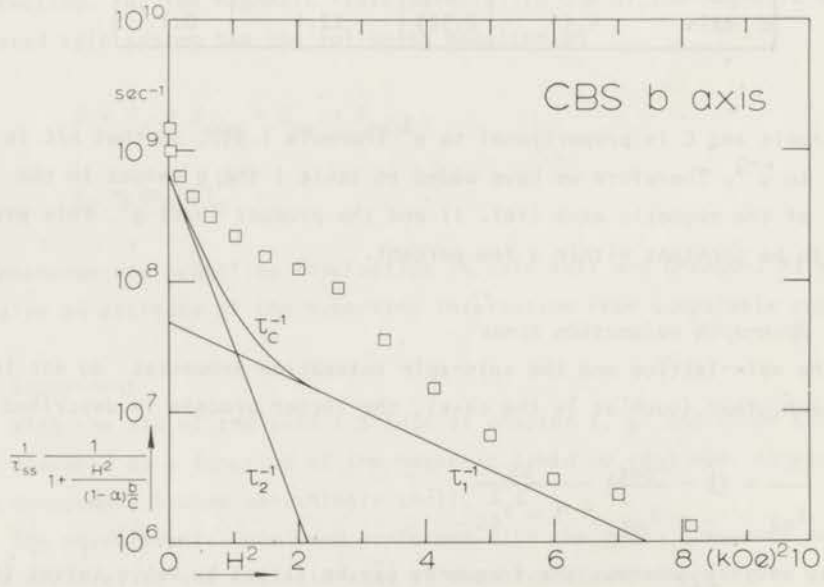

Fig. 6.02b

which the Debye curve has a maximum value. The ratio χ_{ad}/χ_0 to be denoted by α, has been determined from the value of this maximum itself. The ratios in the three different directions of the axes are also given in table 1. The relaxation rates τ_{SS}^{-1} multiplied by $[1 + H^2/((1 - \alpha)b/C)]^{-1}$ (see section 6.4.2), have been plotted in fig. 6.02a (a' axis), fig. 6.02b, (b axis) and fig. 6.02c (c axis).

6.4 *Discussion* 1

6.4.1 *b/C values*

We have for b/C in a high temperature approximation the following expression

$$\frac{b}{C} = \frac{\langle\langle H_{int}^2 \rangle\rangle}{Ng_z^2\mu_B^2 \frac{1}{3} S(S + 1)} \quad , \tag{1.93}$$

where it is assumed that deviations of Curie's law are negligible. H_{int} consists

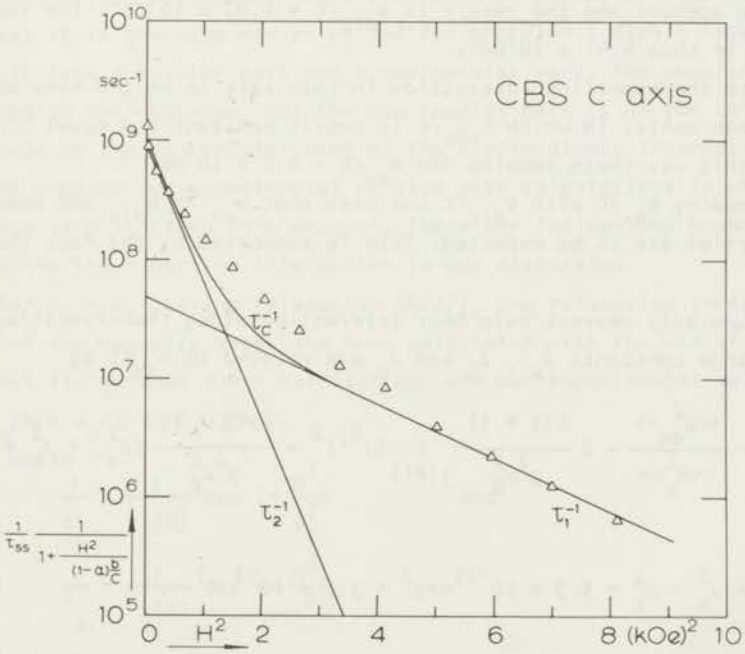

Fig. 6.02c

Figs. 6.02a,b,c $\dfrac{1}{\tau_{SS}} \dfrac{1}{1 + \dfrac{H^2}{(1 - \alpha)(b/C)}}$ versus H^2 in CBS. a: a' axis
b: b axis
c: c axis

The drawn lines are theoretical curves.
$\tau_1^{-1} + \tau_2^{-1}$ has been abbreviated as τ_C^{-1}.

of H_{dip}, H_{ex} and H_{hfs}. For equivalent ions with an isotropic g value, the cross terms $\langle\langle H_{dip} H_{ex} \rangle\rangle$, $\langle\langle H_{dip} H_{hfs} \rangle\rangle$ and $\langle\langle H_{ex} H_{hfs} \rangle\rangle$ vanish, so that

$$\langle\langle H_{int}^2 \rangle\rangle = \langle\langle H_{dip}^2 \rangle\rangle + \langle\langle H_{ex}^2 \rangle\rangle + \langle\langle H_{hfs}^2 \rangle\rangle \quad . \tag{6.03}$$

Consequently

$$\frac{b}{C} = \frac{b_{dip}}{C} + \frac{b_{ex}}{C} + \frac{b_{hfs}}{C} \quad . \tag{6.04}$$

The unknown way in which twinning occurs makes exact calculations impossible. Therefore no attempt has been made in this direction. The inequivalence of the copper ions and the twinning are neglected. We take as g value the average value of 2.21 and as b/C value $4.6 \times 10^5 0e^2$.

A computer calculation has been performed for b_{dip}/C. 342 neighbours have been taken into account and the result is $b_{dip}/C = 1.93 \times 10^4 0e^2$. The sum $b_{ex}/C + b_{hfs}/C$ is thus $4.41 \times 10^5 0e^2$.

We estimate the hyperfine interaction in this salt to be the same as in the copper Tutton salts, in which b_{hfs}/C is nearly constant and equal to $2 \times 10^4 0e^2$ [4]. In this way there remains for $b_{ex}/C = 4.2 \times 10^5 0e$.

If one compares b_{ex}/C with b_{dip}/C one sees that $b_{ex} >> b_{dip}$ and weak coupling properties are to be expected. This is supported by the fact that $\chi'_{bet} << \chi_{ad}$.

If we assume only nearest neighbour interaction along the crystallographic axes, the exchange constants $J_{a'}$, J_b and J_c are related to b_{ex}/C by

$$\frac{b_{ex}}{C} = \frac{\langle\langle H_{ex}^2 \rangle\rangle}{\langle\langle M_z^2 \rangle\rangle} = 2 \frac{S(S+1)}{g^2 \mu_B^2} \sum_{j(\neq i)} (J^{ij})^2 = \frac{4S(S+1)}{g^2 \mu_B^2} (J_{a'}^2 + J_b^2 + J_c^2) \quad . \tag{6.05}$$

Thus

$$J_{a'}^2 + J_b^2 + J_c^2 = 5.9 \times 10^{-35} erg^2 = 3.1 \times 10^{-3} K^3 \quad . \tag{6.06}$$

A crystal of CBS can be thought to consist of layers parallel to the b-c plane. The distance between copper ions in the layers (6.32 Å along the b axis and 6.96 Å along the c axis) is much smaller than the distance between the layers (about $\frac{1}{2}a = 11.2$ Å). We expect that due to this large distance and the internal structure of the crystal, the exchange interaction between copper ions of different layers can be neglected with respect to the exchange within the

layers.

Hence

$$J_b^2 + J_c^2 = 3.1 \times 10^{-3} K^2 \quad . \tag{6.07}$$

6.4.2 *Spin-spin relaxation times*

If the memory spectrum consists of Gaussian lines, the spin-spin relaxation time is given by

$$\frac{1}{\tau_{SS}} = \frac{H^2 + \frac{1}{2}H_{i\ sec}^2}{\frac{1}{2}H_{i\ sec}^2} \left(\frac{1}{\tau_1} + \frac{1}{\tau_2}\right) \quad , \tag{1.105}$$

with τ_1^{-1} and τ_2^{-1} given by (1.106) and (1.107).

The hyperfine interaction is of the same order of magnitude as the dipole dipole interaction, but small compared to the echange interaction. The exact influence of the hyperfine interaction on the relaxation time is uncertain. If we treat it in the same way as we did for the dipole dipole interaction, we can split it into a secular part and a non secular part. The secular part is small compared to the exchange, but the non secular part is of the same order of magnitude as the non secular part of the dipole dipole interaction.

We compare our experimental results with calculations in which only the exchange term is taken into account. There are indications however that we have to involve the hyperfine interaction in our discussion.

For $J_b = J_c$ obeying relaxation (6.07), the relaxation times in the directions of the magnetic axes have been calculated with the aid of a computer. The best fit between these calculations and our experimental values is obtained for $J_b/k = J_c/k = +0.0394$ K.

If we write

$$\frac{1}{\tau_1} = \frac{1}{\tau_1(0)} \exp\left(-\frac{H^2}{\gamma^2}\right) \qquad \text{and}$$

$$\frac{1}{\tau_2} = \frac{1}{\tau_2(0)} \exp\left(-\frac{H^2}{\gamma^2}\right) \quad ,$$

then the results of the calculation, in terms of $\tau_1(0)$, $\tau_2(0)$, γ_1 and γ_2, are given in table 2.

6.5 *Discussion* 2

If we neglect the hyperfine interaction, application of the weak coupling theory for $J_b = J_c = +0.0394$ K gives a particularly good agreement between

Table 2

	$\tau_1(0)$ in 10^{-8}sec	$\tau_2(0)$ in 10^{-10}sec	γ_1 in(kOe)^2	γ_2 in(kOe)^2
a' axis	3.65	5.90	0.881	0.302
b axis	2.04	15.2	1.91	0.332
c axis	2.05	10.2	1.93	0.371

theory and experiment in the c axis. The values computed from theory, come close to the experimental values for low and high fields in the direction of the b axis. In the a' axis there is only agreement for low fields.

The relaxation rate at low fields is mainly determined by τ_2^{-1} and at high fields almost exclusively by τ_1^{-1} (fig. 6.02). Therefore the assumptions made seem to be plausible to describe the experiments with respect to the calculation of τ_2.

The deviations between theory and experiment originate from τ_1^{-1}. The non secular part of the hyperfine interaction gives only extra terms to H_1 and H_{-1} and influences in this manner only τ_1^{-1} and not τ_2^{-1}. The second moment of the line in the memory spectrum at ω_L (proportional to γ_1) has the smallest value in the direction of the a' axis (see table 2). In this direction we may thus expect the largest influence of hyperfine and possibly other interactions which can give a non secular contribution to the total interaction. This could be a Dialoshinsky-Morya exchange term in the Hamiltonian.

The difference between theory and experiment in the b axis for intermediate fields, indicates that the lines of the memory spectrum at ω_L and $2\omega_L$ are not exactly Gaussian.

6.6 *Conclusion*

It is more or less surprising that we find a reasonable agreement between theory and experiment in the b and c axes, in spite of the simplifications made. The agreement is reasonable, in the c axis even good, concerning the magnitude as well as the field dependence of the relaxation rate. In the direction of the long magnetic axis, the a' axis, the agreement is poor. This is caused by the interactions which we have not taken into account and which mainly influence τ_1^{-1}.

References

1) Zimmerman, N.J., Van Santen, J.A. and Van den Handel, J., Physica 57 (1972) 334.

2) Broomhead, J.M. and Nicol, A.D.J., Acta Cryst. 1 (1948) 88.

3) Groth, P., Chem. Krystallographie IV, Wilhelm Englemann, Leipzig (1917).

4) Benzie, R.J., Cooke, A.H. and Whitley, S., Proc. Roy. Soc. London A232 (1955) 277.

A P P E N D I X

We suppose the Hamiltonian of the isolated spin system to consist of the following terms

$$H = H_Z + H_{dip} + H_{ex} + H_{hfs} \quad .$$

The decomposition of H_{dip} and H_{ex} into eigenoperators of the Liouville operator L_Z corresponding with H_Z, has been given in section 1.5.2.

$$H_{dip} + H_{ex} = \sum_k H_k, \qquad k = -2,-1,0,1,2 \text{ and}$$

$$H_0 = H_{dip\ 0} + H_{ex} \quad .$$

We decompose $H_{hfs} \equiv \sum_i \vec{I}^i \cdot \bar{\bar{A}}^i \cdot \vec{S}^i$ into eigenoperators of L_Z in the same way:

$$H_{hfs} = H_{-1\ hfs} + H_{0\ hfs} + H_{1\ hfs} \quad ,$$

with

$$H_{0\ hfs} = \sum_i A_z^i I_z^i S_0^i \quad \text{and}$$

$$H_{\pm 1\ hfs} = \tfrac{1}{2}\sum_i (A_x^i I_x^i \mp i A_y^i I_y^i) S_\pm^i \quad .$$

Here it has been assumed that the magnetic field is applied along one of the principal axes of the A tensor.

Explicit expressions for $\langle\langle H_0^2 \rangle\rangle$, $\langle\langle H_1 H_{-1} \rangle\rangle$, $\langle\langle H_2 H_{-2} \rangle\rangle$, $\langle\langle H_{int}^2 \rangle\rangle$, $\langle\langle [H_0,H_1][H_{-1},H_0] \rangle\rangle$ and $\langle\langle [H_0,H_2][H_{-2},H_0] \rangle\rangle$ for the dipole dipole and exchange interaction have been given in section 1.5.5. If the principal axes of the g and A tensors coincide, it is rather easy to take into account the hyperfine interaction. The expression becomes

$$\langle\langle H_0^2 \rangle\rangle = \langle\langle H_0^{de} \rangle\rangle + \frac{1}{9} I(I+1)S(S+1) \sum_i (A_z^i)^2 \quad ,$$

$$\langle\langle H_{1\ -1} \rangle\rangle = \langle\langle H_1^{de} H_{-1}^{de} \rangle\rangle + \frac{1}{18} I(I+1)S(S+1) \sum_i [(A_x^i)^2 + (A_y^i)^2] \quad ,$$

$$\langle\langle H_2 H_{-2}\rangle\rangle = \langle\langle H_2^{de} H_{-2}^{de}\rangle\rangle \quad ,$$

$$\langle\langle [H_0,H_1][H_{-1},H_0]\rangle\rangle = \langle\langle [H_0^{de},H_1^{de}][H_{-1}^{de},H_0]\rangle\rangle \quad +$$

$$+ \frac{1}{54}\mu_B^4 I(I+1)S^2(S+1)^2 \sum_{i,j\neq}\left\{\{(C_{00}^{ij})^2+(C_{+-}^{ij})^2\}\{(A_x^i)^2+(A_y^i)^2\}+|C_{+0}^{ij}|^2(A_z^i)^2\right\} +$$

$$+ \frac{1}{180} I(I+1)S(S+1)[2S(S+1)+2I(I+1)-3] \sum_i (A_z^i)^2+(A_y^i)^2] \quad \text{and}$$

$$\langle\langle [H_0,H_2][H_{-2},H_0]\rangle\rangle = \langle\langle [H_0^{de},H_2^{de}][H_{-2}^{de},H_0^{de}]\rangle\rangle \quad +$$

$$+ \frac{4}{27}\mu_B^4 I(I+1)S^2(S+1)^2 \sum_{i,j\neq} |C_{++}^{ij}|^2 (A_z^i)^2 \quad .$$

An Algol program has been written in order to calculate these expressions. The program is suitable for a crystal containing two equivalent ions in a unit cell. The principal axes of the anisotropic g and A tensors should coincide. Nearest neighbour exchange interaction along the crystallographic axes and between the two ions in the unit cell is assumed. The ions may contain, besides even isotopes, two odd isotopes.

The program reads:

```
//kaon1502 job (40102ha,0069),'hillaert     relax3',
// time=3 *lines=3
//staf exec algodclg,szc=108k,region.algol=204k,szg=104k,
// opt=opt1,tst=nt,region.go=204k
//algol.sysin dd *
'begin'
 'comment'
 programma ter berekening van de nulde en tweede momenten van de kern-
 funktie,de b/c-waarde en de relaxatietyd voor een gaussische kern-
 funktie.
 de berekening is voor een triklien kristal (assen a,b en c) met twee
 magnetische ionen per eenheidscel (afstand tussen de ionen r1) en een
 anisotrope g-tensor. nemen we het coordinatenstelsel langs de hoofd-
 assen van de g-tensor dan is deze diagonaal (diagonaalelementen gx,gy
 en gz). het magneetveld nemen we steeds evenwydig de z-as.
 de exchange-constanten in de kristalasrichtingen geven we aan met
 ja,jb en jc,de spinwaarde van het ion met s en het aantal kristal-
 afstanden waarover we de berekening uitvoeren met n.
 de kristalassen worden opgegeven in a.e. en de exchangeconstanten in k
 (dus eigenlyk j/k);
 'integer'n,i,j,k,t,u,v,p,q,r;
 'real'ax,ay,az,bx,by,bz,cx,cy,cz,r1x,r1y,r1z,r10,
       gx,gy,gz,ja,jb,jc,bj,gamma1,gamma2,a1x,a1y,a1z,a2x,a2y,a2z,g1,g2,
       bk,bm,hstr,an,wn,gbk,gbm,jambk,jbmbk,jcmbk,bjmbk,ex,bex,
       b1x,b1y,b1z,b2x,b2y,b2z,bxek,byek,bzek,
       sum1,sum2,sum3,sum4,sum5,sum6,sum7,sum8,sum9,sum10,sum11,sum12,
       som1,som2,som3,som4,som5,som6,som7,som8,som9,som10,som11,som12,
       sum13,sum23,sum33,sum43,sum14,sum24,sum34,sum44,
       sum15,sum25,sum35,sum45,sum16,sum26,sum36,sum46,
       subs1,subs2,subs3,subs4,cst1,cst2,
       s,x,i1,y1,i2,y2,
       de00,de01,de02,de0t,de21,de22,hf00,hf01,hf0t,hf21,hf22,
       omeg00,omeg01,omeg02,omeg0t,omeg21,omeg22,mom21,mom22,
       bdegc,bhfgc,bgc,bscgc,
       a1,b1,c1,d1,a2,b2,c2,d2,ma1,ma2,ro1,ro2,roc,ro,or1,or2,orc,or,
       h,hstep,endh;
 sysact(1,8,60);sysact(1,6,132);sysact(1,12,1);sysact(0,12,1);
 return:
 ininteger(0,n);'if'n =999'then''goto'stop;
 inreal(0,s);inreal(0,i1);inreal(0,i2);
 inreal(0,a1x);inreal(0,a1y);inreal(0,a1z);
 inreal(0,a2x);inreal(0,a2y);inreal(0,a2z);
 inreal(0,g1);inreal(0,g2);
 inreal(0,ax);inreal(0,ay);inreal(0,az);
 inreal(0,bx);inreal(0,by);inreal(0,bz);
 inreal(0,cx);inreal(0,cy);inreal(0,cz);
 inreal(0,r1x);inreal(0,r1y);inreal(0,r1z);
 inreal(0,gx);inreal(0,gy);inreal(0,gz);
 inreal(0,ja);inreal(0,jb);inreal(0,jc);inreal(0,bj);
 inreal(0,hstep);inreal(0,endh);
```

```
'begin'
'real''array'rx,ry,rz,r0,azz,apm,rapz,iapz,rapp,iapp,dx,dy,dz,d0,
bzz,bpm,rbpz,ibpz,rbpp,ibpp(/-n:n,-n:n,-n:n/);
sum1:=0;sum2:=0;sum3:=0;sum4:=0;sum5:=0;sum6:=0;sum7:=0;sum8:=0;
sum9:=0;sum10:=0;sum11:=0;sum12:=0;som1:=0;som2:=0;som3:=0;som4:=0;
som5:=0;som6:=0;som7:=0;som8:=0;som9:=0;som10:=0;som11:=0;som12:=0;
sum13:=0;sum23:=0;sum33:=0;sum43:=0;sum14:=0;sum24:=0;sum34:=0;
sum44:=0;sum15:=0;sum25:=0;sum35:=0;sum45:=0;sum16:=0;sum26:=0;
sum36:=0;sum46:=0;subs1:=0;subs2:=0;subs3:=0;subs4:=0;
'for'i:=-n'step'1'until'n'do'
'for'j:=-n'step'1'until'n'do'
'for'k:=-n'step'1'until'n'do'
'begin'
bk:=1.38026'-16;bm:=0.92712'-20;hstr:=1.054206'-27;an:=6.0248'+23;
wn:=1.98574'-16;gbk:=1.38026;gbm:=0.92712;
jambk:=ja*bk;jbmbk:=jb*bk;jcmbk:=jc*bk;bjmbk:=bj*bk;
b1x:=a1x*wn;b1y:=a1y*wn;b1z:=a1z*wn;
b2x:=a2x*wn;b2y:=a2y*wn;b2z:=a2z*wn;
'if'(i=1|i=-1)&j=0&k=0'then'ex:=4*ja*gbk/(gbm*gbm)'else'
'if'i=0&(j=1|j=-1)&k=0'then'ex:=4*jb*gbk/(gbm*gbm)'else'
'if'i=0&j=0&(k=1|k=-1)'then'ex:=4*jc*gbk/(gbm*gbm)'else'ex:=0;
'if'i=0&j=0&k=0'then'
'begin'
azz(/i,j,k/):=0;apm(/i,j,k/):=0;rapz(/i,j,k/):=0;iapz(/i,j,k/):=0;
rapp(/i,j,k/):=0;iapp(/i,j,k/):=0;
'end''else'
'begin'
rx(/i,j,k/):=i*ax+j*bx+k*cx;
ry(/i,j,k/):=i*ay+j*by+k*cy;
rz(/i,j,k/):=i*az+j*bz+k*cz;
r0(/i,j,k/):=sqrt(rx(/i,j,k/)*rx(/i,j,k/)+ry(/i,j,k/)*ry(/i,j,k/)+
rz(/i,j,k/)*rz(/i,j,k/));
azz(/i,j,k/):=2*(3*rz(/i,j,k/)*rz(/i,j,k/)/(r0(/i,j,k/)*r0(/i,j,k/))-1)
*gz*gz/(r0(/i,j,k/)*r0(/i,j,k/)*r0(/i,j,k/))+ex;
apm(/i,j,k/):=((3*rx(/i,j,k/)*rx(/i,j,k/)/(r0(/i,j,k/)*r0(/i,j,k/))-1)
*gx*gx+(3*ry(/i,j,k/)*ry(/i,j,k/)/(r0(/i,j,k/)*r0(/i,j,k/))-1)
*gy*gy)/(r0(/i,j,k/)*r0(/i,j,k/)*r0(/i,j,k/))+ex;
rapz(/i,j,k/):=rx(/i,j,k/)*rz(/i,j,k/)*gx*gz/(r0(/i,j,k/)*r0(/i,j,k/)
*r0(/i,j,k/)*r0(/i,j,k/)*r0(/i,j,k/));
iapz(/i,j,k/):=ry(/i,j,k/)*rz(/i,j,k/)*gy*gz/(r0(/i,j,k/)*r0(/i,j,k/)
*r0(/i,j,k/)*r0(/i,j,k/)*r0(/i,j,k/));
rapp(/i,j,k/):=((3*rx(/i,j,k/)*rx(/i,j,k/)/(r0(/i,j,k/)*r0(/i,j,k/))-1)
*gx*gx-(3*ry(/i,j,k/)*ry(/i,j,k/)/(r0(/i,j,k/)*r0(/i,j,k/))-1)
*gy*gy)/(r0(/i,j,k/)*r0(/i,j,k/)*r0(/i,j,k/));
iapp(/i,j,k/):=6*rx(/i,j,k/)*ry(/i,j,k/)*gx*gy/(r0(/i,j,k/)*r0(/i,j,k/)
*r0(/i,j,k/)*r0(/i,j,k/)*r0(/i,j,k/));
'end';
r10:=sqrt(r1x*r1x+r1y*r1y+r1z*r1z);
dx(/i,j,k/):=r1x+i*ax+j*bx+k*cx;
```

```
dy(/i,j,k/):=rly+i*ay+j*by+k*cy;
dz(/i,j,k/):=rlz+i*az+j*bz+k*cz;
d0(/i,j,k/):=sqrt(dx(/i,j,k/)*dx(/i,j,k/)+dy(/i,j,k/)*dy(/i,j,k/)+
dz(/i,j,k/)*dz(/i,j,k/));
'if'd0(/i,j,k/)>0&d0(/i,j,k/)<(r10+0.001*r10)'then'
bex:=4*bj*gbk/(gbm*gbm)'else'bex:=0;
bzz(/i,j,k/):=2*(3*dz(/i,j,k/)*dz(/i,j,k/)/(d0(/i,j,k/)*d0(/i,j,k/))-1)
*gz*gz/(d0(/i,j,k/)*d0(/i,j,k/)*d0(/i,j,k/))+bex;
bpm(/i,j,k/):=((3*dx(/i,j,k/)*dx(/i,j,k/)/(d0(/i,j,k/)*d0(/i,j,k/))-1)
*gx*gx+(3*dy(/i,j,k/)*dy(/i,j,k/)/(d0(/i,j,k/)*d0(/i,j,k/))-1)
*gy*gy)/(d0(/i,j,k/)*d0(/i,j,k/)*d0(/i,j,k/))+bex;
rbpz(/i,j,k/):=dx(/i,j,k/)*dz(/i,j,k/)*gx*gz/(d0(/i,j,k/)*d0(/i,j,k/)
*d0(/i,j,k/)*d0(/i,j,k/)*d0(/i,j,k/));
ibpz(/i,j,k/):=dy(/i,j,k/)*dz(/i,j,k/)*gy*gz/(d0(/i,j,k/)*d0(/i,j,k/)
*d0(/i,j,k/)*d0(/i,j,k/)*d0(/i,j,k/));
rbpp(/i,j,k/):=((3*dx(/i,j,k/)*dx(/i,j,k/)/(d0(/i,j,k/)*d0(/i,j,k/))-1)
*gx*gx-(3*dy(/i,j,k/)*dy(/i,j,k/)/(d0(/i,j,k/)*d0(/i,j,k/))-1)
*gy*gy)/(d0(/i,j,k/)*d0(/i,j,k/)*d0(/i,j,k/));
ibpp(/i,j,k/):=6*dx(/i,j,k/)*dy(/i,j,k/)*gx*gy/(d0(/i,j,k/)*d0(/i,j,k/)
*d0(/i,j,k/)*d0(/i,j,k/)*d0(/i,j,k/));
sum1:=sum1+azz(/i,j,k/)*azz(/i,j,k/);
sum2:=sum2+apm(/i,j,k/)*apm(/i,j,k/);
sum3:=sum3+(rapz(/i,j,k/)*rapz(/i,j,k/)+iapz(/i,j,k/)*iapz(/i,j,k/));
sum4:=sum4+(rapp(/i,j,k/)*rapp(/i,j,k/)+iapp(/i,j,k/)*iapp(/i,j,k/));
sum5:=sum5+azz(/i,j,k/)*rapz(/i,j,k/);
sum6:=sum6+apm(/i,j,k/)*rapz(/i,j,k/);
sum7:=sum7+azz(/i,j,k/)*iapz(/i,j,k/);
sum8:=sum8+apm(/i,j,k/)*iapz(/i,j,k/);
sum9:=sum9+(rapz(/i,j,k/)*rapz(/i,j,k/)+iapz(/i,j,k/)*iapz(/i,j,k/))
*((12*s*s+12*s+6)*azz(/i,j,k/)*azz(/i,j,k/)-(8*s*s+8*s-6)*azz(/i,j,k/)
*apm(/i,j,k/)+(20*s*s+20*s+15)*apm(/i,j,k/)*apm(/i,j,k/));
sum10:=sum10+apm(/i,j,k/)*rapp(/i,j,k/);
sum11:=sum11+apm(/i,j,k/)*iapp(/i,j,k/);
sum12:=sum12+(rapp(/i,j,k/)*rapp(/i,j,k/)+iapp(/i,j,k/)*iapp(/i,j,k/))
*(azz(/i,j,k/)*azz(/i,j,k/)+2*apm(/i,j,k/)*apm(/i,j,k/));
som1:=som1+bzz(/i,j,k/)*bzz(/i,j,k/);
som2:=som2+bpm(/i,j,k/)*bpm(/i,j,k/);
som3:=som3+(rbpz(/i,j,k/)*rbpz(/i,j,k/)+ibpz(/i,j,k/)*ibpz(/i,j,k/));
som4:=som4+(rbpp(/i,j,k/)*rbpp(/i,j,k/)+ibpp(/i,j,k/)*ibpp(/i,j,k/));
som5:=som5+bzz(/i,j,k/)*rbpz(/i,j,k/);
som6:=som6+bpm(/i,j,k/)*rbpz(/i,j,k/);
som7:=som7+bzz(/i,j,k/)*ibpz(/i,j,k/);
som8:=som8+bpm(/i,j,k/)*ibpz(/i,j,k/);
som9:=som9+(rbpz(/i,j,k/)*rbpz(/i,j,k/)+ibpz(/i,j,k/)*ibpz(/i,j,k/))
*((12*s*s+12*s+6)*bzz(/i,j,k/)*bzz(/i,j,k/)-(8*s*s+8*s-6)*bzz(/i,j,k/)
*bpm(/i,j,k/)+(20*s*s+20*s+15)*bpm(/i,j,k/)*bpm(/i,j,k/));
som10:=som10+bpm(/i,j,k/)*rbpp(/i,j,k/);
som11:=som11+bpm(/i,j,k/)*ibpp(/i,j,k/);
```

```
som12:=som12+(rbpp(/i,j,k/)*rbpp(/i,j,k/)+ibpp(/i,j,k/)*ibpp(/i,j,k/))
*(bzz(/i,j,k/)*bzz(/i,j,k/)+2*bpm(/i,j,k/)*bpm(/i,j,k/));
'end';
'for't:=-n'step'1'until'n'do'
'for'u:=-n'step'1'until'n'do'
'for'v:=-n'step'1'until'n'do'
'for'i:=-n'step'1'until'n'do'
'for'j:=-n'step'1'until'n'do'
'for'k:=-n'step'1'until'n'do'
'begin'
p:=i-t;q:=j-u;r:=k-v;
'if'abs(p)>nabs(q)>nabs(r)>n'then''goto'next;
sum13:=sum13+(rapz(/p,q,r/)*rapz(/p,q,r/)+iapz(/p,q,r/)*iapz(/p,q,r/))
*apm(/t,u,v/)*apm(/i,j,k/);
sum23:=sum23+(rapz(/p,q,r/)*rapz(/p,q,r/)+iapz(/p,q,r/)*iapz(/p,q,r/))
*bpm(/t,u,v/)*bpm(/i,j,k/);
sum33:=sum33+(rbpz(/p,q,r/)*rbpz(/p,q,r/)+ibpz(/p,q,r/)*ibpz(/p,q,r/))
*apm(/t,u,v/)*bpm(/i,j,k/);
sum43:=sum43+(rbpz(/p,q,r/)*rbpz(/p,q,r/)+ibpz(/p,q,r/)*ibpz(/p,q,r/))
*bpm(/t,u,v/)*apm(/i,j,k/);
sum14:=sum14+(azz(/p,q,r/)*apm(/p,q,r/)+azz(/p,q,r/)*apm(/t,u,v/)
+apm(/p,q,r/)*apm(/p,q,r/)+apm(/p,q,r/)*apm(/i,j,k/))*(rapz(/t,u,v/)
*rapz(/i,j,k/)+iapz(/t,u,v/)*iapz(/i,j,k/));
sum24:=sum24+(azz(/p,q,r/)*apm(/p,q,r/)+azz(/p,q,r/)*bpm(/t,u,v/)
+apm(/p,q,r/)*apm(/p,q,r/)+apm(/p,q,r/)*bpm(/i,j,k/))*(rbpz(/t,u,v/)
*rbpz(/i,j,k/)+ibpz(/t,u,v/)*ibpz(/i,j,k/));
sum34:=sum34+(bzz(/p,q,r/)*bpm(/p,q,r/)+bzz(/p,q,r/)*apm(/t,u,v/)
+bpm(/p,q,r/)*bpm(/p,q,r/)+bpm(/p,q,r/)*bpm(/i,j,k/))*(rapz(/t,u,v/)
*rbpz(/i,j,k/)+iapz(/t,u,v/)*ibpz(/i,j,k/));
sum44:=sum44+(bzz(/p,q,r/)*bpm(/p,q,r/)+bzz(/p,q,r/)*bpm(/t,u,v/)
+bpm(/p,q,r/)*bpm(/p,q,r/)+bpm(/p,q,r/)*apm(/i,j,k/))*(rbpz(/t,u,v/)
*rapz(/i,j,k/)+ibpz(/t,u,v/)*iapz(/i,j,k/));
sum15:=sum15+(rapp(/p,q,r/)*rapp(/p,q,r/)+iapp(/p,q,r/)*iapp(/p,q,r/))
*azz(/t,u,v/)*azz(/i,j,k/);
sum25:=sum25+(rapp(/p,q,r/)*rapp(/p,q,r/)+iapp(/p,q,r/)*iapp(/p,q,r/))
*bzz(/t,u,v/)*bzz(/i,j,k/);
sum35:=sum35+(rbpp(/p,q,r/)*rbpp(/p,q,r/)+ibpp(/p,q,r/)*ibpp(/p,q,r/))
*azz(/t,u,v/)*bzz(/i,j,k/);
sum45:=sum45+(rbpp(/p,q,r/)*rbpp(/p,q,r/)+ibpp(/p,q,r/)*ibpp(/p,q,r/))
*bzz(/t,u,v/)*azz(/i,j,k/);
sum16:=sum16+apm(/p,q,r/)*(azz(/p,q,r/)+azz(/i,j,k/))*(rapp(/t,u,v/)
*rapp(/i,j,k/)+iapp(/t,u,v/)*iapp(/i,j,k/));
sum26:=sum26+apm(/p,q,r/)*(azz(/p,q,r/)+bzz(/i,j,k/))*(rbpp(/t,u,v/)
*rbpp(/i,j,k/)+ibpp(/t,u,v/)*ibpp(/i,j,k/));
sum36:=sum36+bpm(/p,q,r/)*(bzz(/p,q,r/)+azz(/i,j,k/))*(rbpp(/t,u,v/)
*rapp(/i,j,k/)+ibpp(/t,u,v/)*iapp(/i,j,k/));
sum46:=sum46+bpm(/p,q,r/)*(bzz(/p,q,r/)+bzz(/i,j,k/))*(rapp(/t,u,v/)
*rbpp(/i,j,k/)+iapp(/t,u,v/)*ibpp(/i,j,k/));
```

```
next:
'end';
x:=s*s+s;y1:=i1*i1+i1;y2:=i2*i2+i2;
cst1:=(6.0248'-9)*gbm**4*x*x;cst2:=(6.0248'-41)*gbm**8*x*x;
de00:=(1.38889'-2)*cst1*(sum1+som1+2*sum2+2*som2);
de01:=0.5*cst1*(sum3+som3);
de02:=(1.38889'-2)*cst1*(sum4+som4);
de0t:=de00+2*de01+2*de02;
bxek:=0.01*(g1*y1*b1x*b1x+g2*y2*b2x*b2x);
byek:=0.01*(g1*y1*b1y*b1y+g2*y2*b2y*b2y);
bzek:=0.01*(g1*y1*b1z*b1z+g2*y2*b2z*b2z);
hf00:=0.111111*an*x*bzek;
hf01:=0.055556*an*x*(bxek+byek);
hf0t:=hf00+2*hf01;
omeg00:=de00+hf00;omeg01:=de01+hf01;omeg02:=de02;omeg0t:=de0t+hf0t;
bdegc:=de0t/(an*0.33333*x*gz*gz*bm*bm);
bhfgc:=hf0t/(an*0.33333*x*gz*gz*bm*bm);
bgc:=omeg0t/(an*0.33333*x*gz*gz*bm*bm);
bscgc:=omeg00/(an*0.33333*x*gz*gz*bm*bm);
subs1:=sum3*(sum1+3*sum2)+sum3*(som1+3*som2)+som3*(sum1+3*sum2)
      +som3*(som1+3*som2);
subs2:=sum5*sum5-sum5*sum6+sum6*sum6+sum7*sum7-sum7*sum8+sum8*sum8
      +sum5*som5-sum5*som6+sum6*som6+sum7*som7-sum7*som8+sum8*som8
      +som5*sum5-som5*sum6+som6*sum6+sum7*sum7-sum7*sum8+som8*sum8
      +som5*som5-som5*som6+som6*som6+som7*som7-som7*som8+som8*som8;
de21:=(4.16667'-2)*cst2*(x*(subs1+2*subs2+2*sum13+2*sum23+2*sum33
       +2*sum43-2*sum14-2*sum24-2*sum34-2*sum44)-0.1*sum9-0.1*som9);
subs3:=sum4*(sum1+sum2)+sum4*(som1+som2)+som4*(sum1+sum2)
      +som4*(som1+som2);
subs4:=sum10*sum10+sum11*sum11+sum10*som10+sum11*som11
      +som10*sum10+som11*sum11+som10*som10+som11*som11;
de22:=(2.31481'-3)*cst2*(x*(subs3+subs4+sum15+sum25+sum35+sum45-2*
      sum16-2*sum26-2*sum36-2*sum46)-0.05*(8*s*s+8*s+9)*(sum12+som12));
hf21:=cst1*((4.62962'-3)*(bxek+byek)*(sum1+som1+sum2+som2)+
      0.166667*bzek*(sum3+som3))+
      (5.55556'-5)*an*x*(g1*y1*(2*x+2*y1-3)*b1z*b1z*(b1x*b1x+b1y*b1y)+
      g2*y2*(2*x+2*y2-3)*b2z*b2z*(b2x*b2x+b2y*b2y));
hf22:=(9.25925'-5)*cst1*bzek*(sum4+som4);
omeg21:=de21+hf21;omeg22:=de22+hf22;
mom21:=omeg21/omeg01;
mom22:=omeg22/omeg02;
outstring(1,'('de eindantwoorden voor het kristal:')');sysact(1,14,3);
outstring(1,'('n=')');outinteger(1,n);sysact(1,2,33);
outstring(1,'('gx=')');outreal(1,gx);sysact(1,2,66);
outstring(1,'('ja/k=')');outreal(1,ja);
outstring(1,'('k dus ja=')');outreal(1,jambk);
outstring(1,'('erg')');sysact(1,2,33);
outstring(1,'('gy=')');outreal(1,gy);sysact(1,2,66);
```

```
outstring(1,'('jb/k=')');outreal(1,jb);
outstring(1,'('k dus jb=')');outreal(1,jbmbk);
outstring(1,'('erg')');sysact(1,14,1);
outstring(1,'('s=')'); outreal(1,s); sysact(1,2,33);
outstring(1,'('gz=')');outreal(1,gz);sysact(1,2,66);
outstring(1,'('jc/k=')');outreal(1,jc);
outstring(1,'('k dus jc=')');outreal(1,jcmbk);
outstring(1,'('erg')');sysact(1,2,66);
outstring(1,'('j'/k=')');outreal(1,bj);
outstring(1,'('k dus j'=')');outreal(1,bjmbk);
outstring(1,'('erg')');sysact(1,14,2);
outstring(1,'('        i1=')');outreal(1,i1);sysact(1,2,40);
outstring(1,'('a1x=')');outreal(1,a1x);
outstring(1,'('cm**-1')');sysact(1,2,80);
outstring(1,'('a2x=')');outreal(1,a2x);
outstring(1,'('cm**-1')');sysact(1,14,1);
outstring(1,'('        i2=')');outreal(1,i2);sysact(1,2,40);
outstring(1,'('a1y=')');outreal(1,a1y);
outstring(1,'('cm**-1')');sysact(1,2,80);
outstring(1,'('a2y=')');outreal(1,a2y);
outstring(1,'('cm**-1')');sysact(1,14,1);
outstring(1,'('gew.perc.1=')');outreal(1,g1);sysact(1,2,40);
outstring(1,'('a1z=')');outreal(1,a1z);
outstring(1,'('cm**-1')');sysact(1,2,80);
outstring(1,'('a2z=')');outreal(1,a2z);
outstring(1,'('cm**-1')');sysact(1,14,1);
outstring(1,'('gew.perc.2=')');outreal(1,g2);sysact(1,14,2);
outstring(1,'('ax=')');outreal(1,ax);
outstring(1,'('a.e.')');sysact(1,2,33);
outstring(1,'('bx=')');outreal(1,bx);
outstring(1,'('a.e.')');sysact(1,2,66);
outstring(1,'('cx=')');outreal(1,cx);
outstring(1,'('a.e.')');sysact(1,2,99);
outstring(1,'('r1x=')');outreal(1,r1x);
outstring(1,'('a.e.')');sysact(1,14,1);
outstring(1,'('ay=')');outreal(1,ay);
outstring(1,'('a.e.')');sysact(1,2,33);
outstring(1,'('by=')');outreal(1,by);
outstring(1,'('a.e.')');sysact(1,2,66);
outstring(1,'('cy=')');outreal(1,cy);
outstring(1,'('a.e.')');sysact(1,2,99);
outstring(1,'('r1y=')');outreal(1,r1y);
outstring(1,'('a.e.')');sysact(1,14,1);
outstring(1,'('az=')');outreal(1,az);
outstring(1,'('a.e.')');sysact(1,2,33);
outstring(1,'('bz=')');outreal(1,bz);
outstring(1,'('a.e.')');sysact(1,2,66);
outstring(1,'('cz=')');outreal(1,cz);
outstring(1,'('a.e.')');sysact(1,2,99);
```

```
 outstring(1,'('rlz=')');outreal(1,rlz);
 outstring(1,'('a.e.')');sysact(1,14,2);
 outstr9ng(1,'('afgedrukt wordt het getal van avogadro*het gemiddelde re
sultaat per ion')');sysact(1,14,2);
 outstring(1,'('het resultaat voor alleen dip-dip. plus exchange interac
tie')');sysact(1,14,1);
 outstring(1,'('<<h(0)*h(0)>>  =')');outreal(1,de00);
 outstring(1,'('erg**2')');sysact(1,2,50);
 outstring(1,'('<<(h(0),h(-1))*(h(+1),h(0))>>=')');outreal(1,de21);
 outstring(1,'('erg**4')');sysact(1,14,1);
 outstring(1,'('<<h(-1)*h(+1)>>=')');outreal(1,de01);
 outstring(1,'('erg**2')');sysact(1,2,50);
 outstring(1,'('<<(h(0),h(-2))*(h(+2),h(0))>>=')');outreal(1,de22);
 outstring(1,'('erg**4')');sysact(1,14,1);
 outstring(1,'('<<h(-2)*h(+2)>>=')');outreal(1,de02);
 outstring(1,'('erg**2')');sysact(1,14,1);
 outstring(1,'('<<hint*hint>>  =')');outreal(1,de0t);
 outstring(1,'('erg**2')');sysact(1,14,2);
 outstring(1,'('b dip-ex/c=')');outreal(1,bdegc);
 outstring(1,'('gauss**2')');sysact(1,14,2);
 outstring(1,'('het resultaat voor de hyperfynbydrage')');
 sysact(1,14,1);
 outstring(1,'('<<h(0)*h(0)>>  =')');outreal(1,hf00);
 outstring(1,'('erg**2')');sysact(1,2,50);
 outstring(1,'('<<(h(0),h(-1))*(h(+1),h(0))>>=')');outreal(1,hf21);
 outstring(1,'('erg**4')');sysact(1,14,1);
 outstring(1,'('<<h(-1)*h(+1)>>=')');outreal(1,hf01);
 outstrin7(1,'('erg**2')');sysact(1,2,50);
 outstring(1,'('<<(h(0),h'-2))*(h(+2),h(0))>>=')');outreal(1,hf22);
 outstring(1,'('erg**4')');sysact(1,14,1);
 outstring(1,'('<<hint*hint>>  =')');outreal(1,hf0t);
 outstring(1,'('erg**2')');sysact(1,14,2);
 outstring(1,'('b hf/c    =')');outreal(1,bhfgc);
 outstring(1,'('gauss**2')');sysact(1,14,2);
 outstring(1,'('het resultaat voor dip-dip. plus exchange plus hyperfyn
 ')');sysact(1,14,1);
 outstring(1,'('<<h(0)*h(0)>>  =')');outreal(1,omeg00);
 outstrin7(1,'('erg**2')');sysact(1,2,50);
 outstring(1,'('<<(h(0),h(-1))*(h(+1),h(0))>>=')');outreal(1,omeg21);
 outstring(1,'('erg**4')');sysact(1,14,1);
 outstring(1,'('<<h(-1)*h(+1)>>=')');outreal(1,omeg01);
 outstrin7(1,'('erg**2')');sysact(1,2,50);
 outstring(1,'('<<(h(0),h(-2))*(h(+2),h(0))>>=')');outreal(1,omeg22);
 outstring(1,'('erg**4')');sysact(1,14,1);
 outstring(1,'('<<h(-2)*h(+2)>>=')');outreal(1,omeg02);
 outstrin7(1,'('erg**2')');sysact(1,2,50);
 outstring(1,'('<<(h(0),h(-1))*(h(+1),h(0))>>/<<h(-1)*h(+1)>>=')');
```

```
outreal(1,mom21);outstring(1,'('erg**2')');sysact(1,14,1);
outstring(1,'('<<hint*hint>> =')');outreal(1,omegOt);
outstring(1,'('erg**2')');sysact(1,2,50);
outstring(1,'('<<(h(0),h(-2))*(h(+2),h(0))>> /<<h(-2)*h(+2)>> =')');
outreal(1,mom22);outstring(1,'('erg**2')');sysact(1,14,2);
outstring(1,'('b/c       =')');outreal(1,bgc);
outstring(1,'('gauss**2')');sysact(1,14,1);
outstring(1,'('b sec/c   =')');outreal(1,bscgc);
outstring(1,'('gauss**2')');sysact(1,14,2);
outstring(1,'('sum1=')'); outreal(1,sum1); sysact(1,2,33);
outstring(1,'('sum4=')'); outreal(1,sum4); sysact(1,2,66);
outstring(1,'('sum7=')'); outreal(1,sum7); sysact(1,2,99);
outstring(1,'('sum10=')');outreal(1,sum10);sysact(1,14,1);
outstring(1,'('sum2=')'); outreal(1,sum2); sysact(1,2,33);
outstring(1,'('sum5=')'); outreal(1,sum5); sysact(1,2,66);
outstring(1,'('sum8=')'); outreal(1,sum8); sysact(1,2,99);
outstring(1,'('sum11=')');outreal(1,sum11);sysact(1,14,1);
outstrin7(1,'('sum3=')'); outreal(1,sum3); sysact(1,2,33);
outstring(1,'('sum6=')'); outreal(1,sum6); sysact(1,2,66);
outstring(1,'('sum9=')'); outreal(1,sum9); sysact(1,2,99);
outstring(1,'('sum12=')');outreal(1,sum12);sysact(1,14,2);
outstring(1,'('som1=')'); outreal(1,som1); sysact(1,2,33);
outstring(1,'('som4=')'); outreal(1,som4); sysact(1,2,66);
outstring(1,'('som7=')'); outreal(1,som7); sysact(1,2,99);
outstring(1,'('som10=')');outreal(1,som10);sysact(1,14,1);
outstrin7(1,'('som2=')'); outreal(1,som2); sysact(1,2,33);
outstring(1,'('som5=')'); outreal(1,som5); sysact(1,2,66);
outstring(1,'('som8=')'); outreal(1,som8); sysact(1,2,99);
outstring(1,'('som11=')');outreal(1,som11);sysact(1,14,1);
outstrin7(1,'('som3=')'); outreal(1,som3); sysact(1,2,33);
outstring(1,'('som6=')'); outreal(1,som6); sysact(1,2,66);
outstring(1,'('som9=')'); outreal(1,som9); sysact(1,2,99);
outstring(1,'('som12=')');outreal(1,som12);sysact(1,14,2);
outstring(1,'('sum13=')');outreal(1,sum13);sysact(1,2,33);
outstring(1,'('sum23=')');outreal(1,sum23);sysact(1,2,66);
outstring(1,'('sum33=')');outreal(1,sum33);sysact(1,2,99);
outstring(1,'('sum43=')');outreal(1,sum43);sysact(1,14,1);
outstring(1,'('sum14=')');outreal(1,sum14);sysact(1,2,33);
outstring(1,'('sum24=')');outreal(1,sum24);sysact(1,2,66);
outstring(1,'('sum34=')');outreal(1,sum34);sysact(1,2,99);
outstring(1,'('sum44=')');outreal(1,sum44);sysact(1,14,1);
outstring(1,'('sum15=')');outreal(1,sum15);sysact(1,2,33);
outstring(1,'('sum25=')');outreal(1,sum25);sysact(1,2,66);
outstring(1,'('sum35=')');outreal(1,sum35);sysact(1,2,99);
outstring(1,'('sum45=')');outreal(1,sum45);sysact(1,14,1);
outstring(1,'('sum16=')');outreal(1,sum16);sysact(1,2,33);
outstring(1,'('sum26=')');outreal(1,sum26);sysact(1,2,66);
outstring(1,'('sum36=')');outreal(1,sum36);sysact(1,2,99);
```

```
outstring(1,'('sum46=')');outreal(1,sum46);sysact(1,14,2);
outstring(1,'('subs1=')');outreal(1,subs1);sysact(1,2,33);
outstring(1,'('subs2=')');outreal(1,subs2);sysact(1,2,66);
outstring(1,'('subs3=')');outreal(1,subs3);sysact(1,2,99);
outstring(1,'('subs4=')');outreal(1,subs4);sysact(1,14,2);
a1:=hstr*0.33333*x*sqrt(6.28319*mom21)*an/omeg01;c1:=1/a1;
b1:=gz*gz*bm*bm/(2*mom21);d1:=-b1;
a2:=0.25*hstr*0.33333*x*sqrt(6.28319*mom22)*an/omeg02;c2:=1/a2;
b2:=2*gz*gz*bm*bm/mom22;d2:=-b2;
sysact(1,2,30);outstring(1,'('****************************************
**********************************')');sysact(1,2,30);
outstring(1,'('* dus voor een gaussische kernfunktie:
                *')');sysact(1,2,30);
outstring(1,'('* ro1=(')');outreal(1,a1);outstring(1,'(')*exp((')');
outreal(1,b1);outstring(1,'(')*h**2) sec. *')');sysact(1,2,30);
outstring(1,'('* ro2=(')');outreal(1,a2);outstring(1,'(')*exp((')');
outreal(1,b2);outstring(1,'(')*h**2) sec. *')');
sysact(1,2,30);outstring(1,'('****************************************
**********************************')');sysact(1,14,2);
'if'n<2'then''goto'cont;
sysact(1,2,11);outstring(1,'('h')');sysact(1,2,37);
outstring(1,'('ro1')');sysact(1,2,63);outstring(1,'('ro2')');
sysact(1,2,89);outstring(1,'('roc')');sysact(1,2,115);
outstring(1,'('ro')');sysact(1,14,1);
'begin'
'for'h:=0'step'hstep'until'endh'do'
'begin'
ma1:=b1*h*h;ma2:=b2*h*h;
'if'ma1<85&ma2<85'then''begin'
ro1:=a1*exp(ma1);ro2:=a2*exp(ma2);
'end''else''begin'ro1:=1;ro2:=1;'end';
roc:=ro1*ro2/(ro1+ro2);
ro:=1/(h*h/bscgc+1)*roc;
outreal(1,h);sysact(1,2,27);
outreal(1,ro1);sysact(1,2,53);outreal(1,ro2);sysact(1,2,79);
outreal(1,roc);sysact(1,2,105);outreal(1,ro);sysact(1,14,2);
'end';'end';
cont:
sysact(1,2,30);outstring(1,'('****************************************
**************************************')');sysact(1,2,30);
outstring(1,'('* ofwel voor een gaussische kernfunktie:
                *')');sysact(1,2,30);
outstring(1,'('* 1/ro1=(')');outreal(1,c1);outstring(1,'(')*exp((')');
outreal(1,d1);outstring(1,'(')*h**2) sec**-1 *')');sysact(1,2,30);
outstring(1,'('* 1/ro2=(')');outreal(1,c2);outstring(1,'(')*exp((')');
outreal(1,d2);outstring(1,'(')*h**2) sec**-1 *')');
sysact(1,2,30);outstring(1,'('****************************************
**************************************')');sysact(1,14,2);
```

```
'if'n<2'then''goto'again;
sysact(1,2,11);outstring(1,'('h')');sysact(1,2,37);
outstring(1,'('1/ro1')');sysact(1,2,63);outstring(1,'('1/ro2')');
sysact(1,2,89);outstring(1,'('1/roc')');sysact(1,2,115);
outstring(1,'('1/ro')');sysact(1,14,1);
'begin'
'for'h:=0'step'hstep'until'endh'do'
'begin'
ma1:=b1*h*h;ma2:=b2*h*h;
'if'ma1<85ama2<85'then''begin'
or1:=c1*exp(-ma1);or2:=c2*exp(-ma2);
'end''else''begin'or1:=1;or2:=1;'end';
orc:=or1+or2;
or:=(h*h/bscgc+1)*orc;
outreal(1,h);sysact(1,2,27);
outreal(1,or1);sysact(1,2,53);outreal(1,or2);sysact(1,2,79);
outreal(1,orc);sysact(1,2,105);outreal(1,or);sysact(1,14,2);
'end';'end';
again:
outstring(1,'('einde van de opgave')');sysact(1,15,1);
'end';
'goto'return;
stop:
'end';
//go.sysin dd *
```

Explanation of the notation

n is the number of lattice-distances for which the calculation is performed,

S is the spin value,

i1 and i2 are the nuclear spin values,

a1x, a1y, a1z, a2x, a2y and a2z are the values of the hyperfine constants in cm^{-1},

g1 and g2 are the weight percentages of the odd isotopes,

ax, ay, az, bx, by, bz, cx, cy and cz are the components of the crystal axes (in Å), along the chosen x,y,z frame,

r1x, r1y and r1z are the components (in Å) of the distance between the two ions in the unit cell,

gx, gy and gz are the components of the g tensor,

ja, jb and jc are the exchange constants (in K) along the crystallographic axes,

bj is the exchange constant (in K) between the two ions in the unit cell,

h step is the value with which the external field is increased,

end h is the end value of the magnetic field,

azz(|i,j,k|) = $A^{ij}_{zz} = -2C^{ij}_{00}$,

apm(|i,j,k|) = $A^{ij}_{+-} = -2C^{ij}_{+-}$,

apz(|i,j,k|) = $A^{ij}_{+z} = -1/3\ C^{ij}_{+0}$, and

$app(|i,j,k|) = A^{ij}_{++} = -4C^{ij}_{++}$.

For calculation of the relaxation time it is uncertain whether the hyperfine interaction should be decomposed in the same way as we did for the dipole dipole and exchange interaction. Moreover we do not know whether for ions consisting of different isotopes it is allowed to take into account an average contribution of the hyperfine interaction.

S A M E N V A T T I N G

De magnetisatie van een paramagnetisch kristal komt na een plotselinge verandering van het uitwendig magneetveld trapsgewijze tot evenwicht. Als bij lage temperaturen de tijden, welke de verschillende trappen kenmerken, voldoende uiteenlopen, onderscheiden we:

1) snelle processen, dat zijn de parallel veld resonanties en de spin-spin relaxatie, en
2) langzame processen, dat zijn de rooster-bad relaxatie en de spin-rooster relaxatie.

Bij uiteenlopende tijden kan men het kristal opgebouwd denken uit twee thermodynamische systemen: het spinsysteem, dat de magnetische eigenschappen van het kristal beschrijft en het rooster waaraan de overige eigenschappen worden toegekend. De wisselwerkingstermen in de Hamiltoniaan van het spinsysteeem zijn veel groter dan de termen welke de interacties tussen het spinsysteeem en het rooster en het rooster en het bad beschrijven.

De karakteristieke tijden van de verschillende processen zijn veelal te snel om het verloop van de magnetisatie rechtstreeks waar te nemen. Daarom wordt de Fourier getransformeerde van de funktie, welke dit verloop beschrijft, gemeten. Is het relaxatie-proces te beschrijven met één exponentiële funktie dan wordt de karakteristieke tijd daarvan de relaxatietijd genoemd. De Fourier getransformeerde leidt dan tot de Debye formules voor het reële en imaginaire deel van de dynamische susceptibiliteit.

In de hoofdstukken 3, 5 en 6 worden spin-spin relaxatieprocessen beschreven. Centraal daarbij staat een vergelijking van de theoretische en de experimentele resultaten. Met het oog hierop wordt in hoofdstuk 1 een overzicht gegeven van de spin-spin relaxatie theorie. De resultaten zijn geschreven in een zodanige vorm dat ze met de computer verwerkt kunnen worden.

De veldafhankelijkheid van de spin-spin relaxatietijd en de magnetische soortelijke warmte van een éénkristal $Ce_2Mg_3(NO_3)_{12}\cdot 24H_2O$ loodrecht op de trigonale as wordt in hoofdstuk 3 beschreven. De gemeten spin-spin relaxatietijden worden vergeleken met de strong coupling theorie van P. Mazur en R.H. Terwiel en theoretische voorspellingen van G. Sauermann. Een redelijke overeenstemming wordt daarbij gevonden. De gemeten magnetische soortelijke warmte is iets groter dan de theoretisch berekende.

In hoofdstuk 5 worden temperatuur afhankelijke spin-spin relaxatietijden in éénkristallen $CoCs_3Cl_5$ en $CoCs_3Br_5$ parallel aan de tetragonale as beschreven,

tezamen met de magnetische soortelijke warmte. Een verklaring van de exponentiële temperatuur afhankelijkheid van de spin-spin relaxatietijden wordt gegeven door de theorie, zoals gepresenteerd door P.W. Verbeek in zijn proefschrift, uit te breiden tot deze zouten. De magnetische soortelijke warmte in het chloride is in overeenstemming met de gegevens omtrent de exchange wisselwerking van paren cobalt ionen in $ZnCs_3Cl_5$. Voor het bromide echter moet een aanzienlijk grotere exchange interactie worden aangenomen.

Het verschillend karakter van deze twee zouten bij lage temperaturen komt in het veldverloop van de relaxatietijden tot uiting.

De spin-spin relaxatietijden en de magnetische soortelijke warmte van éénkristallen $Cu(C_6H_5SO_3)_2 \cdot 6H_2O$ in de richting van de magnetische assen worden in hoofdstuk 6 beschreven. De magnetische gegevens van het zout zijn ontleend aan N.J. Zimmerman c.s. Berekening van de magnetische soortelijke warmte, waarbij alleen rekening is gehouden met de dipool dipool wisselwerking, wijst op de aanwezigheid van een aanzienlijke exchange interactie.

Toepassing van de weak coupling theorie geeft, ondanks de gemaakte vereenvoudigingen, een goede overeenstemming tussen de experimentele en theoretisch berekende resultaten in twee asrichtingen. Een mogelijke verklaring voor de afwijkingen in de derde asrichting wordt gegeven.

De spin-spin relaxatiemetingen zijn verricht met behulp van een twin T brug. Deze wordt beschreven in hoofdstuk 2. De mogelijkheid om met een twin T brug van deze vorm beide componenten van de susceptibiliteit te meten is reeds door Verstelle aangetoond. De meetmethode is uitgebreid en vervolmaakt waardoor de brug automatisch in evenwicht wordt gehouden en in een frequentiegebied van 100 kHz tot 30 MHz de twee componenten van de susceptibiliteit continu als funktie van het magneetveld tot 5 kOe kunnen worden geregistreerd.

Voor de spin-rooster relaxatiemetingen aan CMN, zoals deze worden beschreven in hoofdstuk 4, is ook gebruik gemaakt van de door A.J. De Vries ontworpen brug.

In lage velden werden by 4 K de twee relaxatieprocessen, corresponderende met de twee tijden welke volgen uit een simpel thermodynamisch model bestaande uit het spin systeem, de laagfrequent fononen en het bad, duidelijk waargenomen. In hoge velden wordt één relaxatieproces waargenomen, waarvan de relaxatietijd in een groter wordend veld steeds toeneemt tot in relatief grote velden (30 kOe). De temperatuur afhankelijkheid van deze relaxatietijd wordt voor alle velden beschreven met behulp van een z.g. Orbach proces.

In een appendix wordt het computer programma gegeven waarmee de magnetische soortelijke warmte en de spin-spin relaxatietijden zijn berekend.

Op verzoek van de faculteit der Wiskunde en Natuurwetenschappen volgt hier een overzicht van mijn studie.

Na het behalen van het eindexamen H.B.S.-B aan het Jansenius Lyceum te Hulst, waar mijn belangstelling voor de exacte vakken werd aangewakkerd door K. van den Ende en Drs. A. van Hecke, begon ik in 1959 mijn studie aan de Rijksuniversiteit te Leiden. Het kandidaatsexamen met de hoofdvakken wiskunde en natuurkunde en bijvak sterrekunde legde ik in 1963 af.

Sinds november van dat jaar ben ik verbonden aan de werkgroep paramagnetische spin-spin relaxatie, welke onder supervisie staat van Prof. Dr. C.J. Gorter en waarvan Dr. J.C. Verstelle de dagelijkse leiding heeft. Aanvankelijk assisteerde ik Dr. K. van der Molen en Drs. H. Lieffering.

In 1966 legde ik het doctoraal examen experimentele natuurkunde af. Na verhuizing naar de nieuwe vleugel van het Kamerlingh Onnes Laboratorium werd een begin gemaakt met het experimentele werk.

Sinds 1965 ben ik als assistent verbonden aan het natuurkundig prakticum waarbij het accent heeft gelegen op de praktica, welke op electronica gericht waren. Na mijn doctoraal examen werd ik aangesteld als doctoraal assistent en in januari 1968 benoemd tot wetenschappelijk medewerker.

Dit proefschrift is tot stand gekomen met steun van vele medewerkers van het Kamerlingh Onnes Laboratorium. Op de allereerste plaats Dr. J.C. Verstelle waarmee vrijwel dagelijks over de problemen werden gesproken, vaak zelfs op de fiets, onderweg naar huis. Vervolgens Dr. P.W. Verbeek en Drs. H. van Noort welke belangrijk hebben bijgedragen tot de theoretische en electronische inhoud van dit proefschrift.

Hoofdstuk 6 is tot stand gekomen in samenwerking met Drs. P. van Tol. Bij de metingen werd ik geassisteerd door Drs. C. de Lezenne Coulander, H. van Tol en W.L.C. Rutten. Bij de metingen in hoofdstuk 4 is gebruik gemaakt van de apparatuur in de groep van Dr. A.J. van Duyneveldt. In het theoretische hoofdstuk is dankbaar gebruik gemaakt van: "Seminar über Fragen der Magnetischen Relaxation", Darmstadt 1965/1966, dat welwillend ter beschikking werd gesteld door Prof. Dr. G. Weber. Met Prof. Dr. G. Weber, Prof. Dr. G. Sauermann en medewerkers van de Technische Hochschule in Darmstadt is een vruchtbare discussie gevoerd. De technische apparatuur is vervaardigd in de werkplaats van J. Turenhout en de glazen apparatuur in de werkplaatsen van B. Kret en C.J. van Klink. De kristallen werden vervaardig door Mevr. M.A. Otten-Scholten en Dr. H.W.J. Blöte. De tekeningen werden in een vlot tempo vervaardigd door W.J. Brokaar en de foto's werden afgedrukt door W.F. Tegelaar. De Engelse tekst

werd gecorrigeerd door Dr. R. Thiel en het manuscript werd getypt door Mevr. E. de Haas-Walraven. Tot hen allen zeg ik: *bedankt*.